CRYSTALLIZATION AND INTERCALATION BEHAVIOUR OF LAYER DICHALCOGENIDES

Thesis submitted for the Degree of
Doctor of Philosophy

of the University of London by

VICTOR MANUEL CHAPELA CASTAÑARES

Department of Chemical Engineering and Chemical Technology
Imperial College of Science and Technology
May, 1979

ABSTRACT

Lamellar transition metal dichalcogenides powders have been prepared by direct synthesis inside quartz tubes.

Single crystals were subsequently grown in a gradient zone furnace by iodine vapour transport technique at 900°C.

Both powders and single crystals have been intercalated by reaction with different chemical compounds. The intercalation process was monitored by powder and single crystal X-ray methods.

Some 30 new chemical species have been intercalated into 2H-TaS_2 conforming with the currently accepted empirical rules and new groups of complexes are now available for research.

Among the several new groups of materials successfully intercalated into TaS_2 are the trisubstituted amines, the amino acids and polypeptides.

Trisubstituted amines N $R_1R_2R_3$ were intercalated from the liquid state by standard methods. The series $R_1=R_2=R_3$

where $R=-(CH_2)_{n-1}-CH_3$; n=1,2,3,4,8,10

$(CH_3)_2$ N-$(CH_2)_n$-N$(CH_3)_2$; n=1,2,3,4

$H_{3-n}N(CH_2CH_2OH)_n$; n=1,2,3

H_{3-n} N $(CH_2CH_2)_n$ NH_{3-n}; n=1,2,3

form superconducting intercalated complexes.

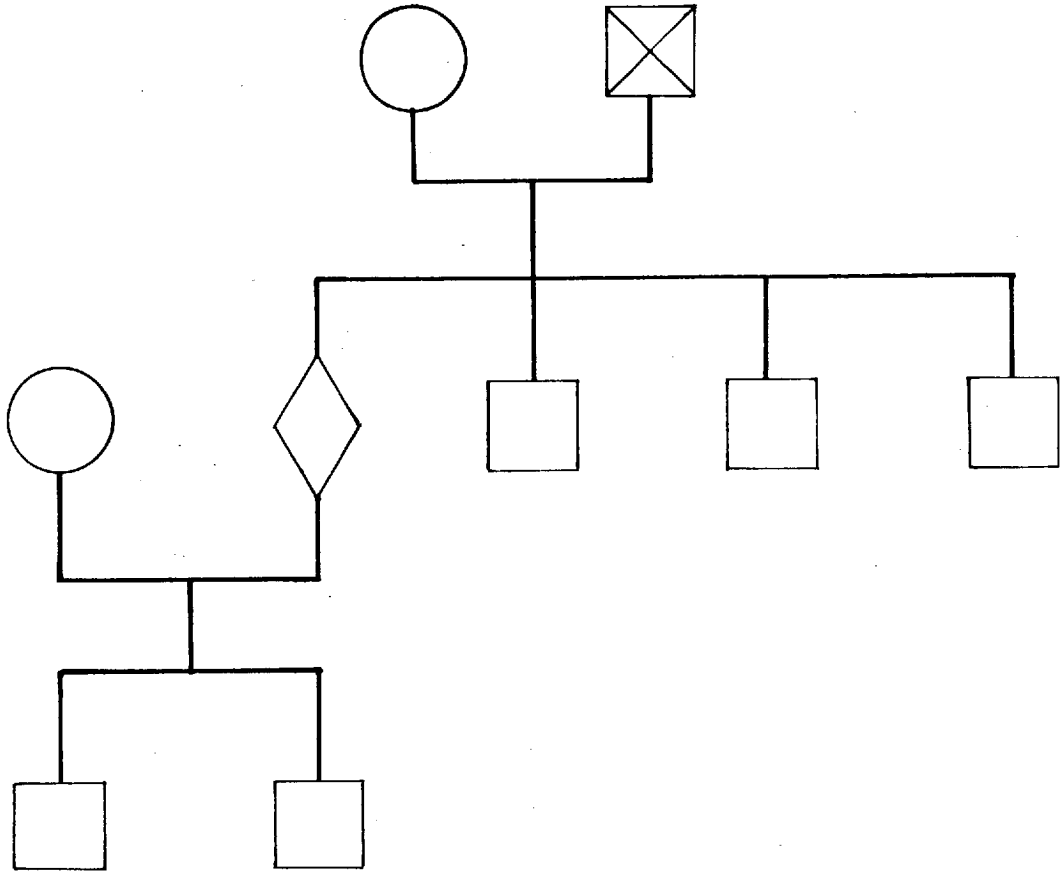
The intercalation of amino acids and polypeptides into TaS_2 was achieved using aqueous solutions. Amino acids included glycine, valine, proline and β alanine. Polypeptides included diglycine, triglycine, tetra-glycine, pentaglycine and diketopiperazine. Attempts were made to polymerize glycine and to intercalate the polyglycine. Results are reported and discussed.

The c axis repeat distance of the intercalated compounds was measured. Of interest was the decreasing behaviour of the van der Waals expanded gap in the case of glycine and its n-mers ($1<n<5$).

The superconducting transition temperature of the complexes was measured and shows an increment of the transition temperature as reported previously for the intercalation complexes.

As a result of all these findings, it is suggested that the model currently accepted of the lone pair orbital to explain the interaction between the intercalated species and the TaS_2 layer should be revised to include the possibility that the nitrogen lone pair in the polypeptides and the acidamides p orbital could interact with the metallic layers.

To my family



I have a clock, a pencil and a paper.
The clock mumbles me the brevity of my life.
The pencil compels me to work.
The paper induces me to write
the history of my best acts.
But before I have to perform them!

Miguel Angel Cevallos
"A man lost in the Universe"
Editorial Cultura
México 1954

ACKNOWLEDGEMENTS

I thank my supervisor Dr. G.S. Parry for his guidance and friendship. I also thank Prof. G. Allen for his advice and encouragement. Dr. J. Gómez Lara and C. Doubé helped with stimulating discussion.

I would like to acknowledge to my beloved wife Noráh Yolanda her love and encouragement after nine years of very happy marriage and friendship that made possible to close this cycle.

I would also like to thank Dr. Forgan from Birmingham University for making available to me the Department of Physics facilities for measuring the superconducting transition temperature.

I also wish to thank Dr. Waight from the Chemistry Department of Imperial College of Science and Technology, for obtaining the mass spectrograms of several complexes.

I am indebted to Mrs. Rhoda Surgenor for typing the manuscript.

I acknowledge financial support by Universidad Nacional Autonoma de México - Banco de México scholarship program and the leave of absence from the Centro de Investigación de Materiales.

CONTENTS

ABSTRACT 2

ACKNOWLEDGEMENTS 6

CONTENTS 7

LIST OF TABLES 10

LIST OF FIGURES 11

CHAPTER 1 Introduction 15

1.1 Intercalation 15

1.2 Clay intercalation 16

1.3 Graphite intercalation 18

1.4 Metal dichalcogenide intercalation 19

1.5 Pyridine and ammonia intercalation into TaS_2 23

1.6 Proposed model's for achieving new superconductors 26

1.6.1 Little's model 26

1.6.2 Ginzburg's model 28

CHAPTER 2 Crystal Structure and Layer Packing 32

2.1 Description of layer transition metal dichalcogenides 32

2.1.1 Octahedral co-ordination group 35

2.1.2 Trigonal prismatic co-ordination group 36

CHAPTER 3 Preparation of Material and Crystal Growth 40

3.1 Introduction 41

3.2 Experimental equipment and procedures 42

3.2.1 Materials 42

3.2.2 Procedure to form the dichalcogenides 43

3.2.3 Vacuum line design and construction 44

3.2.4 Furnace design and construction 46

3.3 Results and discussion 51

CHAPTER 4 Intercalation of SN Compounds 55

4.1 Introduction to chemistry of S_4N_4 55

4.1.1 Disulphur dinitride S_2N_2 and polysulphurnitride SN)x 56

4.2 Reactions of tetrasulphur tetranitride with ammonia and with alcohols 58

4.3 Preparation of S_4N_4 tetrasulphur tetranitride 60

4.3.1 Method 1 61

4.3.2 Method 2 62

4.4 Intercalation experiments with SN compounds 66

4.5 Discussion 71

CHAPTER 5 Intercalation of Triamines 72

5.1 Introduction 72

5.2 Intercalation sets 72

5.3 Results of intercalation of triamines 74

5.4 The relative orientation of the intercalated triamines inside TaS_2 85

5.5 Discussion 90

CHAPTER 6 Intercalation of Amino Acids 93

6.1 Introduction 93

6.2 The peptide bond 95

6.3 Intercalation experimental procedures 102

6.3.1 Procedures to intercalate amino acids and polypeptides 102

6.3.2 Attempts to intercalate polyglycine 104

6.4 Results 106

6.5 Discussion 108

CHAPTER 7 Characterization of Intercalated Crystals 112

7.1 Introduction 112

7.2 Thermogravimetric determinations 113

7.3 Superconductivity 115

7.4 X-ray diffraction 120

7.4.1 Powder diffraction equipment 120

7.4.2 Procedure 122

7.4.3 Interpretation 123

7.4.4 Intercalated single crystals 125

CHAPTER 8 General Discussion and Future Work 131

REFERENCES 142

LIST OF TABLES

4.1 Intercalation experiments of S_4N_4 plus alcohols into TaS_2 66

4.2 Mass spectrometry results on $S_4N_4{}^{15}$ and S_4N_4 70

5.1 Results of intercalation of triamines into TaS_2 76

5.2 Thermogravimetric analyses of triamines 78

6.1 Results of intercalation of amino acids into TaS_2 105

8.1 Expanded gap prediction from the squashed molecules 133

LIST OF FIGURES

1.1 The montmorillonite layer structure viewed along the a axis. 16

1.2 Expanded gap in graphite intercalation 19

1.3 Graph showing the results on amides intercalation, the expanded gap and the mol ratio versus the number of carbons in the acid chain 20

1.4 The superconducting T_{onset} (circles) expanded gap (triangles) versus the number of carbons on aliphatic chain of the primary amines 22

1.5 The pyridine orientation with the lone pair of the nitrogen which lies parallel to the layer plane and the molecule plane perpendicular to the layer plane 25

1.6 Little's model showing the spine A and the side chains B attached to the spine, which should be highly polarizable molecule 27

1.7 Ginzburg's model, two dimensional dielectric-metal-dielectric sandwich system 29

2.1 MX_2 layer sandwich showing the van der Waals gap 33

2.2 MX_2 layered structure (regular or undistorted) 34

2.3 Basic MX_2 unit a) Trigonal prismatic co-ordination; b) octahedral co-ordination 34

2.4 Illustration of the plan of the structure and the $(11\bar{2}0)$ plane with octahedral co-ordination (AbC stacking) 36

2.5 Illustration of the plan of the structure and the $(11\bar{2}0)$ plane with trigonal prismatic co-ordination (AbACbC stacking) 37

2.6 Illustration of the plan of the structure and the ($11\bar{2}0$) plane with trigonal prismatic co-ordination (AbABaB stacking) 38

2.7 ($11\bar{2}0$) planes of polytypes of transition metal dichalgonides 39

3.1 Vacuum line set up showing the L shaped glass tube and glove bag 43

3.2 Vacuum line set up showing the L shaped glass tube and without the glove bag 45

3.3 Graph of the temperature of the furnace against 20-turn helical potentiometer dial setting of the temperature controller 48

3.4 Photograph of the AEI controller showing the profile cam and microswitch 49

3.5 Arrangement of the furnaces and controller 50

3.6 Temperature vs. distance showing the profile of the gradient zone furnace 51

3.7 1T-TaS_2 crystals obtained by direct synthesis, the scale is $1mm^2$ 52

4.1 Diagram of S_4N_4 molecule 56

4.2 Resonance formulae of polymerization of S_4N_4 57

4.3 Reaction of S_4N_4 with ammonia to obtain the ammoniate 59

4.4 Fission of the ammoniate in ammonia solutions 59

4.5 Diagram of $S_4N_4H_4$ molecule 60

4.6 Apparatus previously used to obtain S_4N_4 with NH_4Cl and S_2Cl_2 63

4.7 Apparatus used for preparing S_4N_4 nitrogen 15 64

5.1 Expanded gap and T_{onset} versus the (n) number of 79

carbons on the alkaly chain of the normal triamines of set (a) 79

5.2 Detail of expanded gap (with error bars) versus the n, also the composition (x) corresponding to the formula TaS_2 (n-triamines)$_x$ of set (a) 80

5.3 Graph of the expanded gap and superconducting T_{onset} versus the number of carbons (n) in the linking chain (set b) 81

5.4 Expanded gap and composition (x) (corresponding to the formula TaS_2 (triamines)$_x$ versus the number of carbons (n) in the linking chain (set b) 82

5.5 Expanded gap and superconducting T_{onset}, showing error bars and transition widths, versus the n-ethanolamines of set (c) 83

5.6 Expanded gap and superconducting T_{onset} ,showing error bars and transition widths, versus the n-ethylenediamines of set (d) 85

5.7 Top and side photographs of the three substituted amines, showing molecular dimensions of set (a) 88

5.8 Top and side photographs of the n-ethylenediamines, showing molecular dimensions (set d) 89

6.1 Peptide bond showing 3 possible rotations 95

6.2 Peptide bond without rotation of the C-N bond 96

6.3 Representation of the nitrogen atom with sp^2 hybridization 97

6.4 Representation of an oxygen atom with sp hybridization 98

6.5 Top and side view of the bonding on a peptide bond 99

6.6 Energy levels diagram of a peptide bond 100

6.7 Expanded gap and superconducting T_{onset}, showing error bars and transition widths, versus the number of glycine units of polyglycine 107

7.1 Diagram of the A.C. susceptibility probe 116

7.2 Diagram of the heater of the probe 116

7.3 Diagram showing the location of the Allen-Bradley carbon resistance thermometer 117

7.4 Temperature control circuit

7.5 General view of the powder diffractiometer set up 121

7.6 Powder diffractometer (X-ray source, sample holder and detector) 122

7.7 Oscillation camera for single crystals examination 126

7.8 Single crystal oscillation photograph 2H-TaS_2 128

7.9 TaS_2 intercalated with glycine, single crystal c-axis perpendicular to the beam 129

7.10 TaS_2 intercalated with diglycine, single crystal c-axis perpendicular to the beam 129

7.11 TaS_2 intercalated with triglycine, single crystal c-axis perpendicular to the beam 130

7.12 TaS_2 intercalated with glycine, single crystal c-axis parallel to the beam 130

8.1 Top and side photographs of the first four n-glycine polypeptides, showing the α_2 orientation 134

8.2 Proposed mechanism for initiation of intercalation 138

CHAPTER 1

INTRODUCTION

1.1 Intercalation

Intercalation is the insertion of atoms (or molecules) between the layers of a host structure. Intercalation has been studied in different layered compounds mainly clays, graphite and metallic dichalcogenides.

Of particular interest are the methods and procedures adopted to study intercalation products. X-ray diffraction is used to confirm intercalation and to determine certain structural aspects of these layered materials. Intercalation materials may be either transparent or opaque, broadly this corresponds to matrix structures that are electrical insulators or conductors. If the material is transparent, polarized I.R. can be used to explore the chemical nature of the intercalated species; other techniques commonly used to study intercalation compounds are differential-thermal analysis (DTA), that may detect internal order-disorder transitions and thermal-gravimetric analysis (TGA) to establish weight uptake and hence the composition of the product.

The electrical properties of these layer compounds range from insulators (intercalated clays) to metallic superconductors (intercalated dichalcogenides).

1.2 Clay Intercalation

The reasons to talk about clays are the similarities in intercalation behaviour found during this research between the clays intercalation and the dichalcogenides intercalation and that in order to introduce some concepts regarding intercalation the clays are simpler systems.

Most of the clay layers have positive charged cations sandwiched in between the layers which are solvated by water molecules (Figure 1.1).

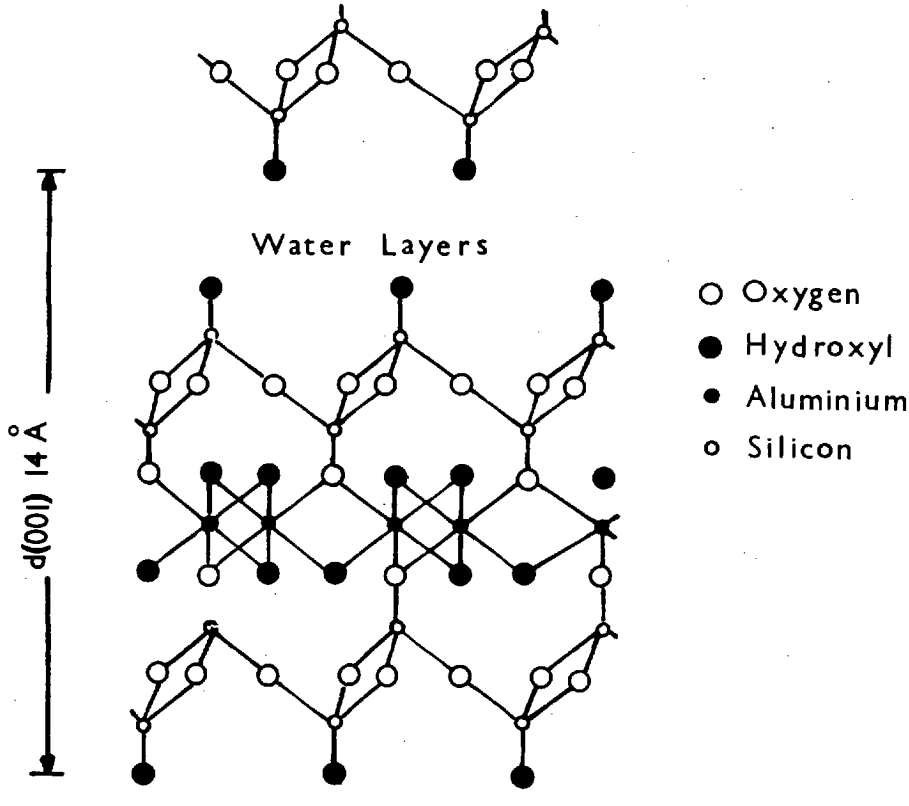


Figure (1.1)

Two types of water can be distinguished. The first type (I) constitutes the inner (primary) hydration shell around the exchangeable cation, i.e. the water which is directly co-ordinated to the cation. The second type (II)

forms the outer (secondary) co-ordination sphere of the cation; as it is indirectly linked to the cation and possesses greater mobility, this water is more labile than that of type I. The substitution of the cation could also lead to an intercalation complex. Hence it is possible to visualize three types of intercalation in clays according to which molecules are exchanged.

1. - Many polar organic molecules such as pyridine, nitrobenzene and benzoic acid can therefore displace type II water in montmorillonite.

2. - If the saturating cation is weakly polarizing (e.g. Na^{+}, Ba^{2+}) type I water may similarly be displaced.

3. - Finally inorganic cations may be replaced by alkylammonium ions by bringing the clays into contact with aqueous solution of the appropriate alkylammonium chloride.

The molecular orientation in the intercalated clays is of two kinds: in the first type, designated α_1 refers to an interlayer arrangement in which the plane of carbon zig-zag is perpendicular to the silicate layer; in the second type, the α_2 arrangement, the plane of carbon zig-zag is parallel to the silicate layer (Theng 1974).

Clays form complexes with alcohols as well as aliphatic and aromatic amines; homologous series of alcohols ($CH_3(CH_2)_{n-1}OH$), primary amines ($CH_3(CH_2)_{n-1}NH_2$) and

tertiary amines ($(CH_3(CH_2)_{n-1})_3N$) have produced intercalated complexes.

Amino acids and polypeptides have been intercalated and polymerized in between clays in an attempt to explain the abiotic synthesis of proteins.

Systematic changes of the properties can be made by changing the number of carbons or amino acids in the chain of the intercalated molecule that cannot be done with intercalations of simple atoms like alkaline metals.

1.3 Graphite Intercalation

Graphite intercalation has been known for a long time. Gmelins (1968) makes reference to graphite intercalation work by C. Schafhaeutl in 1840. Systematic studies have shown that a wide range of chemicals can be intercalated in between the host layers, e.g. alkali metals, Lewis acids, superacids, fuming nitric, sulfuric acids and bromine (Ubbelohde 1977). It is interesting to note the amphoteric character of graphite regarding intercalation behaviour. Of particular importance is the fact that it was possible to produce materials with different properties to the original graphite. For example graphite can be considered as a semimetal but after intercalation with bromine it becomes a good electrical conductor. The ability of changing the electronic properties of the host material by intercalation processes has been one of the reasons for undertaking this research with the metallic dichalcogenides.

It is customary to discuss the basal spacing of graphite intercalation compounds and intercalation complexes in general in terms of Δ value, delta value or expanded gap (also called expanded van der Waals gap), which is the difference between the observed expanded spacing of the intercalated complex (B) and the thickness of the individual unintercalated layered compound (A). (Figure 1.2)

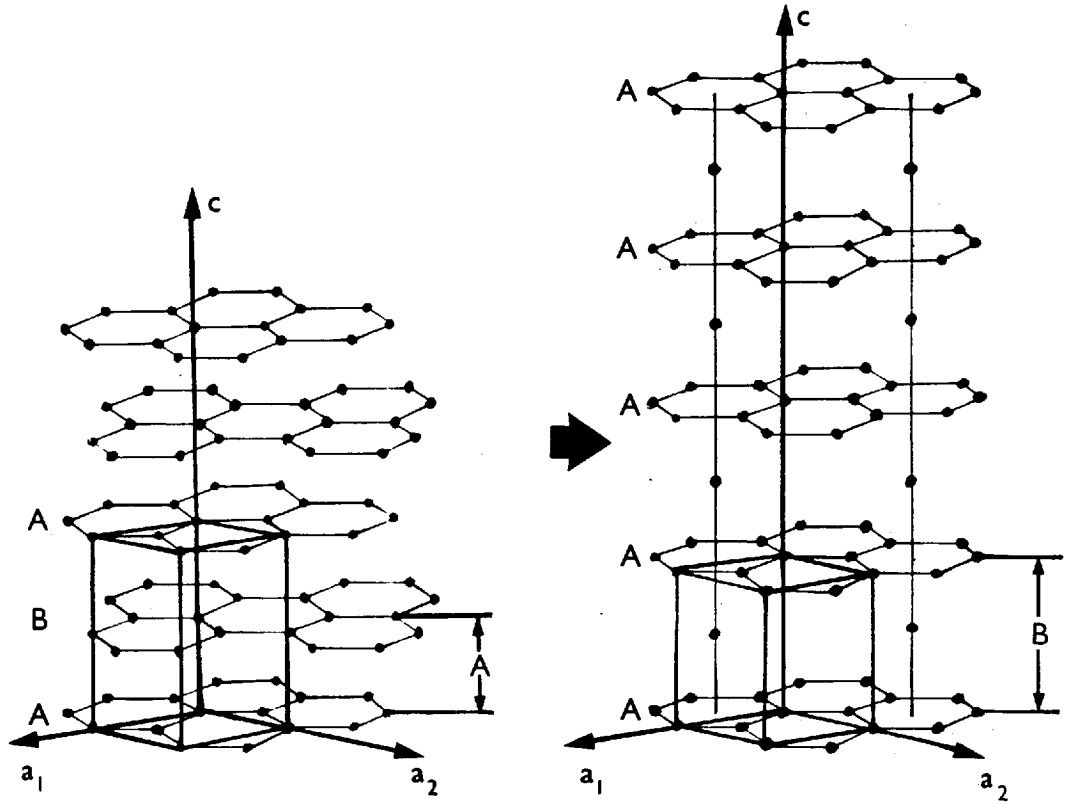


Figure (1.2)

1.4 Metal Dichalcogenide Intercalation

The first intercalation into layer dichalcogenide was reported by Rüdorf (1959). He intercalated alkaline metals into MoS_2 and WS_2 from an ammonia solution.

Intercalation of organic molecules into MX_2 structures was first reported by Weiss and Ruthart (1969); they described intercalation of hydrazine and some aliphatic

amides into TiS_2. The behaviour of the amides with respect of the number of carbon atoms in the chain is that the expanded gap decreases from the formamide (1 carbon) to caproamide (6 carbons) from 10.6Å to 4.8Å. As well as the mol ratio which decreases also from 0.87 to 0.55 as indicated on the graph of figure (1.3).

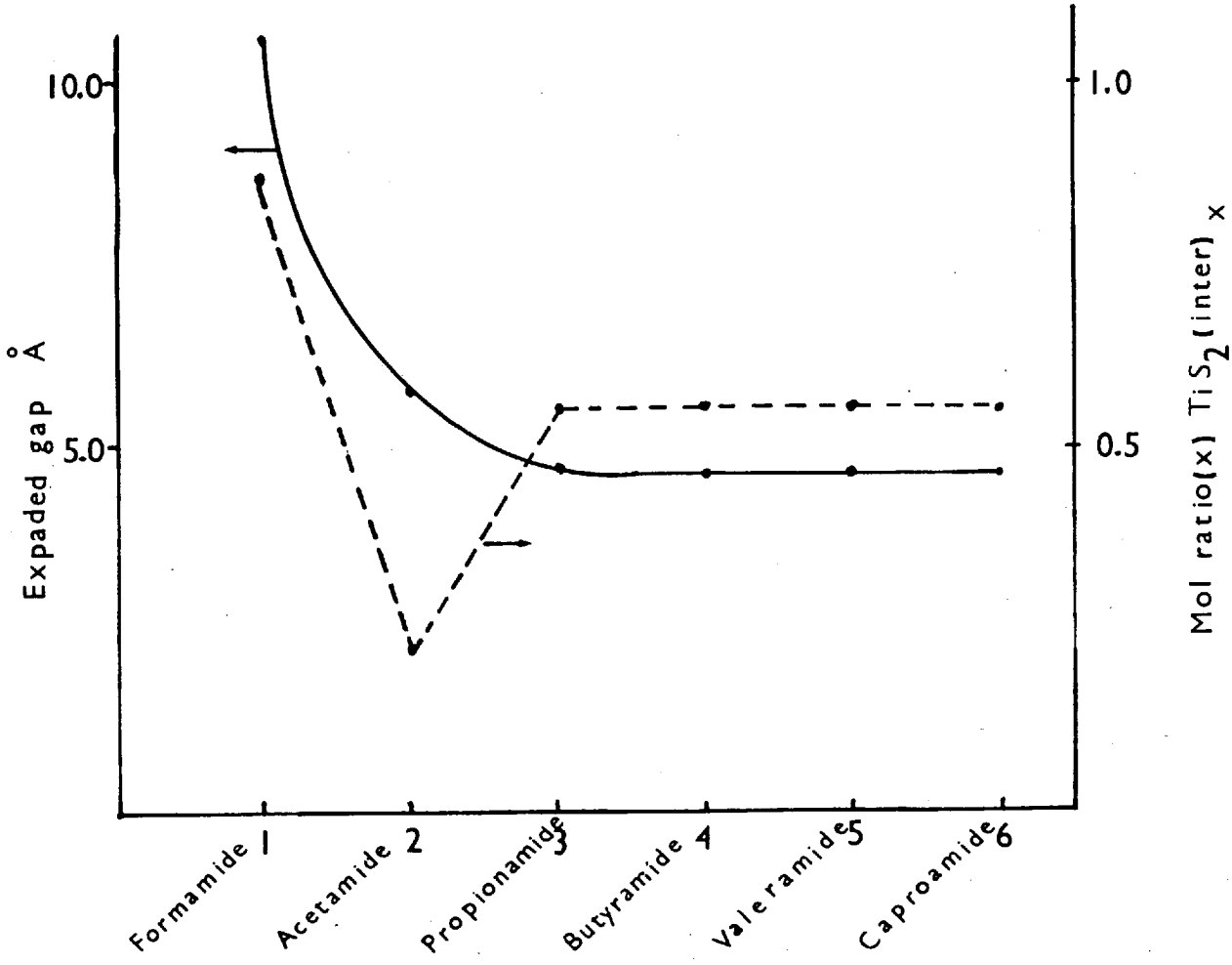


Figure (1.3)

An extensive study of intercalation of organic molecules into layer dichalcogenides and the effect of electronic properties particularly the conductivity and the onset of superconductivity was made by Gamble et. al. (1971), Di Salvo et. al. (1971) and Geballe et. al. (1971).

They studied the intercalation behaviour of a very large list of amines and substituted pyridines as well as hydroxides and other Lewis bases; and they found that the pK_a greater than 4 was a simple practical index for the idea that Lewis basicity was the controlling factor in intercalation of the compounds investigated.

The low temperature electronic properties of these intercalated compounds were studied and it was established that superconductivity occurred on all the intercalated compounds between $1.5^{o}K$ and $5.3^{o}K$ and that the onset of superconductivity was controlled by the nature of the intercalate but was insensitive to a separation of the superconducting planes of up to 57 angstroms i.e. octadecylamine molecules intercalated into TaS_2.

From the study of intercalation of alkylamines ($CH_3(CH_2)_nNH_2$) Gamble et. al. (1971) proposed that the chains lie parallel to the layer when the chains were small ($n < 4$) but perpendicular to the layers when the chains were large ($n > 12$). As can be noted in figure (1.4).

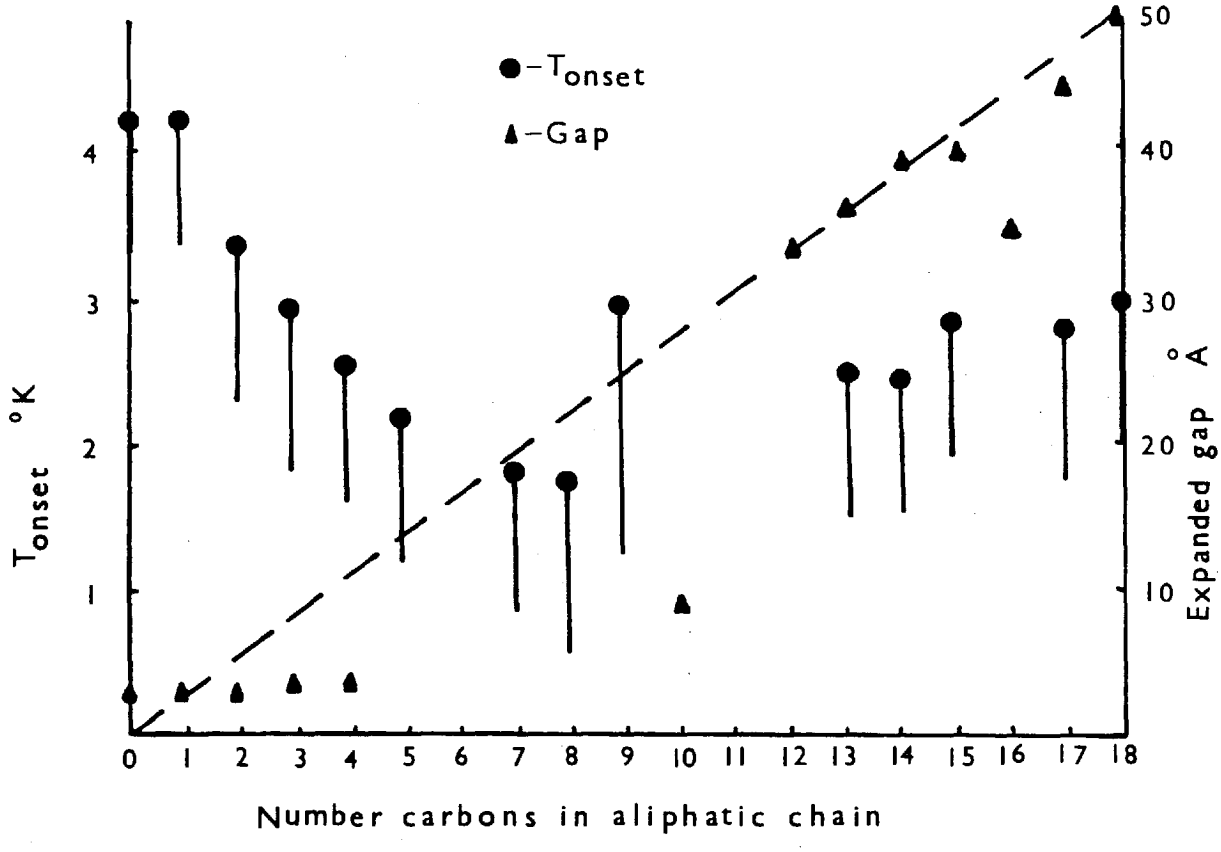


Figure (1.4)

Judging only from the increase in interlayer spacing in angstroms for the amines and amides intercalation complexes is not easy to propose a nitrogen lone pair orientation. The situation is different in the intercalation complexes of TaS_2 and substituted pyridines (Gamble et. al. 1971) where there were two exceptional cases, 2,6 dimethyl-pyridine and 2,4,6 trimethylpyridine having expanded gaps of 3.55 and 3.63 $\mathring{A}$ respectively. In order to explain these expanded gaps, that were measured by simple powder X-rays diffractometry, the molecule molecular plane must lie parallel to the TaS_2 planes, so that the nitrogen lone pair in the sp^2 hybridized orbital now can easily be visualized as also lying parallel to the TaS_2 planes.

1.5 Pyridine and Ammonia Intercalated into TaS_2

The case of pyridine and ammonia intercalated compounds has provided an interesting example of the difficulties that can arise because of the limited number of experimental techniques available for studying metallic dichalcogenides, initially the orientation of the molecular plane and the nitrogen lone pair were established (Gamble et. al. 1970), as perpendicular to the TaS_2 layers in order to explain the almost stoichiometric ratio of the dichalcogenide to the ammonia and pyridine, of 1 and 0.5 respectively.

The interaction between the dichalcogenide and the intercalated pyridine molecule was proposed by Gamble et. al. (1970) as a co-ordination bond between the nitrogen lone pair and d_z2 orbital of the tantalum. This co-ordination demanded the perpendicular orientation of the pyridine molecular plane with the nitrogen lone pair pointing towards a tantalum atom.

Later on, in another article, Gamble et. al. (1971) inferred that the plane of the molecule should lie parallel to the tantalum disulphide planes and that the interaction should be a charge donation from the nitrogen to the sulphur atoms.

An X-ray single crystal study by Parry et. al. (1974) showed that the findings were inconsistent with the parallel alignment of the pyridine molecule relative to the TaS_2 layers and suggested in agreement with Gamble et. al. (1970) that the nitrogen lone pair is also

perpendicular to the TaS_2 layer in order to have a favourable position to interact with the d orbitals of the tantalum. This implied that the pyridine molecule occupied a specific site over the sulphur plane.

The case of ammonia is also interesting. Cousseau (1973) postulated on the basis of traditional chemical arguments that the lone pair orbital of the nitrogen lies perpendicular to the TaS_2 in disagreement with the recent NMR studies on $TaS_2 \cdot NH_3$ of Gamble et. al. (1975) where they measured an anisotropic proton spin-lattice relaxation time in single crystals of $TaS_2 \cdot NH_3$ and conclude that the lone pair orbital should lie parallel to the TaS_2 lamellae.

Neutron diffraction studies have accentuated the superiority of this technique as compared to X-ray diffraction in structural investigations that require the nitrogen atom to be located within the expanded van der Waals gap in this type of compounds.

Neutron diffraction by samples of pyridine and pentadeuteriopyridine intercalated in NbS_2 (Riekel et. al. 1976) and on samples of ammonia and D_3N in TaS_2 (Riekel et. al. 1976) has shown by one-dimensional Fourier synthesis that the hydrogen atoms could be located near the sulphur layer, where minima were found for $NbS_2\ (Py)_{0.5}$ and maxima for $NbS_2(DPy)_{0.5}$ (this difference arises because the scattering cross section of H^1 is negative while that of H^2 is positive). A further hydrogen and nitrogen atom were found to reside midway

between the layers figure (1.5).

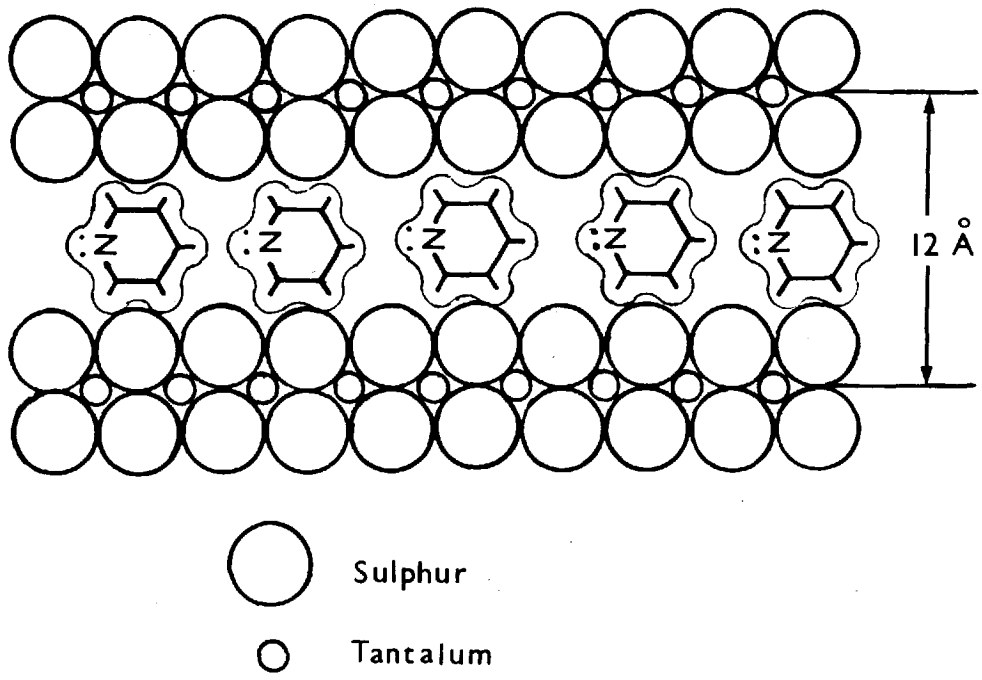


Figure (1.5)

In the case of ammonia the structure factor calculation, for $TaS_2 \cdot NH_3$, based on neutron powder diffraction data for the 001 series favour the model according to which the C_3 axis of the ammonia molecules lies parallel to the layer plane and hence the lone pair orbital should also lie parallel to the layer planes.

The interesting conclusion of these studies is that the nitrogen atom is midway between the dichalcogenide layers and the lone pair of the nitrogen is parallel to the layers. On the basis of these studies, localized charge transfer between pyridine and ammonia to the dichalcogenide layer would be highly unlikely except on an initial event

during the intercalation process. The nature of the equilibrium bonding of intercalated organic molecules and the host lattice remains a problem yet to be solved.

A study by Schöllhorn et. al. (1977) have demonstrated that ammonia intercalated into TaS_2 can be understood as a polyelectrolyte system consisting of $(TaS_2)^{x-}$ layers with delocalized negative charges and the interlayer spacings being populated by readily mobile and exchangeable NH_4^+ cations solvated by NH_3 molecules. They have found that TaS_2 layers act as oxidizing agent in the reaction and part of the NH_3 is oxidized to elemental nitrogen and the concomitant protons can be transferred to NH_3 molecules to form NH_4^+ ions. The ionic structural model provides a simple explanation of the unusual arrangement of the NH_3 molecule (C_3 axis parallel to the layer as shown by neutron scattering experiments). With the ratio of NH_4^+/NH_3=1:9 each NH_4^+ acquires a complete two dimensional solvation sphere: the solvate molecules must be arranged with the lone pair directed to the positive charge centres.

1.6 Proposed Models for Achieving New Superconductors

1.6.1 Little's model

Little (1964) has speculated on a new kind of superconductivity in which conduction electrons and molecular excitons may interact to increase the superconducting transition temperature.

The model proposed by Little can be regarded as one dimensional, because he considered a molecule consisting of two parts, a long chain called the "spine" (A) and a series of side chains attached to the spine (B). The spine (A) would be filled with electrons and may or may not form a conducting system. The side chains (B) would have to have virtual oscillation of charge, meaning this that the sidechains should be highly polarizable molecules Figure (1.6).

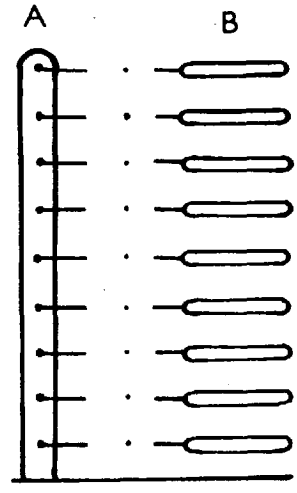


Figure (1.6)

From an experimental practical point of view this means a system with an extensive delocalization of electrons in the spine like in a conjugated double bonds or metal to metal bonding chains. The side chains could be dye molecules or small molecules like cyanide group or simple atoms. Many systems with these general characteristics have been proposed and tested in the past 15 years but

superconductivity has not been found.

The only system on which this geometrical model can be applied and which has produced a superconductor is $SN)_x$. (Greene et. al. 1975), even though the mechanism for superconductivity cannot be regarded that of Little's.

1.6.2. Ginzburg's model

Ginzburg (1968) has also proposed a model for attaining high superconducting transition temperatures which may be regarded as two dimensional. He proposed an excitonic mechanism for superconductivity on "unusual" conducting systems like filamentary compounds, layer compounds and "sandwiches" of the dielectric-metal-dielectric type.

The model proposed is a two dimensional dielectric-metal-dielectric system where the idea is that the attraction between the electrons is enhanced by the exchange of excitons propagating mainly in the dielectric regions of the "sandwich". Figure (1.7).

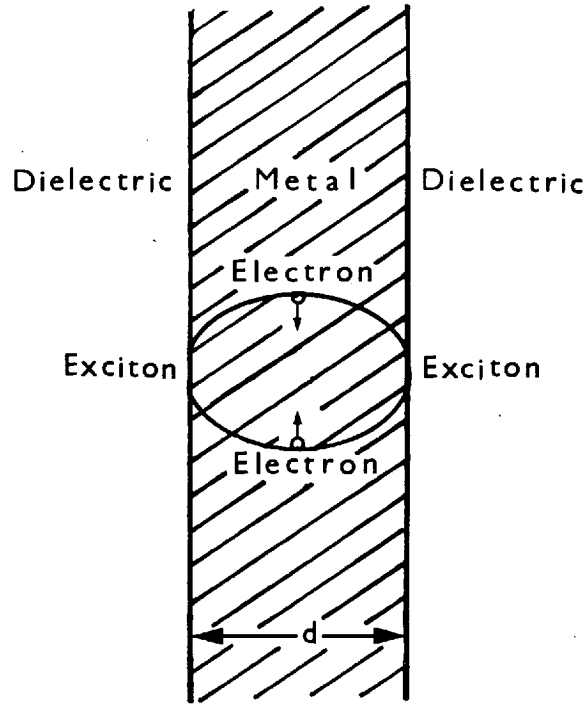


Figure (1.7)

In contrast with Ginzburg's model it must be pointed out that the effect of a dielectric coating on the critical superconducting transition temperature of films has been studied in the past by Gamble et. al. (1968) and Glover III (1960). Dielectric organic molecules were deposited over superconducting films, this changed the superconducting transition temperature of the metal, the charge transfer from the organic molecule to the superconducting metal was the responsible for increasing the Tc. Similarly the transition temperature of a superconducting thin film can be increased or decreased by just electrostatically charging it with positive or negative charge.

As pointed out by Ginzburg (1972) "The exciton mechanics seems to be ineffective for layered compounds intercalated

with molecular species because molecules of large size 10-20 Å are necessary to obtain low excited levels $\hbar\Omega$<leV. To overcome this difficulty it is necessary to try to put into dichalcogenides (or into other layered compounds) layers of a semiconductor type instead of molecular layers. In such semiconducting layers delocalized excitons with favorable values of $\hbar\Omega$ probably can exist which weakly damp even at $q \sim q_F$."

The suggestion by Ginzburg (1972) can be interpreted as suggesting that a long molecule of a polymer with semiconducting characteristics intercalated into a dichalcogenide could behave as an excitonic superconductor.

It has been pointed out by Gamble et. al. (1971) that given the mild conditions under which many intercalations proceed and the large number of basic functional groups that can be used to carry a molecule between the layers, molecular species of almost any description can be designed to form intercalation complexes with certain of the layered dichalcogenides.

With the ultimate aim of combining the one dimensional model by Little and the two dimensional model of Ginzburg, in order to obtain a composite model where the dichalcogenide of transition metal will act as the two dimensional element and the intercalate polymer will act as the one dimensional element, it was then decided to investigate the intercalation of polymers in between the transition metal dichalcogenides layers.

The first requirement was to obtain control over the supply of host crystals and the crystallization experiments are described in Chapter 3. TaS_2 was chosen as the transition metal dichalcogenide because it is by far the easiest to intercalate. The search for new intercalation species commenced with the cyclic tetramer of $SN)_x$ (Chapter 4). These experiments were inconclusive and revealed large gaps in the understanding of covalent inorganic chemistry of sulphur-nitrogen systems. Intercalation of triamines (Chapter 5) were followed by intercalation of amino acids (Chapter 6) and intercalation of the first homologous polymeric series. Chapters 4, 5 and 6 are written to include all experiments performed on the intercalated complexes including thermogravimetry and superconducting transition temperatures. Such features which are relevant to only one of the groups of compounds, are dealt within the discussion at the end of each chapter. Chapter 7 described the techniques used for characterization of the intercalated complexes. The general discussion (Chapter 8) deals with common and contrasting features found in the experimental results and propose guidelines for future work.

CHAPTER 2

CRYSTAL STRUCTURE AND LAYER PACKING

2.1 Description of Layer Transition Metal Dichalcogenides

Layer compounds are those which crystallize in atomically thin sheets, within which the chemical bonds are strong but between which the bonding is weak van der Waal's type.

The transition metal layer dichalcogenides of general formula MX_2, where M represents a transition metal and X is a chalcogenide i.e. sulphur, selenium or tellurium have proved to be a particularly interesting group of materials in which to study the relationship between crystal and electronic structures. Their electrical properties vary from those of insulators to superconducting metals.

In all of these compounds, the MX_2 layer are three atoms thick. The top and bottom layers of the layer are formed by chalcogen atoms, and the middle layer by the transition metal atoms (Wilson et. al. 1969).

This study is mainly concerned with the groups Va transition metal dichalcogenides TaS_2 and NbS_2. However, the structural properties of all groups IVa, Va and VIa share common behaviour.

Each MX_2 layer consists of a sandwich as shown in Figure (2.1).

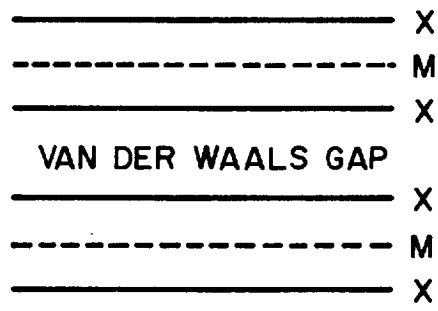


Figure (2.1)

This structure leads to strongly anisotropic properties for these compounds, the most obvious of which is their easy cleavage parallel to the layers.

The undistorted structures of layer dichalcogenides (sometimes known as regular structures) are easily visualized. The bottom layer is formed from a close packed layer of chalcogen atoms, Figure (2.2A). The middle layer of metal atoms is placed so that they occupy every other depression formed by the bottom chalcogen layer Figure (2.2B). The top chalcogen layer can be placed in one of two ways: either directly above the original chalcogen layer or in the unfilled depressions left in the original chalcogen layer (those not filled by a cation) Figure (2.2C).

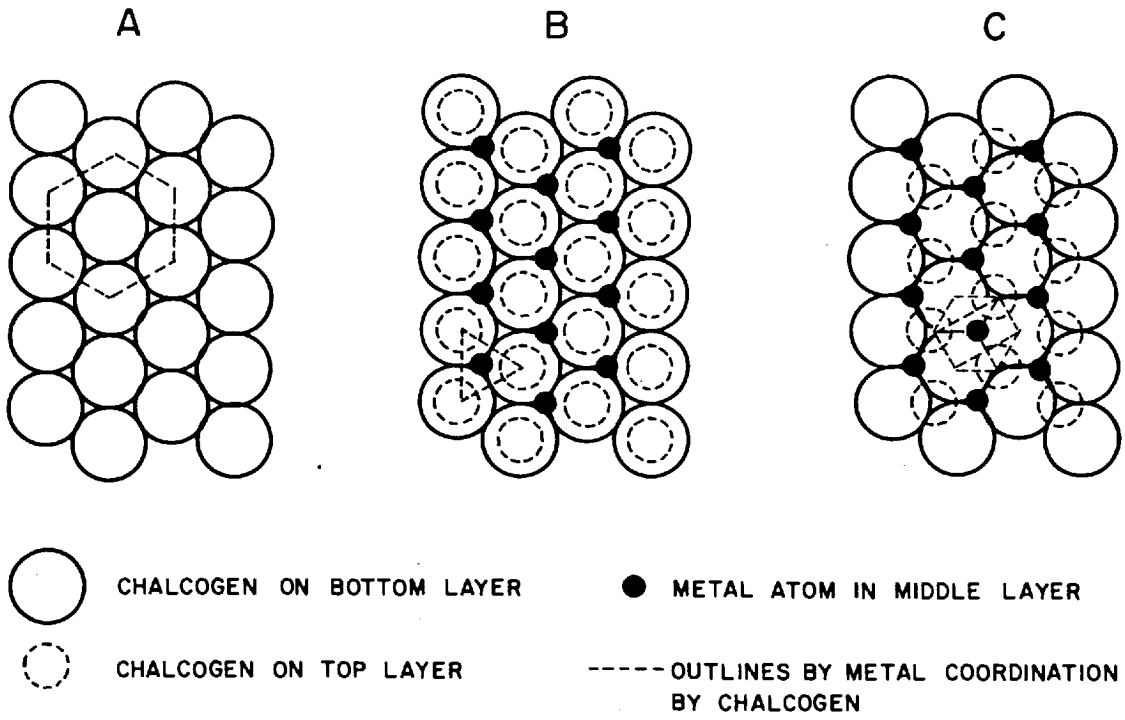


Figure (2.2)

The former choice results in a trigonal prismatic co-ordination of the metal by the chalcogen atoms Figure (2.3A) and the latter in an octahedral co-ordination of the metal Figure (2.3B).

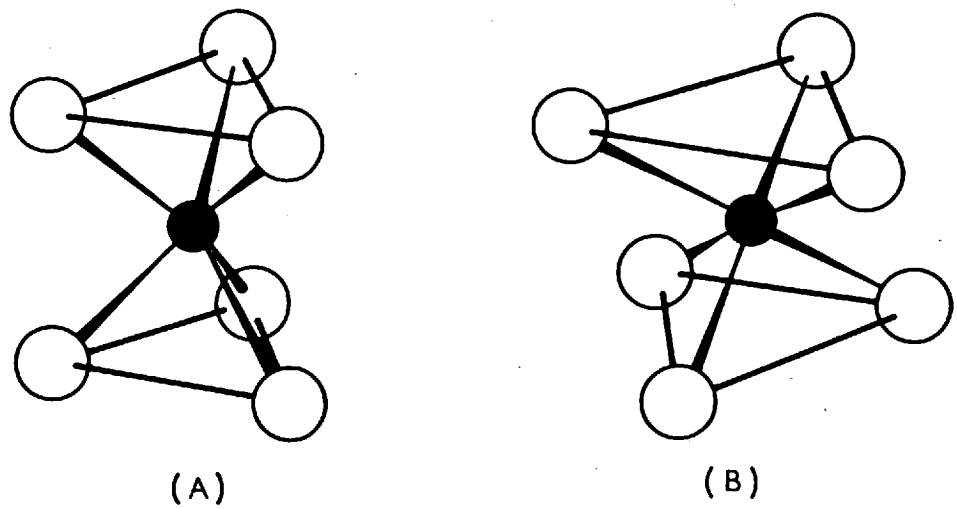


Figure (2.3)

From the above description it is clear that the atoms can only occupy three equivalent positions along the plane of the sheet: in other words all atoms lie on one of the three special sites whose fractional co-ordinates in the 2 dimensional hexagonal cell are: (0,0), ($\frac{1}{3}$, $\frac{2}{3}$) or ($\frac{2}{3}$, $\frac{1}{3}$). Conventionally these are denoted by the letters A, B or C.

It is noteworthy that the high symmetry octahedral co-ordination occurs in a wide variety of compounds while the lower symmetry trigonal prismatic co-ordination is relatively rare outside these materials. Part of the reason lies in the fact that octahedral co-ordination gives a close packed structure, while trigonal prismatic gives a lower density structure.

All the undistorted materials have centrosymmetric structures, and many of them exhibit polytypes with the following space groups at room temperature:

2.1.1 Octahedral co-ordination

The regular materials with octahedral co-ordination belong to this trigonal group. The metal atoms are situated at the position (0, 0, 0,) and the chalcogens at $\pm$ ($\frac{2}{3}$, $\frac{1}{3}$, z) where z (ideal) = $\frac{1}{4}$. This structure type is referred as the cadmium iodine structure and there is only one MX_2 sandwich per unit cell.

The stacking sequence is therefore AbC. The reason that this structure has trigonal rather than hexagonal symmetry

derives from the octahedral disposition of the chalcogens about the metal atoms.

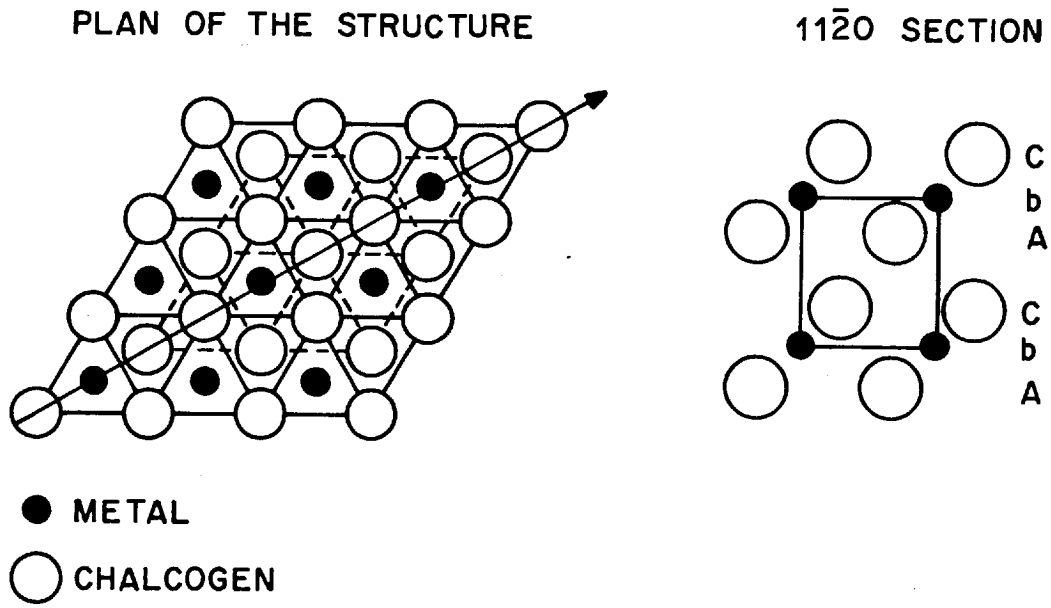


Figure (2.4)

2.1.2 Trigonal prismatic co-ordination

The regular materials with trigonal prismatic co-ordination belong to this group. There are two MX_2 layers per unit cell, and the two sequences assumed by the pure materials are both called 2H. These sequences are:

a) AbA CbC: here the metal positions are $\pm$ (0, 0, $\frac{1}{4}$) and chalcogen positions are $\pm$ ($\frac{1}{3}$, $\frac{2}{3}$, z) and $\pm$ ($\frac{1}{3}$, $\frac{2}{3}$, $\frac{1}{2}$ - z) where z(ideal)= 0.113. The difference between this structure and that of the octahedral materials lies in the disposition of the chalcogen atoms. It is this which gives a different symmetry and a two layer structure. The metal atoms in both case lie on a primitive hexagonal sublattice.

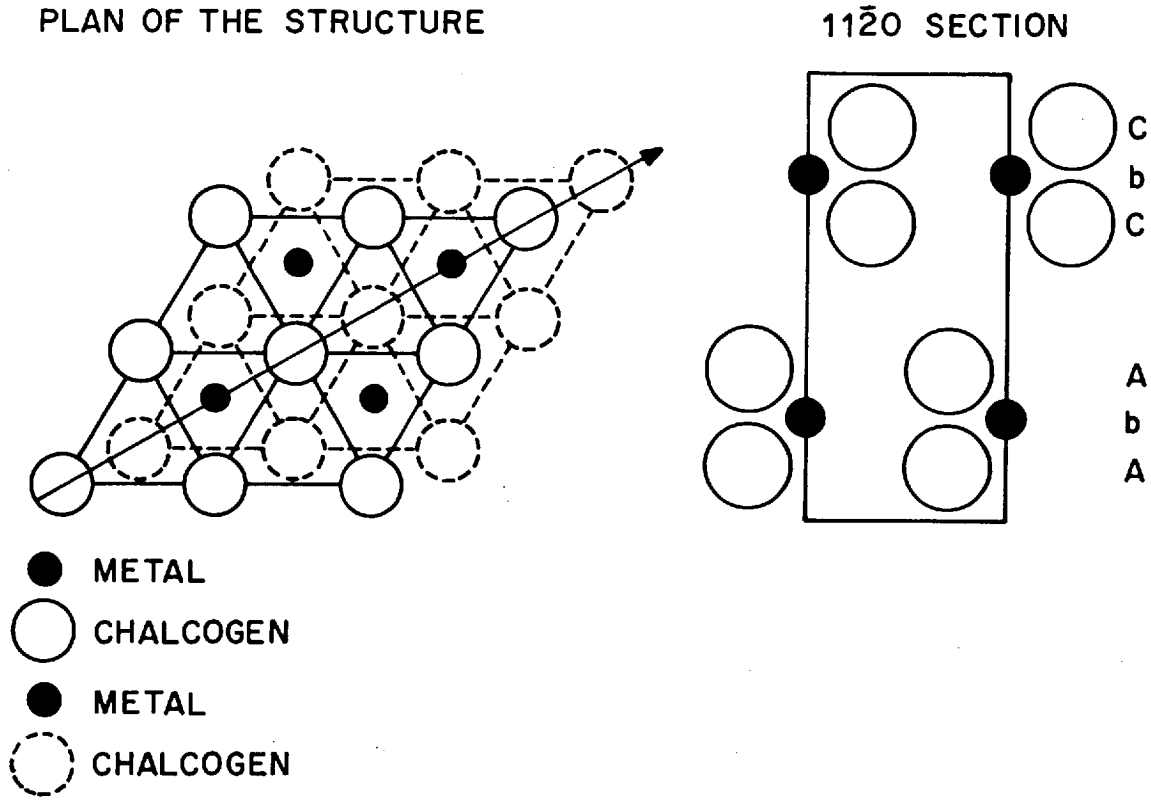


Figure (2.5)

b) AbA BaB the metal position are $\pm$ ($\frac{1}{3}$, $\frac{2}{3}$, $\frac{1}{4}$), and the chalcogen positions $\pm$ ($\frac{2}{3}$, $\frac{1}{3}$, $\frac{1}{2}$ - z), where again z (ideal) = 0.113.

It is worth noting that this is the first stacking sequence so far considered in which the metal atom position do not superimpose in successive layers. Crystal structures of 2H-TaS_2 and 2H-NbS_2 are based on stacking sequence (a).

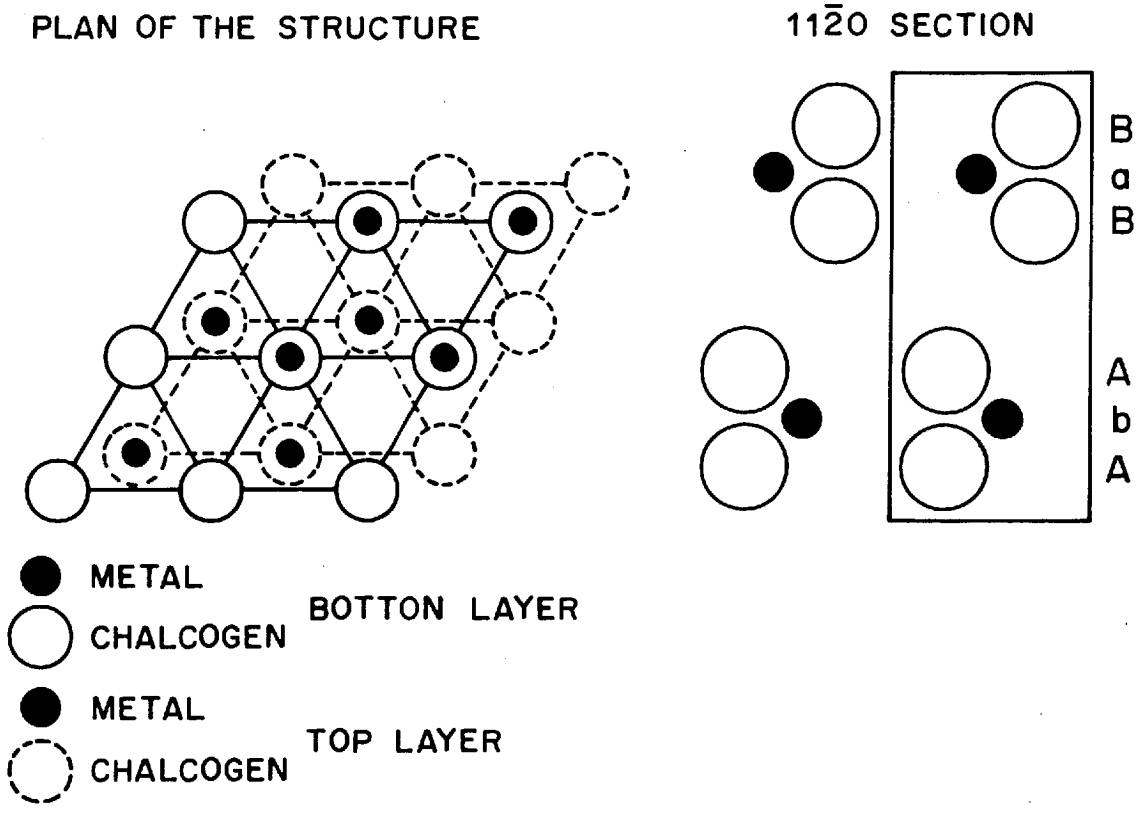


Figure (2.6)

The structure which has three MX_2 layers per unit cell, is designated 3R for the rhombohedral stacking sequence AbA BcB CaC. The metal atoms are trigonally co-ordinated. However, several four layered structures are observed; in one, (4Ha), all metals atoms are at the centre of a trigonal prism but in another, (4Hb), half have octahedral environments. By mixing up the layer symmetry and stacking order, many structures are possible but only a few other than those above have been observed, Figure (2.7) one of which is a random stacking phase (not shown in the Figure).

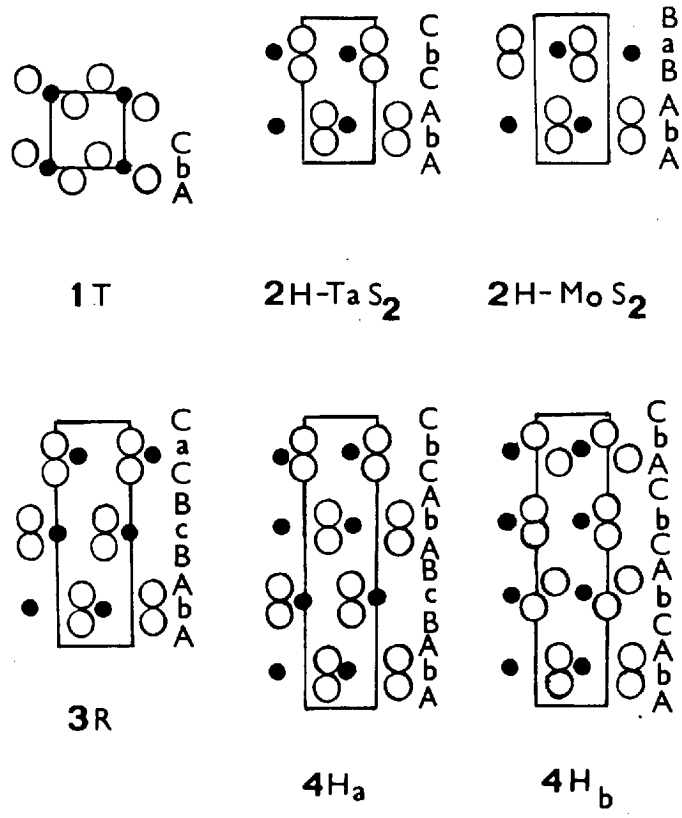

C b A
1T
C b C A b A
2H-Ta S2
B a B A b A
2H-Mo S2
C a C B c B A b A
3R
C b C A b A B c B A b A
4Ha
C b A C b C A b C A b A
4Hb

Figure (2.7)

CHAPTER 3

PREPARATION OF MATERIAL AND CRYSTAL GROWTH

3.1 Introduction

The direct synthesis of the dichalcogenides was the method used to obtain tantalum and niobium disulphides. The two elements were made to react directly and the desired products were obtained. The optimum temperature for the reaction is 950°C; it is therefore important to give careful consideration to the design of equipment to ensure complete reaction and avoid the possibility of an explosion.

For example, sulphur begins to react with tantalum and niobium at about 400°C which is close to its boiling point 441°C. The heats of reaction are large 150 - 200 Kcal/mol and the rates of reaction doubles every 10 - 20°C. The synthesis was made within a quartz tube and for design purposes the pressure within the tube had to be kept within 10 - 20 atmospheres. As the sulphur vapour pressure doubles every 50°C an inherent requirement of the preparative technique was that the temperature of the reacting elements rises very slowly.

An unexpected consequence of the experimental procedures adopted was that large single crystals of 1T-TaS_2 grew during the reaction. Single crystals of TaS_2 and NbS_2 were also grown by conventional vapour transport methods using ground single crystals in the case of TaS_2.

The transport method consists in using a chemical transporting agent (such as one of the halides) (Schaefer (1964), Nitsche (1967), Nitsche (1964), Nitsche (1962) and Nitsche (1961)) to produce a reaction.

$$MS_2 + 2Hal \rightleftharpoons M\,Hal_2 + 2S$$

The equilibrium constant K (T) increases with temperature for exothermic reactions and is usually small at the temperatures concerned. Polycrystalline MS_2 was placed in the hot end (T_1) of an evacuated quartz tube and crystals were grown in the cooler end (T_2), usually 50 - 200°C cooler. The MS_2 reacts with the transporting agent and all the products at these temperatures have relatively large vapour pressures or are gaseous. The concentrations of the products are determined by K (T_1), so that at the cooler end where K (T_2) is lower, the gas is supersaturated and crystals will nucleate and grow in that region.

The transporting agent must be chosen so that it will not only react with the sample at the transporting temperature to give volatile or gaseous products, but also so that upon cooling, the original MS_2 and transporting agent are reformed. The transporting agent should not permanently react with the material to be transported. For example, I_2 is reported to be a good transporting agent for TaS_2 above 700°C, but Br_2 reacts permanently to give TaS_yBr_x compounds. Other transporting agents that have been used include halides, chalcogenides, volatile halide salts, ammonia, water, hydrogen halides and some mixtures of these.

The number of crystals nucleated along the line of the temperature gradient increases with transport rate which itself increases with the tube diameter, the concentration of transport agent, the temperature difference (ΔT), the mean temperature, and in some cases the transporting agent.

All the successful intercalation described in this thesis involved the 2H form of TaS_2 and the transformation from the 1T form was carried out by heating the material to 550°C. This phase change involves a considerable increase in volume of the unit cell (1.5%) because the stacking sequence and co-ordination are changed from AbC to AbACbC shown on section 2.1.1 and 2.1.2. Stresses are built up during the phase transformation which makes it difficult to obtain good crystals of 2H-TaS_2 by this method. However attempts to grow the 2H-TaS_2 phase directly at 500°C have not been very successful either. In NbS_2 the 2H polytype forms directly so the problem is avoided.

3.2 Experimental Equipment and Procedures

3.2.1 Materials

Two sources of the metals were used: Ventron Alpha Inorganics Inc. and Koch Light Laboratories Ltd. The first supplied purity of 99.9999992% at 325 mesh for niobium and 99.9% at 325 mesh for tantalum, the second supplied purities of 99.9% for niobium and 99.7% for tantalum.

The sulphur used was supplied by Koch Light Laboratories

Ltd., and has a purity of 99.9999%.

3.2.2 Procedure to form the dichalcogenides

The vacuum line was designed to provide 10^{-8} torr to four quartz tubes in which mixtures of transition metal and chalcogen could be degassed and sealed under vacuum at 10^{-5} torr. The quartz tube was a single piece with a 14-23 ground quartz joint and a constriction. The internal diameter of the quartz tube was 13 mm, the wall thickness 1 mm and the length was approximately 35 cm.

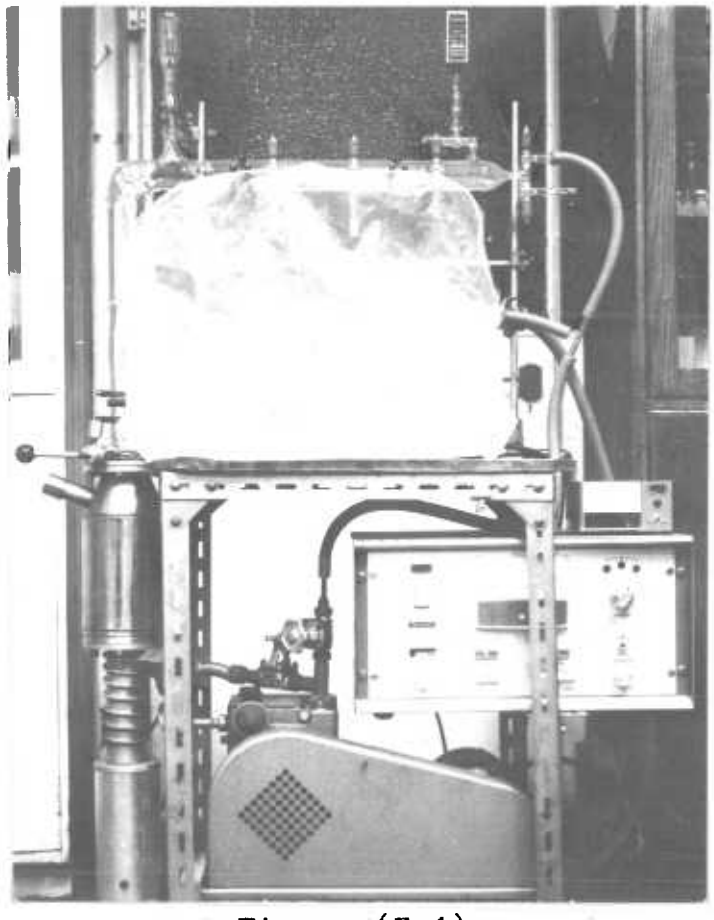


Figure (3.1)

Special attention was given to the design to allow a polyethylene glove bag to surround the four quartz tubes (compare Figure (3.1) with Figure (3.2) and notice the

position of the glove bag). The glove bag could be removed to seal the tubes, or it could be filled with pure argon so that the mixed powders could be transferred in an inert atmosphere. This ensured that oxygen was not present inside the quartz tube when they were sealed.

Special attention was also paid to certain aspects of experimental techniques to minimize the possibility of explosion: thus the constriction where the tube was going to be sealed off, was first cleaned with cotton wool in order to remove tantalum and niobium and so prevent them reacting with the quartz during sealing and thus causing weakness at that point.

After some preliminary experiments the following temperature programme was established for all the compounds prepared. After rapid heating to 350°C in about one hour, the temperature was then increased by 130°C per day for 5 days until the reaction temperature of 950°C was reached. At this reaction temperature of 950°C the reactants, one vapour and the other in solid state, were left for a week to complete the reaction. The tubes were extracted and then rapidly quenched by leaving them to cool at room temperature. In the case of TaS_2 the metastable 1T phase was produced while for NbS_2 the stable 2H form was produced directly.

3.2.3 Vacuum line design and construction

A rotary vacuum pump (Speedivac Edwards Ed 150), was

connected via a valve and a flexible hose to a water cooled oil diffusion pump (Edwards F203), on top of which were screwed a liquid nitrogen cold trap and butterfly valve model QSB2. One "L" shaped glass line, 5 cm. inside diameter, was connected with the butterfly valve using a "o" ring flange arrangement (the "L" shaped glass line can be identified in the photograph of Figure (3.2)).

The L-shaped glass tube had four teflon seal high vacuum valves and 14-23 male joints where the quartz tubes were going to be connected. These valves leak at 10^{-8} torr. A 14-23 female ground joint for the Pirani gauge and a ground joint for the Ionization gauge head were also attached, as shown in Figure (3.2). Apiezon "L" grease with vapour pressure of 10^{-10} torr was used on all ground glass joints.

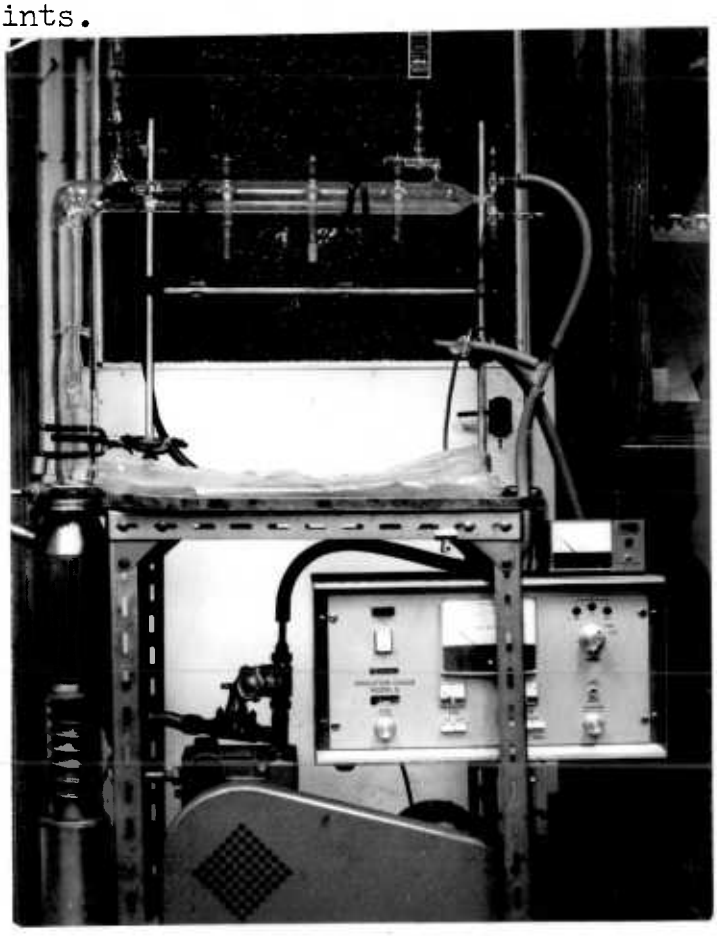


Figure (3.2)

The Pirani gauge model G6B was connected to the Vacuum Generators electronics Pirani unit model P1R1, while the Ionization gauge (model 164M) was driven by the Edwards model 5 Ionization gauge vacuum meter.

In a typical run the four quartz tubes were connected to the glass line via the male ground joints, which were previously coated with apiezon "L" grease. The complete system was roughed out by the mechanical pump by opening the butterfly and teflon seal valves.

The vacuum was monitored with the pirani gauge. The diffusion pump was switched on and was left heating, after about 30 minutes the filament and cathode of the Ionization gauge were degassed. The pressure was then monitored with the Ionization gauge. Two days of continuous pumping were necessary to reach 10^{-8} torr. Before transferring the mixed and weighted powders to the quartz tubes, the glove bag was filled and purged 3 times with argon. After the transfer of the mixed powders, the vacuum system was pumped down and the glove bag removed. When the vacuum reading was below 10^{-7} torr the quartz tubes were sealed using a methane-oxygen torch.

3.2.4 Furnace design and construction

Two types of furnaces were made: one was used to react the chalcogen with the transition metal, and the other permitted the dichalcogen crystals to be grown by vapour transport method.

The desired characteristics of the reaction furnaces were their temperature stability and the capability to increase the temperature by 130 centigrades degrees a day.

The reaction furnace was constructed using a sintered alumina tube (Thermal Syndicate Ltd.) 2" nominal diameter (5.0 cm. ID x 5.9 cm. OD) and 45 cm. long. The alumina tube was wound with about 60 turns of Kanthal wire, 0.048" diameter. The total electrical resistance was 1.25 ohms.

Temperature control was achieved by using a Resistance Thermometer Temperature Controller (Associated Electrical Industries Ltd.). The controller was a fully proportional temperature controller giving precise control of temperature in the range 0-1200^{o}C. It was designed to operate in conjunction with a platinum resistance temperature sensor whose nominal resistance was 10 ohms at 0^{o}C. Such a thermometer was constructed of 0.125 microns diameter platinum wire wound non inductively, supported on a sintered alumina rectangle 2.5 cm. x 1.2 cm. and covered with asbestos paper. The temperature sensing device was placed in thermal contact with the electrical heated alumina tube.

The temperature of the reaction furnace when being controlled by the platinum resistance thermometer, was measured independently by a chromel-alumel thermocouple and a Coprico Thermocouple Potentiometer type P6. A graph showing the variation of temperature with the

setting of the 20-turn helical potentiometer, is shown in Figure (3.3).

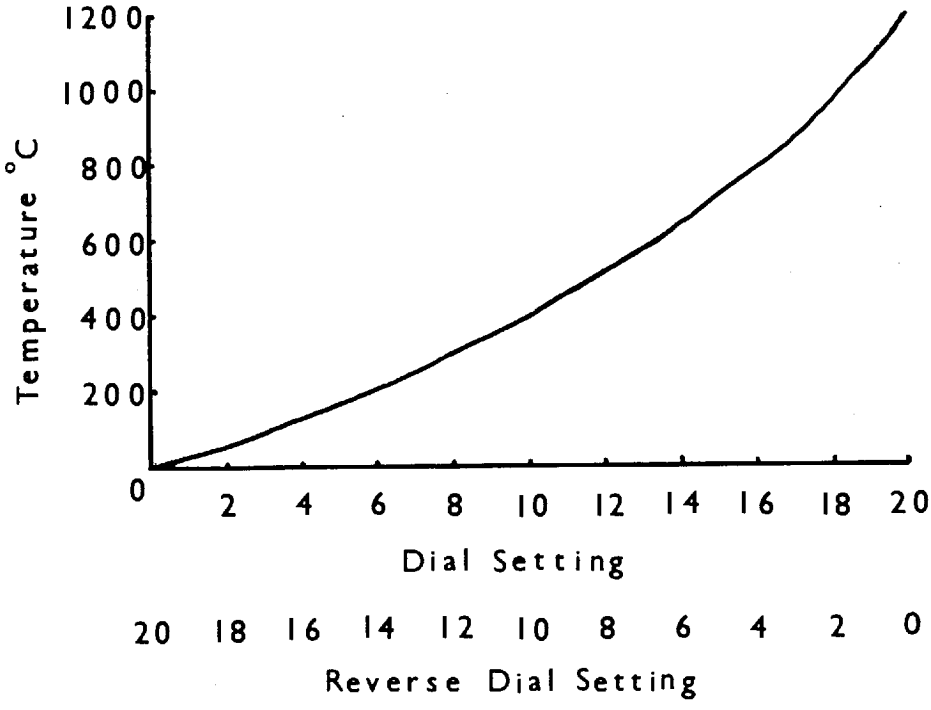


Figure (3.3)

As explained in the introduction it was essential to have a continuous and very slow increment on the temperature and this was achieved by slow rotation of the temperature setting knob of the 20-turn helical potentiometer on the AEI controller.

Two synchronous motors were used in series. One, rotating at 2 revolutions an hour, switched on and off the other (8 revolutions a day) by means of a microswitch. The programme to switch on and off the second motor involved a cam driven by the first motor whose circumference was shaped to an appropriate profile. The profile cam switched on the other synchronous motor for just 15 minutes in every

hour. Hence the second synchronous motor just made two revolutions in 24 hours corresponding to 100 - 150°C a day Figure (3.4).

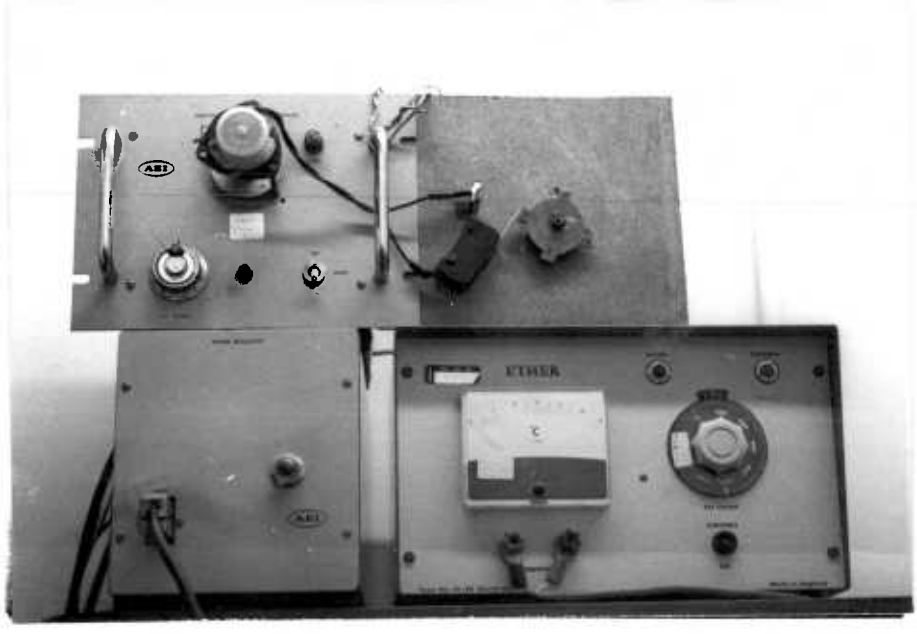


Figure (3.4)

As assembled, the 20-turn helical potentiometer of the AEI Resistance Thermometer Controller was set to increase the temperature of the furnace by a clockwise rotation. The second synchronous motor rotated the knob in an anti-clockwise direction and hence the connections to the potentiometer were interchanged in order to obtain continuous heating.

The furnaces used to grow crystals by the vapour transport method were basically gradient zone furnaces. The gradient zone effect was achieved by having two independent furnaces beside each other. Kanthal tape (1/16 x 0.0056" and 2.07 ohms/foot) was wound around an alumina tube (5.0 cm. ID x 5.9 cm. OD and 77.5 cm. long) to form two heaters of 130 turns each, over each half of the tube.

Each section of the furnace was controlled independently by a Eurotherm type 070-071 temperature controller. The temperature sensing transducer a chromel-alumel thermocouple was set at the middle of each furnace. The Figure (3.5) shows a view of the furnaces.

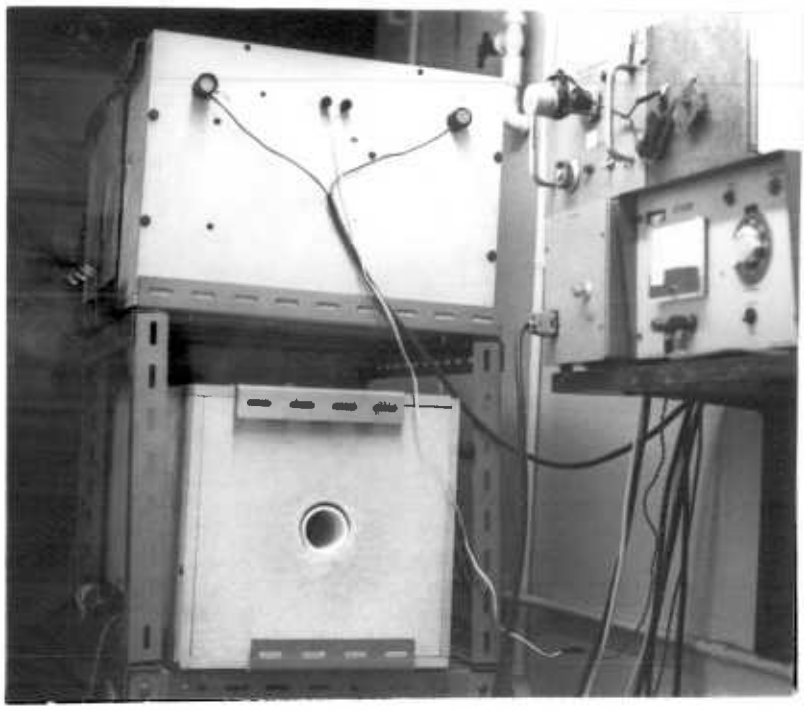


Figure (3.5)

The furnace temperatures were measured independently with chromel-alumel thermocouple as before. The temperature profile of the gradient zone furnace was checked by slowly moving the thermocouple through the middle part of the furnace and measuring the distances corresponding to temperature intervals of 10 degrees. The plot of those points is shown in the Figure (3.6) and was used to locate the position inside the furnace of the quartz tube in which the vapour transport crystallization was made.

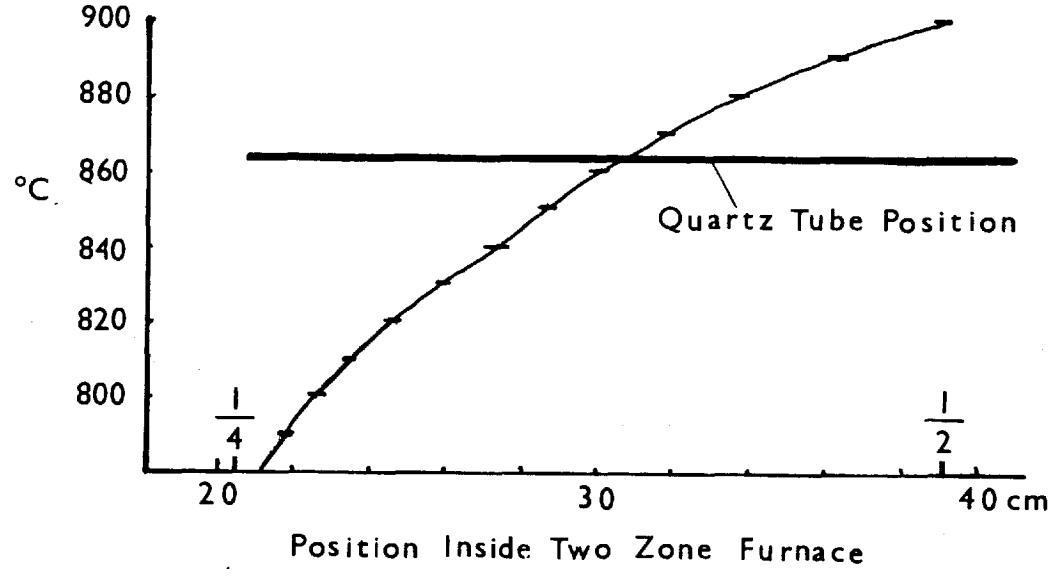


Figure (3.6)

During an experimental run, the recommendations of Di Salvo (1971) were followed. The temperature difference between the two sections of the furnace, ΔT, was set at about 100°C and the iodine concentration was made to be about 5 mg/cm^3. The iodine was handled in the dry atmosphere inside the glove bag. It was weighed on a small quartz spring balance whose scale was calibrated at intervals of 10 g. After the iodine had been inserted into the quartz tube containing the dichalcogenide, the tube was attached to the vacuum line. The glove bag was then removed. The quartz tubes were also sealed using a methane-oxygen torch.

3.3 Results and Discussion

One of the unexpected results of these experiments to prepare material for intercalation, was that the best

single crystal of 1T-TaS_2 but not NbS_2 were prepared during the reaction at 950°C and not by the iodine vapour transport mechanism. During preliminary experiments in growing TaS_2 it was found that a small amount of sulphur remined at the bottom of the tube. A small excess of sulphur was therefore added with the intention of shifting the equilibrium towards stoichiometry in good agreement with the finding of Saito (1977). The result was a beautiful crop of metallic yellow 1T-TaS_2 crystals Figure (3.7).

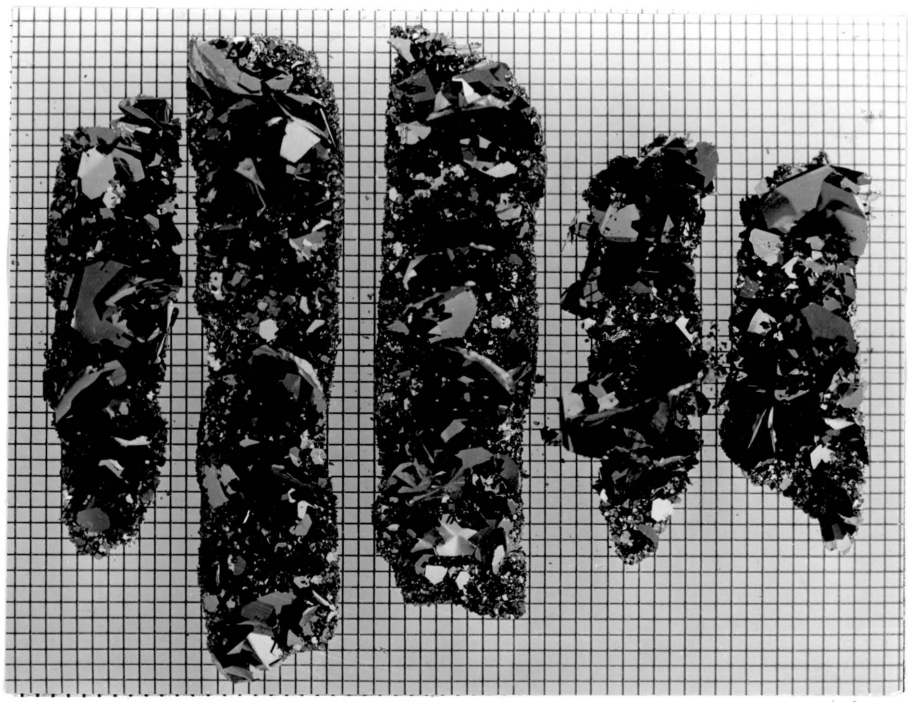


Figure (3.7)

However, when attempts were made to transform these crystals to 2H-TaS_2 at 550°C for 4 days, the transformation was accompanied by the formation of a micro-crystalline filamentous web of TaS_3. This was presumed to be due to the excess sulphur and the effect completely disappeared when excess sulphur was deposited as droplets on the top of the tube (away from the crystals) during cooling. This cooling was done by placing a cold object on the tube

while it was cooling. It was then possible to remove the crystals from the tube and seal them into a Pyrex tube before placing them in the oven to transform to 2H.

The best 2H-TaS_2 crystals were obtained in this way, so it was concluded that the excess sulphur was generally beneficial to the crystal growth process: there was no evidence that the resulting crystals were non-stoichiometric. It is believed that the excess of sulphur acted as a transporting agent, the sulphur was reacting with the tantalum and at the same time helping the crystals to grow. TaS_3 is a volatile substance at the reaction temperature. From the reaction

$$TaS_2 + S_g \rightleftharpoons TaS_{3_g}$$

it can be seen how the excess sulphur can explain the large crystals obtained, because it worked as a transporting agent. The presence of TaS_3 microcrystals as a web can be explained also by the same reaction because the right hand side of the equation is favoured at lower temperature. Hence this equation is a vapour transport equation.

NbS_2 was also reacted and the crystals obtained were not as big and perfect as in the case of TaS_2. In this case no transformation was necessary because 2H-NbS_2 is the stable form after quenching.

$NbSe_2$ and $TaSe_2$ were also reacted but unfortunately the furnace controller failed and the temperature inside rose

to 1200°C. The quartz tubes deformed and broke due to the internal pressure and oxidation of the products occurred. It must be remembered that fused quartz softens around 1200°C.

Both TaS_2 and NbS_2 were successfully grown inside the gradient zone furnaces but the quality of the crystals obtained was poorer than those obtained directly after the synthesis and they were not used for intercalation experiments.

CHAPTER 4

INTERCALATION OF SN COMPOUNDS

4.1 Introduction to Chemistry of S_4N_4

In 1835 it was found that reaction between sulphur monochloride and ammonia gave a compound which contained only sulphur and nitrogen; but it was not until 1850 that the exact composition of this compound was worked out, and not until 1896 that a determination of the molecular weight gave the formula S_4N_4. Tetrasulphur tetranitride, S_4N_4, is a solid at room temperature. It forms orange-yellow crystals of the class C_{2h} and space groups $P2_1/n$. It is diamagnetic and strongly endothermic, the melting point is 178°C, (Goehring 1956).

There are three convenient methods for the preparation of S_4N_4: by reacting ammonia or ammonium chloride with sulphur chlorides and by disproportionation of sulphur in liquid ammonia.

It has been shown that hydrolysis of tetrasulphur tetranitride always gives ammonia or ammonium ions as well as sulphur oxyacids, which is in good agreement with the fact that the electronegativity of nitrogen is greater than that of sulphur. In weakly alkaline solutions the hydrolysis occurs according to the reaction

$$2S_4S_4 + 6(OH^-) + 9\ H_2O \rightarrow 2S_3O_6^{2-} + S_2O_3^{2-} + 8NH_3$$

whereas in strong alkaline solutions the reaction proceeds according to

$$S_4N_4 + 6(OH^-) + 3H_2O \rightarrow 2SO_3^{2-} + 4NH_3$$

The result of the hydrolysis is typical of a substance in which sulphur has the oxidation number -3, as this can then easily undergo dismutation, half into S^{2-} and half in S^{4-}.

The structure determination leads to the molecule shown in the Figure (4.1). The nitrogen atoms are coplanar while the sulphur atoms are alternately above and below the plane, being situated at the corners of a tetrahedron.

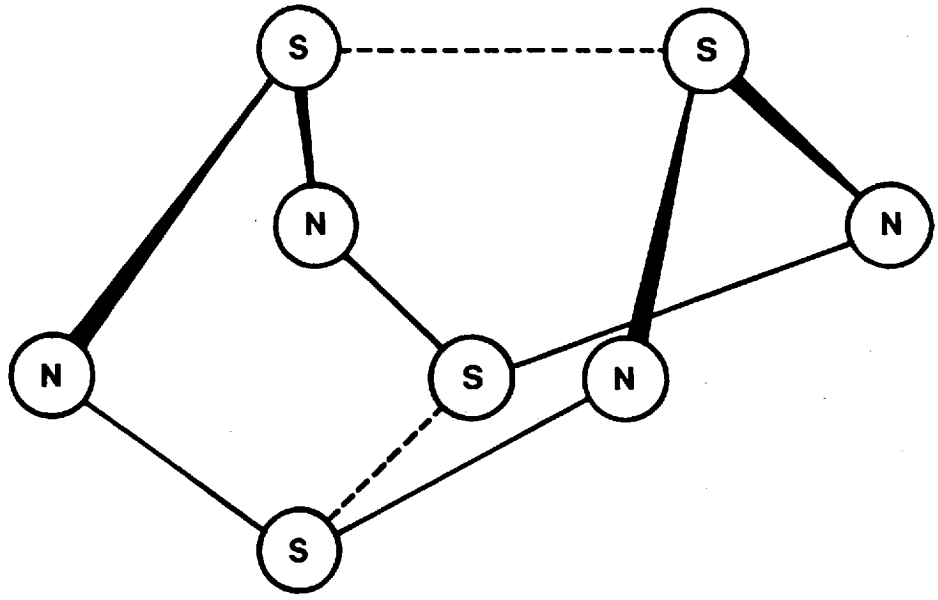


Figure (4.1)

4.1.1 Disulphur dinitride S_2N_2 and polysulphurnitride $(SN)_x$

The ring system of tetrasulphur tetranitride can be cleaved easily. If one heats S_4N_4 vapour to 300°C/0.01 torr and

cools the issuing gases strongly, one obtains an easily volatile white solid, soluble in organic solvents, with the formula S_2N_2. The disulphur dinitride is stable only at low temperatures. Even at room temperature it polymerizes to a substance $(SN)_x$, which is brass-coloured in massive quantities but dark blue in thin layers, insoluble in organic solvents and decomposes if attempts are made to dissolve it in other solvents.

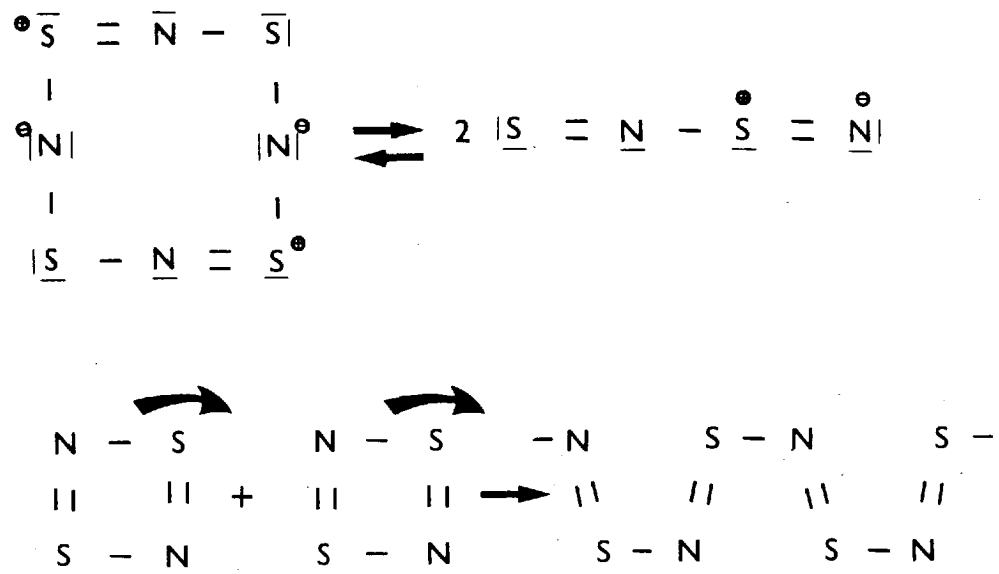


Figure (4.2)

The polysulphur nitride which is formed by the previous reaction, figure (4.2), is diamagnetic, forms fibre like crystals with metallic sheen, and shows the remarkable property of becoming superconductor at $0.3^{o}K$ (Walatka et. al. 1973),(Greene et. al. 1975) and (Greene et. al. 1975).

If one considers the compounds $(SN)_2$, $(SN)_4$ and $(SN)_x$, one sees that with increasing molecular weight the number of limiting valence formulae required for complete description of the electronic state of the compound is increased. Increasing this way the possibilities for resonance, that deepens the colour. It also stabilizes the compounds: disulphur dinitride is very sensitive to shock and decomposes explosively into its elements above 30°C; tetrasulphur tetranitride is sensitive to shock and also decomposes explosively when heated rapidly to above 130°C; polysulphurnitride, so far as is known, is non-explosive on shock or when heated.

4.2 Reactions of Tetrasulphur Tetranitride with Ammonia and with Alcohols

Cleavage of the tetrasulphur tetranitride ring system into two molecules of disulphur dinitride can be effected not merely by heat but apparently also by many chemical reactions. This occurs, for instance, on treatment with ammonia or with alcohols. Tetrasulphur tetranitride and ammonia give an ammoniate $S_2N_2 \cdot NH_3$. In a similar reaction, disulphur dinitride gives an ammoniate $S_2N_2 \cdot NH_3$. From the X-ray diffraction patterns and the absorption spectra, it now appears that these two ammoniates are identical (Gesierich 1954). The volatile disulphur dinitride can be sublimed from these ammoniates even at room temperatures, so it must be assumed that tetrasulphur tetranitride is cleaved during its reaction with ammonia. Figure (4.3).

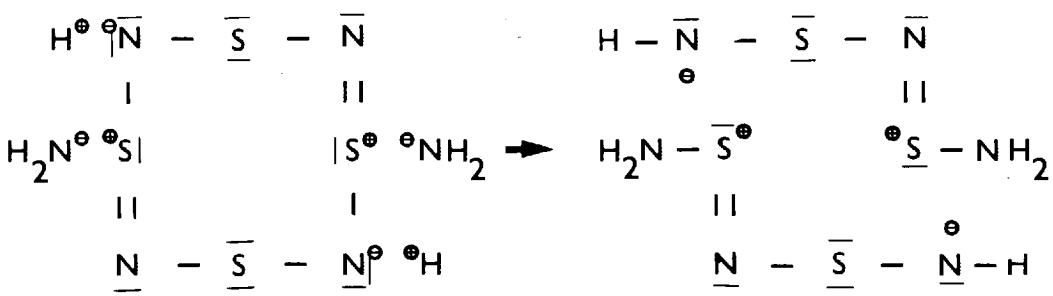


Figure (4.3)

In liquid ammonia this ammoniate behaves as a normal inorganic acid amide and is a proton donor. Accordingly a solution of the ammoniate in liquid ammonia conducts electricity. The fission of the ammoniate (I) into an imide (II) of sulphoxylic acid as well as an imide (III) of the orthosulphurous acid (Figure 4.4) can occur spontaneously in ammonia solutions.

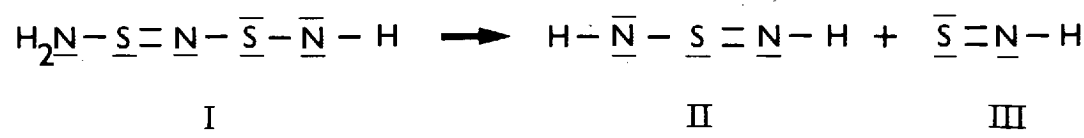


Figure (4.4)

The reactions of disulphur dinitride and tetrasulphur tetranitride with alcohols are analogous to those with ammonia. Formation of a product analogous to the compound (I) can be demonstrated by means of the absorption spectra of the solutions (Gesierich 1954).

Tetrasulphur tetranitride is readily reduced to tetrasulphur tetraimide $S_4N_4H_4$. This tetrasulphur tetraimide crystallizes as colourless needles of the class C_{2h}, the melting point is 152°C. The oxidation number of the sulphur in $S_4N_4H_4$ is + 2 and since the infrared spectrum clearly shows NH frequencies but not SH frequencies, the formula of Figure (4.5) is firmly established (Lippincott and Tobin 1951).

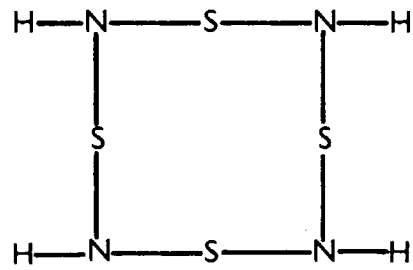


Figure (4.5)

4.3 Preparation of S_4N_4 Tetrasulphur Tetranitride

The S_4N_4 used for intercalation experiments was prepared by two methods. The first one (Becke-Goehring 1960 and Villena-Blanco 1967) uses the following reactions:

$$6SCl_2 + 16NH_3 \rightarrow S_4N_4 + 2S + 12NH_4Cl$$
$$6S_2Cl_2 + 16NH_3 \rightarrow S_4N_4 + 8S + 12NH_4Cl$$

from which it is easy to understand the necessity of a stream of chlorine to transform the monochloride to dichloride by the reaction:

$$S_2Cl_2 + Cl_2 \rightarrow SCl_2$$

The second method used for preparation of S_4N_4 (Jolly and Becke-Goehring 1962) made use of the following reaction:

$$6S_2Cl_2 + 4NH_4Cl \rightarrow S_4N_4 + 8S + 16HCl$$

and was adapted to prepare small quantities of S_4N_4 with 99% isotopic concentration of nitrogen 15.

4.3.1 Method 1

Carbon-tetrachloride and sulphur dichloride were added to a three necked flask into which were inserted a paddle stirrer, a gas inlet and a thermometer. While stirring the mixture briskly the ammonia was passed as rapidly as possible but without causing material to splash from the flask or allowing the temperature of the reaction mixture to rise above 50°C.

After approximately 2 hours, the reaction stopped and the entire mixture turned a "golden poppy" colour. The ammonia flow was then stopped.

The reaction mixture was filtered through a large sintered glass or Buchner funnel and the damp solid material was vigorously shaken with 1 litre of water for 5 to 10 min.

The remaining solid was filtered off and allowed to dry thoroughly for 2 days.

The dry material was placed in an extraction thimble and

extracted with dioxane in a Soxlet extractor until the eluate was only weakly coloured orange-yellow. Sufficient dioxane was used so that there was no possibility of concentrating the solution in the pot so much that the extracted S_4N_4 would decompose. Tetrasulphur tetranitride will explode if heated in a dry flask. When the eluate cooled to room temperature, some of the S_4N_4 crystallized out. This material was filtered off and dried in air. The filtrate was evaporated to dryness at a temperature lower than 60°C. The residue from the evaporation was recrystallized from hot benzene to remove sulphur. S_4N_4 with a melting point as high as 170°C has been obtained. The infrared spectrum of S_4N_4 given by (Lippincot and Tobin 1953) was compared with one obtained using a synthetized S_4N_4, checking with the data reported.

4.3.2 Method 2

The second method used for preparation of S_4N_4 (Jolly and Becke-Goehring 1962) made use of the following reaction:

$$6S_2Cl_2 + 4NH_4Cl \rightarrow S_4N_4 + 8S + 16\ HCl$$

The method was developed to work with large quantities of NH_4Cl, about 800 g. of 1 g. pellets, and had the advantage that very little attention need to be given to the apparatus during a run. Also, a minimum of solvent manipulation was required.

The reaction was carried out by passing a stream of air and S_2Cl_2 vapour through hot ammonium chloride pellets. The exit gases passed through an air cooled condenser, wherein a purple-brown solid deposited. This solid was S_4N_4, sulphur and ammonium chloride, together with smaller amounts of $S_3N_2O_2$. Figure (4.6) shows the apparatus used for this synthesis. The S_4N_4 was isolated by extraction of the purple-brown solid by refluxing with dioxane followed by a recrystallization from hot benzene.

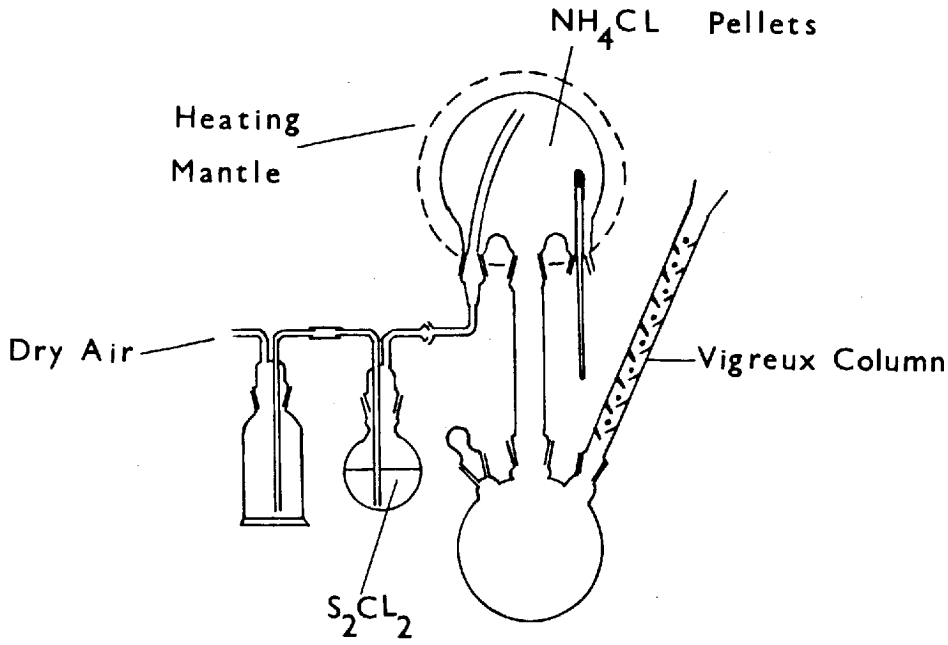


Figure (4.6)

During the intercalation experiments there was a need to distinguish between an N and a CH_2 group, which have the same atomic mass, and then it was thought to adapt this second method to work with 1 gram of NH_4Cl instead of 800 grams in order to be suitable to prepare small quantities of S_4N_4 with the isotope nitrogen 15 instead of

the common nitrogen 14.

The modified apparatus used to prepare S_4N_4 with nitrogen 15 is shown in Figure (4.7).

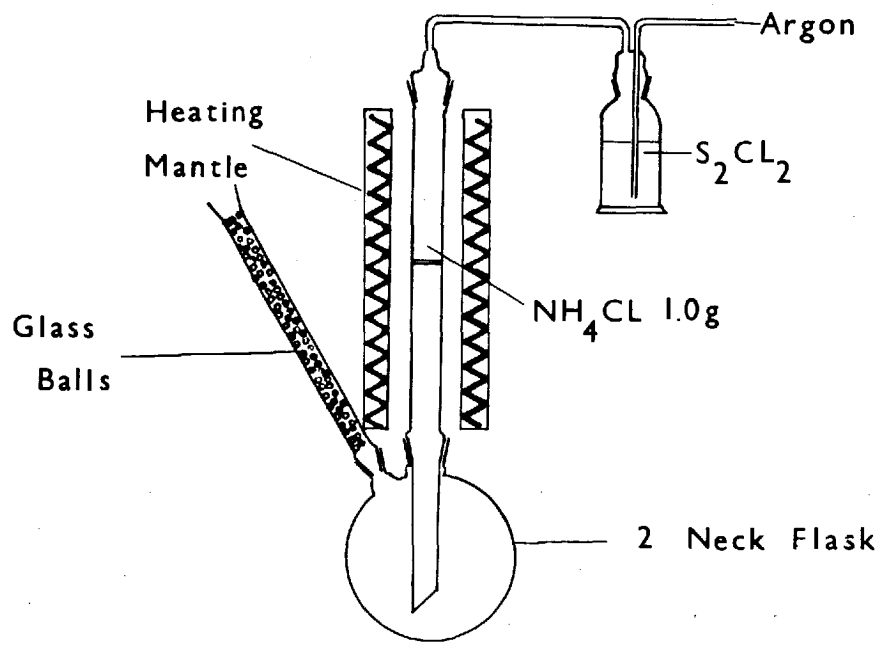


Figure (4.7)

The sulphur monochloride (S_2Cl_2) was carried by a current of argon instead of dry air because oxygen in the air would give rise to $S_3N_2O_2$ (trisulphur dinitrogen dioxide), an undesirable impurity that may have reduced the yield. The argon was bubled through a vessel containing S_2Cl_2 and the vapour was passed over NH_4Cl heated to 170-175°C. A sintered porous glass disc at the midpoint of the tube functioned as a support for the NH_4Cl powder. The reaction products passed through the sintered porous glass disc into a 2 neck 500 ml. flask. A packed column with 5 mm. glass balls was attached to the other neck.

In a typical run, the gram of NH_4Cl was slightly compressed against the sintered glass disc. Some argon was bled through the system to flush out any oxygen present and at the same time the temperature of the NH_4Cl was increased to 170°C. The argon was bubbled through the container of S_2Cl_2 and the mixture of S_2Cl_2 vapour and argon passed into the reaction vessel. A brown-purple mist began to fill the flask and the packed-column. The flow rate of 500 cc/min and the optimum temperature of 170-175°C recommended by Jolly and Becke-Goehring (1962) were used with excellent results. A time of 12 hours was needed to react one gram of NH_4Cl completely.

The product was refluxed with dioxane, dried at room temperature and recrystallized from benzene giving a product with a melting point of 170°C.

The experimental procedure was tested using ordinary NH_4Cl and found to work.

Using this adapted method, one gram of ammonium chloride nitrogen 15 (99% isotopic concentration) from Merck Sharp and Dohme Limited yielded 400 mg. of tetrasulphur tetranitride nitrogen 15.

The samples were taken to Dr. Waight, Chemistry Department, Imperial College, who very kindly performed the mass spectrometry on them. Mass spectrometry of the S_4N_4 prepared with enriched NH_4Cl nitrogen 15 gave the following results:

TABLE 4.1

Chemical identification	Mass number	Chemical identification	Mass number	Chemical identification	Mass number
		N_2^{15}	30	N_2	28
S	32	$S\ N^{15}$	47	SN	46
S_2	64	$S_2N_2^{15}$	94	S_2N_2	92
S_3	96	$S_3N_3^{15}$	141	S_3N_3	138
S_4	128	$S_4N_4^{15}$	188	S_4N_4	184
S_5	160	$S_4N_2^{15}$	158	S_4N_2	156
S_6	192	$S_3N_2^{15}$	126	S_3N_2	124
S_7	224	S_3N^{15}	111	S_3N	110
S_8	256	S_2N^{15}	79	S_2N	78

the corresponding mass difference due to the difference in mass of the two nitrogen isotopes was observed and enabled the number of nitrogen atom in the molecular fragments to be confirmed. The molecular fragment S_4N_3 were looked on both spectra (the $S_4N_4^{15}$ and S_4N_4) and not found.

4.4 Intercalation Experiments with SN Compounds

The experiments with SN compounds were conceived as an alternative route to the experiments by Che-Hsiung Hsu et. al. (1973) of intercalating $SN)_x$ into TaS_2. These authors report their findings as follows:
"By heating 4H-TaS_2 in a sealed tube with $SN)_x$ at 135°C the lattice expands by 3.4 Å and a Tc of 3°K is observed."

The study of the reported chemistry of SN compounds suggested that there may be another way to intercalate SN polymer, mainly to intercalate say S_4N_4 and then attempt to polymerize to $SN)_x$ in situ.

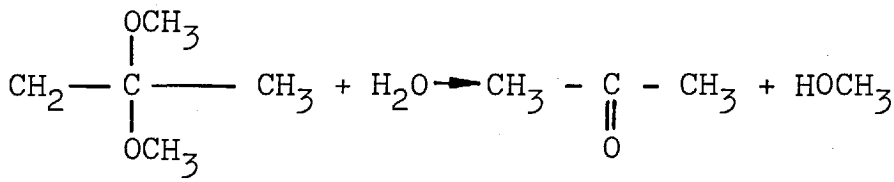
The first experiments were made with a S_4N_4 sample kindly given to us by Dr. A.D. Joffe of the Cavendish Laboratory, Cambridge. In these experiments a solution of S_4N_4 in benzene was boiled with both powder and single crystals of 2H-TaS_2 for different intervals of time, up to one month. In all cases, the results were negative, no intercalation could be detected by X-ray diffraction methods. The next step was to try to cleave S_4N_4 with NH_3 and alcohols. When liquid NH_3 was used, the S_4N_4 and TaS_2 were sealed inside a glass tube with an amount of solid NH_3, that had been previously frozen inside the tube. When allowed to warm up to room temperature, the ammonia as mentioned in section (4.2) reacted with the S_4N_4 to form the ammoniate $S_2N_2 \cdot NH_3$. The tube was left inside a metallic box just in case of an explosion because the vapour pressure of NH_3 at 20°C is 10 atm. The time allowed for the intercalation reaction was one week. Some control samples were also prepared with S_8 and pure ammonia. The results of these experiments were that the X-ray powder diffractograms of the product and of the control sample prepared with ammonia were identical and the conclusion was that only NH_3 had intercalated.

The reaction of S_4N_4 with alcohols yielded the formation of a $S_2N_2 \cdot HOCH_3$ by cleaving the S_4N_4 ring, as mentioned in section (4.2). In this case the TaS_2 powder, S_4N_4 and an

alcohol (methyl-, ethyl-, propyl- or amyl-alcohol) were boiled and stirred in a flask with water condenser for long periods of time, up to a month.

The intercalation processes were followed with the powder diffractometer. In all cases, the powder was decanted and mounted on the sample holder, a diffractogram taken and the powder was then put back until intercalation was completed. Complete intercalation showed only a 3 Å expanded gap corresponding to ammonia intercalation.

It was then thought that perhaps the water in solution was causing the formation of ammonia and which was subsequently intercalating. In order to prevent such a reaction 2, 2 dimethoxy propane was added to the mixture of S_4N_4 and alcohol. 2, 2 Dimethoxy propane, or DMP, is a reagent commonly used to dry solutions of methyl alcohol because it reacts with water to produce acetone and methyl alcohol.



When DMP was added to prevent water reacting with the mixture of S_4N_4, methyl alcohol and TaS_2 the increment in the van der Waals expanded gap was 3.4 Å and then it was thought SN was intercalated. But, it was observed that if DMP, S_4N_4, and TaS_2 were reacted without alcohol the same result was obtained and the increment on the gap was indistinguishable from that in the previous experiment. A blank run was made with DMP and TaS_2 alone to see if DMP was intercalated: there was no evidence of any reaction

even after three weeks.

At this stage of the research two TaS_2 intercalated samples were sent for mass spectrometry. These two samples were the product of intercalation of S_4N_4 + methyl alcohol and S_4N_4 + ethyl alcohol. The spectra showed very clearly sulphur from S_8 to S and ammonia. It was observed on both spectra a very strange peak with a 230 mass, that could have been explained by S_5N_5 , $S_4N_4 \cdot CH_3OH$ or $S_3N_2 \cdot CH_3CH_2OH$, but the sulphur isotopic ratio just indicated S_2 and the number of nitrogen atoms was completely unknown.

Therefore a set of eight experiments were designed to investigate what was happening. In the experiments TaS_2 was reacted with S_4N_4, methyl alcohol and DMP. The S_4N_4 used was normal and labelled with N^{15}, and the methyl alcohol used was normal and fully labelled with deuterium. Table (4.2) shows the list of experiments with the amounts used, a reaction temperature of 75°C and reaction time of 3 weeks were the reaction conditions used.

The purpose of the experiments was to detect with the aid of the mass spectrometer what chemical species was really intercalating.

TABLE 4.2

	S_4N_4 mg	$S_4N_4^{15}$ mg	$HOCH_2CH_3$ ml	$HOCH_3$ ml	$DOCD_3$ ml	DMP ml	Acetone ml
1	100		3				
2	100			3			
3	100					1	2
4	100			3		0.5	
5	100				3		
6		100		3			
7		100				1	2
8		100		3		0.5	
9		100			3		

Because the amounts of chemicals available were very much smaller than those previously used, a small but unfortunately significant change in technique was made. Instead of continuous stirring and boiling inside a flask with water condenser, the substances were sealed inside glass tubes and set inside a constant temperature furnace at 75°C for three weeks.

The results of these sets of experiments were unexpected and very discouraging. A deposit of crystalline sulphur was detected inside the tubes where S_4N_4 and methanol mixture were used.

The X-ray powder diffractometry showed in some cases partially intercalated TaS_2 and the presence of other substance thought to be sulphur.

Mass spectrometry of the deposit showed very clearly just sulphur.

At this stage, it was decided to defer further experiments until adequate resources were available. Clearly the use of mass spectrometry coupled with isotopic enrichment of reacting species could be a powerful tool for exploring the difficult area of establishing the chemical nature of intercalated species, as well as extending our knowledge of sulphur–nitrogen chemistry.

4.5 Discussion

It appears that the S_4N_4 reactions with alcohols are not very well understood and that this is an area for further chemical research. The products of reaction are not very well characterized, they are also unstable. It is believed that $S_2N_2 \cdot (NH_3$ or alcohol) is proton donor and hence a Lewis acid. This would account for why these species were found not to intercalate TaS_2. An interpretation of what is happening on the experiments in table (4.2) is that TaS_2 is reacting with the very oxidizing solution of S_4N_4 and methyl alcohol to give another tantalum compound. It is imperative to repeat the $SN)_x$ intercalation experiment by Che-Hsiung Hsu (1973) using $SN)_x$ prepared from S_4N_4 labelled with N^{15} in order to check their results. Mass spectroscopy has to be used to be able to be certain that $SN)_x$ has been intercalated.

CHAPTER 5

INTERCALATION OF TRIAMINES

5.1 Introduction

Triamines are those substances where each of the three hydrogens of ammonia have been substituted by organic groups. In general triamines have been represented by $NR_1R_2R_3$.

Some triamines have been intercalated previously such as triethylamine by Thomas (1972) and tributylamine by Gamble (1971). The values found by Thomas and Gamble were: for triethylamine 10.0, 9.7 and 9.0 Å and for tributylamine 10.28 Å. The resulting expanded gap values are very small considering the shape of the molecules of the triamines involved.

However no systematic exploration of the intercalation behaviour of triamines has been undertaken. It was thought that experiments on intercalation of triamines could provide additional information on the orientation of lone pair of the nitrogen. It was also of some interest to observe the behaviour of the superconducting transition temperature with relation to the intercalated layer structure of the complexes.

5.2 Intercalating Sets

The triamines were divided into 5 sets:

a) The set where $R_1=R_2=R_3$ and R's were aliphatic chains of increasing length represented by the formula

$$R=-(CH_2)_{n-1}-CH_3;\ n=1,2,3,4,8,10.$$

b) The set of chemicals with general formula

$$CH_3)_2\ N-(CH_2)_n-NCH_3)_2;\ n=1,2,3,4$$

These are liquids of very disgusting odour.

c) The set of n-ethanolamines with general formula

$$H_{3-n}\ N(CH_2CH_2OH)_n;\ n=1,2,3.$$

Corresponding to monoethanolamine, diethanolamine and triethanolamine respectively.

These three ethanolamines were proposed to be intercalated to prove the prediction that an amine group can act as "tractor group" and permit intercalation of a side chain terminating in an hydroxyl-group or a carboxyl-group. In this case, the ethanol group $-CH_2CH_2-OH$ was chosen, because it forms chemically stable amines. Next chapter (6) deals with the side chain terminating in a carboxyl-group i.e. amino acids.

d) The set of n-ethylenediamines which has the general formula

$$H_{3-n}\ N\ (CH_2CH_2)_n\ NH_{3-n};\ n=1,2,3$$

corresponding to monoethylenediamine, diethylenediamine or pirazine, triethylenediamine or 1,4 diazabicyclo (2,2,2) octane respectively.

e) The final set included miscellaneous triamines like triphenylamine, tribenzylamine and ethylenediaminetetra-ethylacetate with the following formulae:

triphenylamine

$N(C_6H_5)_3$

tribenzylamine

$N(CH_2C_6H_5)_3$

ethylenediaminetetraethylacetate

$(CH_3-CH_2-O-\overset{O}{\overset{\|}{C}}-CH_2)_2\ N-CH_2-CH_2-N\ (CH_2-\overset{O}{\overset{\|}{C}}-O-CH_2-CH_3)_2$

The substances in these groups were intercalated in liquid phase. Even though some of them are solids at room temperature, the intercalation temperature was chosen so they were above their melting points.

The substances used in set (a) were liquids at room temperature, except trimethylamine which is a gas. A 33% weight alcoholic solution was used for the experiment in this case. The intercalated products were obtained at the temperature and times indicated in Table (5.1).

The procedure used for the intercalation of all chemical substances of these groups was the same; glass tubes were sealed on air with 200 mg of 2H-TaS_2 and an excess of the triamine. The tubes were kept inside a furnace at constant temperature for increasing periods of time. If intercalation has not occurred then the temperature was increased or a longer period of time was used.

5.3 Results of Intercalation of Triamines

The table (5.1) includes the results of the research concerning triamines. It can be observed that most of the triamines were intercalated to stage 1 into 2H-TaS_2 within a reaction time of 3 weeks. The only exceptions are those triamines with bulky substituents i.e. triphenylamine, tribenzylamine and ethylenediaminetetraethylacetate where there was no change in the X-ray diffraction pattern of the 2H-TaS_2 at the end of 3 weeks.

The separation of layers is obtained from powder X-ray diffractometry of the samples. The estimated standard deviation (e.s.d.) was obtained with a least square fitting method as described on section(7.4.3). The expanded gap was obtained by subtracting 6.04 Å (the original TaS_2 planes separation) from the separation of the layers, in agreement with the definition given in section(1.3). In the case of tripropylamine and tributylamine two different spacings were simultaneously produced on each of them. Hence the two phases are reported on the table, the one with an asterisk corresponds to the majority component 80% for tripropylamine and 70% for tributylamine.

The superconducting transition temperature onset and the transition width form the two last columns of table (5.1). The meaning of "not detected" entry is that the superconducting transition was not observed on the temperature range scanned. The temperature range was from 1.2°K to 15°K. The definition of T_{onset} and description of the method used for detecting the superconducting transition is given in section(7.3).

TABLE 5.1

Substance	Reaction Condition Time Week	Temp. °C	Separation of layers Å	e.s.d. Å	gap Å	Tonset °K	Width °K
set a)							
trimethylamine	3	100	9.658	(0.015)	3.61	5.0	0.8
triethylamine	3	100	10.194	(0.007)	4.15	2.8	0.5
tripropylamine	3	100	10.128	(0.049)	4.08*	3.7	1.4
			10.482	(0.025)	4.44		
tributylamine	3	100	10.004	(0.018)	3.95*	2.9	0.7
			10.154	(0.061)	4.11		
trioctylamine	3	100	19.139	(0.062)	13.09	2.6	0.4
tridecylamine	3	100	23.341	(0.042)	17.30	2.65	0.4
set b)							
tetramethyl NNN'N' diaminomethane	3	100	9.704	(0.012)	3.66	4.95	2.2
tetramethyl NNN'N' diaminoethane	3	100	9.607	(0.017)	3.56	4.95	2.2
tetramethyl NNN'N' diaminopropane	3	100	9.788	(0.008)	3.74	4.2	1.15
tetramethyl NNN'N' diaminobutane	3	100	9.716	(0.041)	3.67	4.6	1.1
tetramethyl NNN'N' diamino2butene	3	100	9.917	(0.050)	3.87	4.2	1.6

TABLE 5.1 (continued)

	Reaction Condition Time Week	Temp. °C	Separation of layers Å	e.s.d. Å	gap Å	Tonset °K	Width °K
set c)							
ethanolamine	3	100	9.994	(0.028)	3.95	not detected	
diethanolamine	3	100	10.467	(0.008)	4.42	4.70	0.8
triethanolamine	2	160	9.913	(0.044)	3.87	not detected	
set d)							
ethylenediamine	3	20	9.63	(0.015)	3.59	decompose in air	
diethylenediamine	1	150	10.000	(0.051)	3.96	4.55	1.35
triethylenediamine	3	160	9.855	(0.023)	3.81	2.9	0.4
set e)							
tribenzylamine	4	160		NO REACTION			
triphenylamine	4	160		NO REACTION			
EDTA tetraethylester	4	100		NO REACTION			

* Majority component (70% for tributylamine, 80% for tripropylamine)

The values of the chemical ratio x related to the formula

$$TaS_2 \text{ (intercalated)}_x$$

were obtained from thermogravimetric experiments (Chapter 7). These values (x) for the triamine intercalation complexes are tabulated on table (5.2). No thermogravimetric results are quoted for some of the intercalation complexes because these were unattainable due to problems of removing all excess viscous liquid without altering the composition of the sample.

TABLE 5.2

	T_i °C	T_f °C	X
set a)			
trimethylamine	80	480	0.418
triethylamine	60	470	0.469
tripropylamine	60	470	0.209
tributylamine	70	480	0.240
set b)			
tetramethyl NNN'N' diaminomethane	60	480	0.259
tetramethyl NNN'N' diaminoethane	80	480	0.217
tetramethyl NNN'N' diaminopropane	100	480	0.194
tetramethyl NNN'N' diaminobutane	60	480	0.176
tetramethyl NNN'N' diaminobutene	70	480	0.179

The values of the chemical ratio x for the triamines show decreasing values from trimethyl to tributyl amines as well as the values for the set b) which decreases as the molecular weight increases. The set a) of triamines intercalated to stage 1 very well. The expanded gap variation with the number of carbons on the alkyl chain is shown on Figure (5.1). The expanded gap increases discontinuously from 3.61 Å for n=1 to 17.30 Å for n=10.

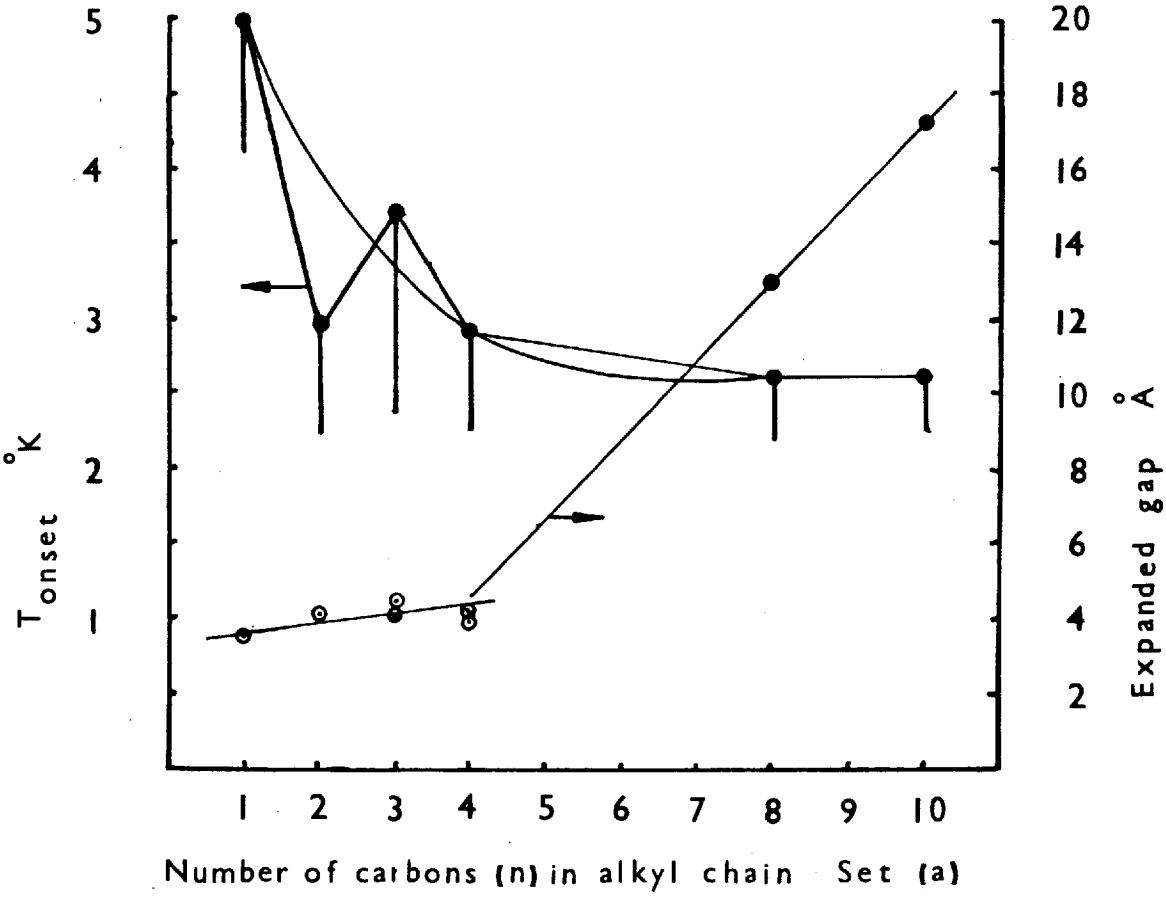


Figure (5.1)

The superconducting T_{onset} varied between $2^{o}K$ and $5^{o}K$ (Figure 5.1) with very broad transition widths. The ideal smooth decreasing behaviour (curved line) is in contrast to the observed zig-zag variation of the T_{onset} with the number of carbons on the alkyl chain.

The composition (x) is plotted against the number of carbons (n) on alkyl chain on Figure (5.2), also the graph shows the 4 first points of Figure (5.1) with more detail and the error bars i.e. the e.s.d. values.

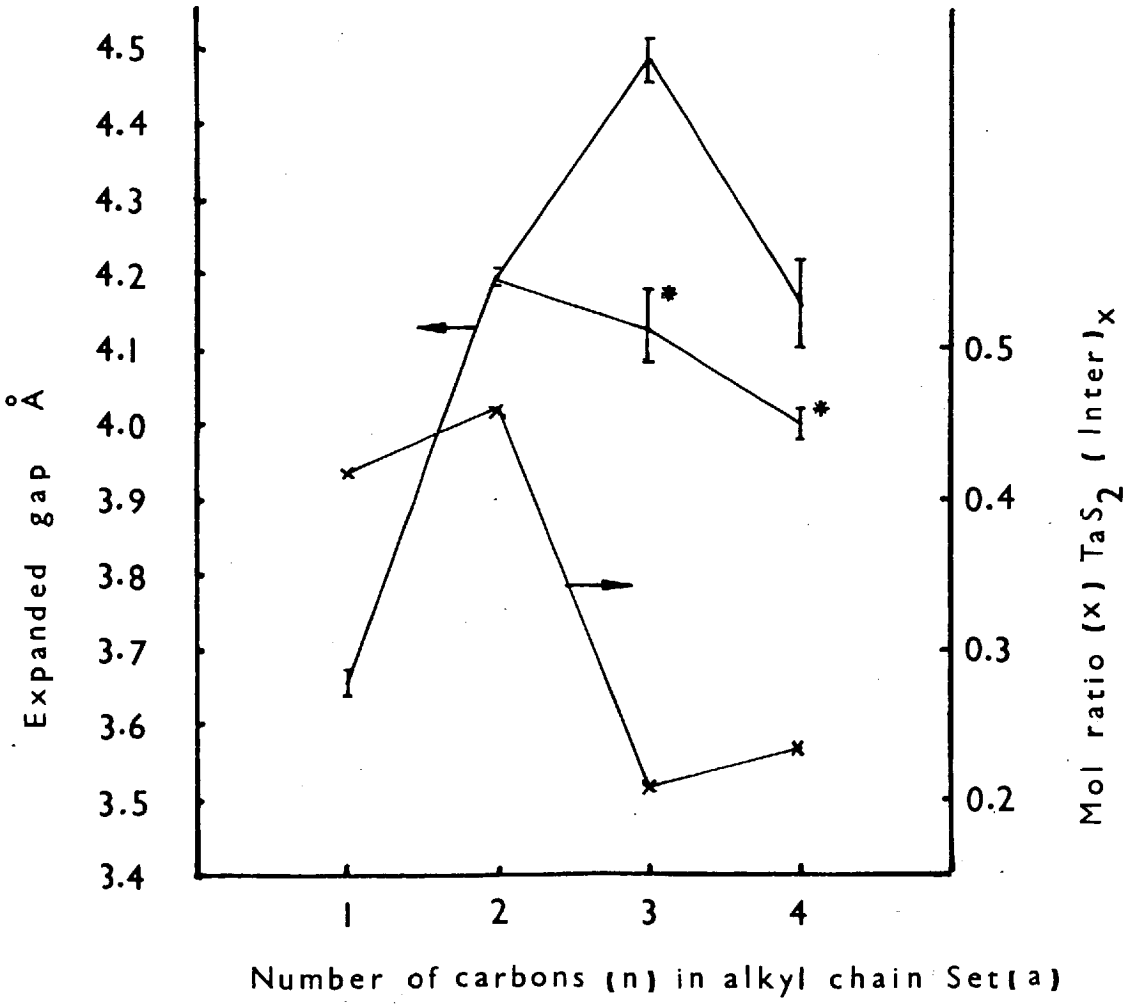


Figure (5.2)

Intercalation of chemicals in set b) did not change the expanded gap very much by going from n=1 to n=4 as can be seen in Figure 5.3. The values are between 3.55 Å and 3.75 Å even the linking chain is increasing from n=1 to n=4. The extra point is a similar molecule but instead of increasing the number of CH_2 on the linking chain there is a double bond at the middle of the butane linking chain changing it to 2 butene.

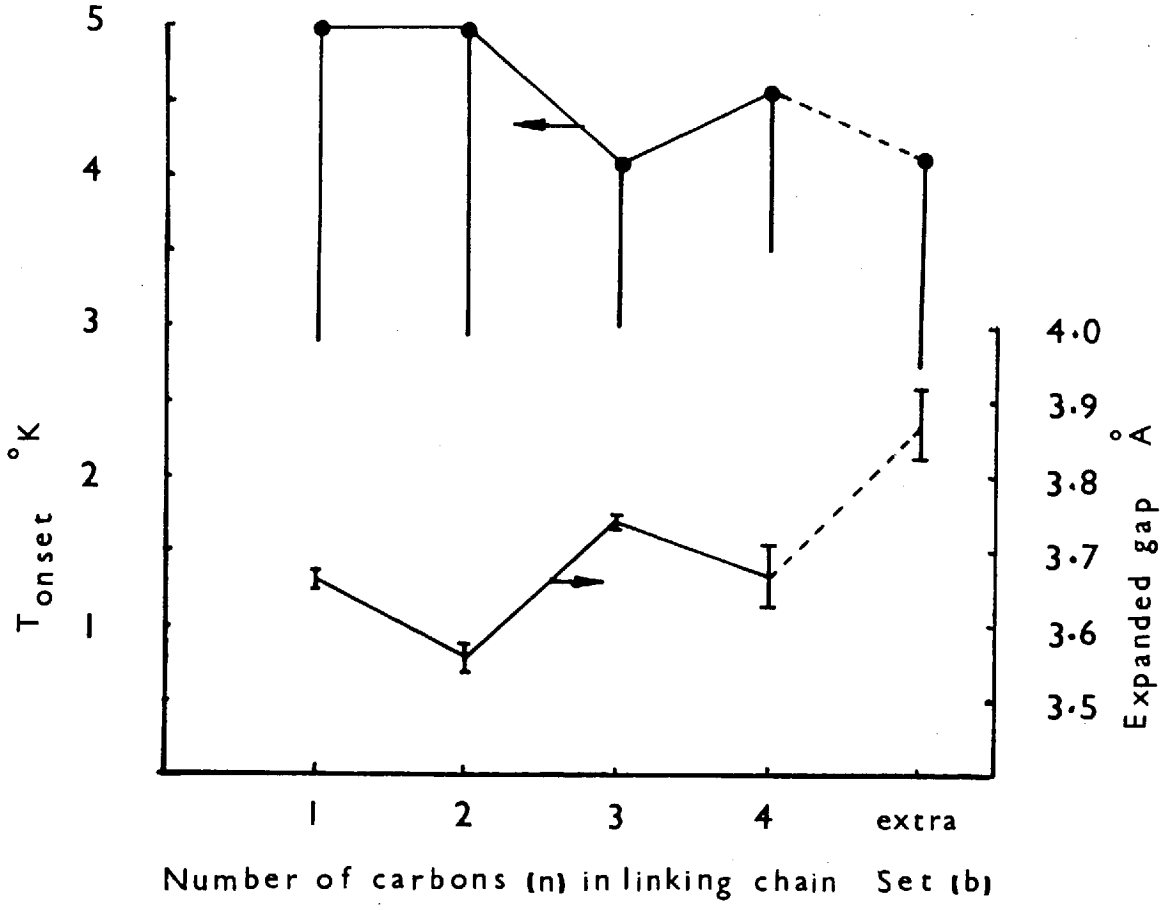


Figure (5.3)

The transition widths of these intercalation compounds, set b) were found to be the broadest of all the intercalated triamines.

The chemical composition (x) varies very smoothly from 0.259 for tetramethyl NNN'N' diaminomethane to 0.179 for tetramethyl NNN'N' diaminobutene as shown on Figure (5.4)

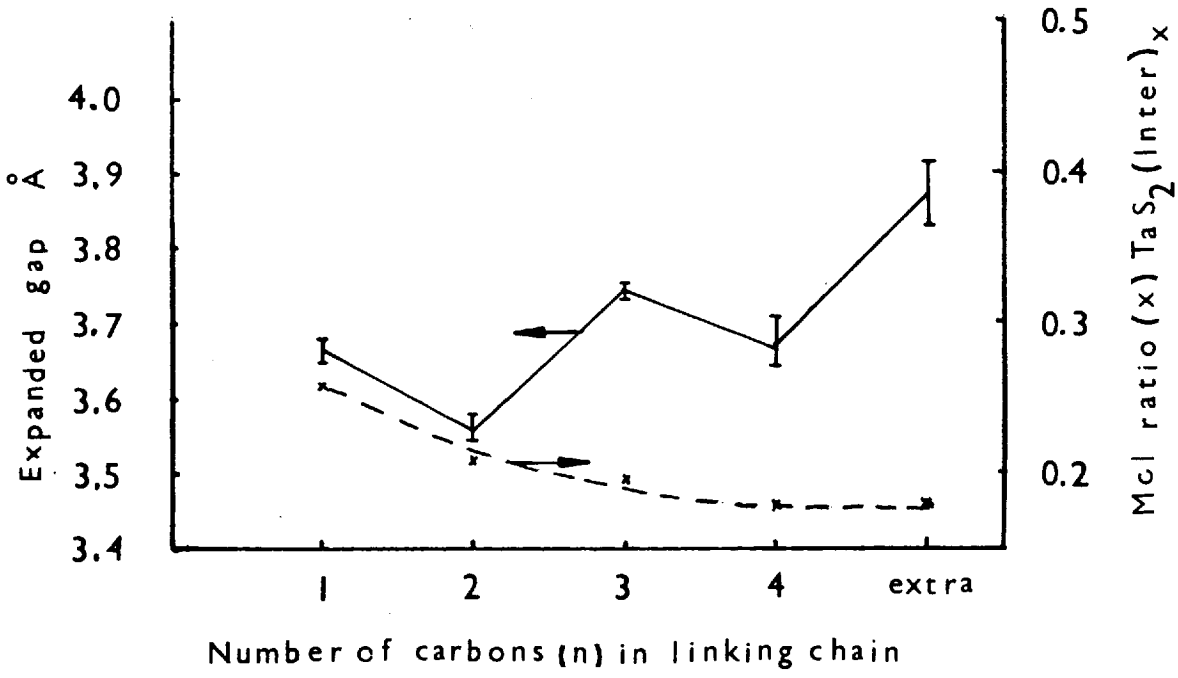


Figure (5.4)

Ethanolamines on set c) intercalated satisfactorily, showing that an amino group can initiate intercalation of a hydrocarbon chain with a hydroxyl group attached to it. The expanded gap goes from 3.95 Å to 4.42 Å and then decreases to 3.87 Å when is plotted against the number (n) of ethanol groups of the molecule i.e. mono, di and tri.

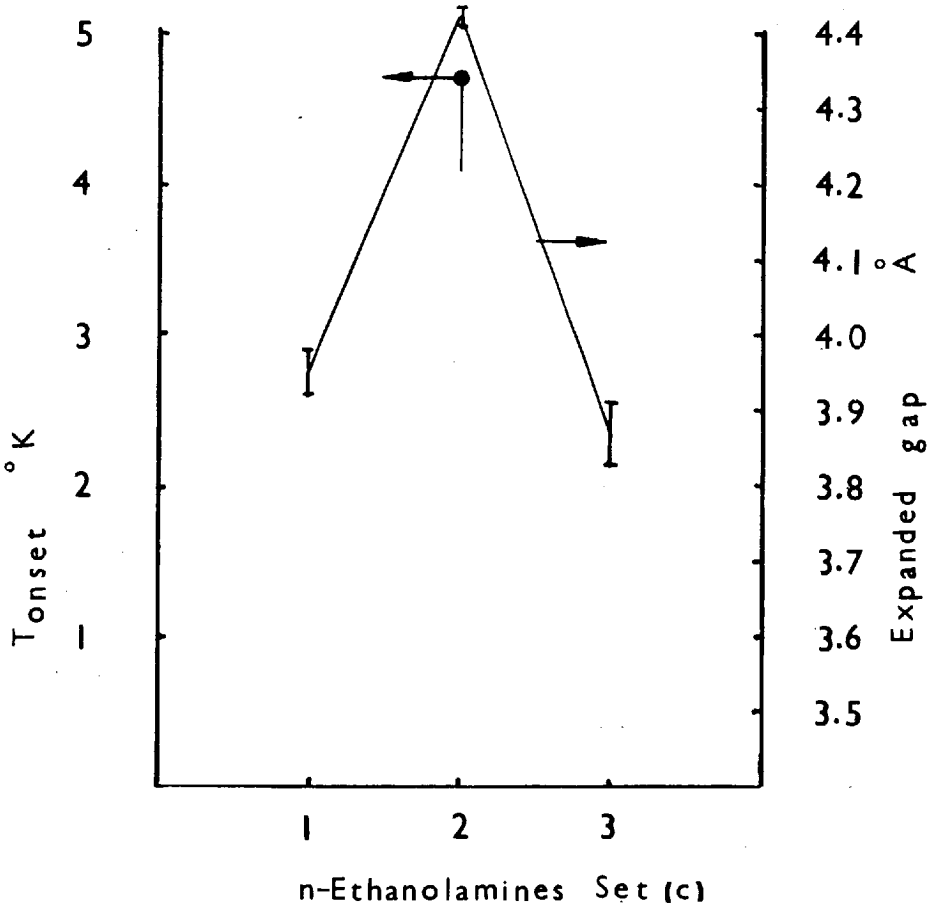


Figure (5.5)

The absence of an observable superconducting transition for ethanolamine and triethanolamine was unexpected, because diethanolamine had a T_{onset} of 4.7°K as shown in figure (5.5).

The set d) offered some difficulty in the choice of intercalation temperature. Ethylenediamine proved to be unstable in air, as has been pointed out by Thomas (1972). The difficulty is believed to be its hygroscopic character which makes it difficult to handle without decomposition.

Diethylenediamine is a solid at room temperature with a melting point at 109°C and a boiling point at 145°C, so the liquid range is not very large and it was decided to intercalate from the gaseous phase at a temperature of 150°C. Triethylenediamine also had this short temperature range in which it is a liquid, with a melting point at 159°C and the boiling point at 198°C. After several trials at different intercalation temperatures a temperature of 160°C was used with the material contained within a sealed glass ampoule.

The X-ray powder diffraction pattern of triethylenediamine showed some degree of disorder (broad peaks and not very well defined) while the pattern for ethylenediamine showed two sets of peaks corresponding one to the spacing of unintercalated TaS_2 and the other the first stage intercalated TaS_2 with ethylenediamine.

The spacing reported on table 5.1 (9.63 Å) for ethylenediamine with an average error of 0.015 was determined from this second group of peaks.

The superconducting transition temperature T_{onset} variation for the di and tri ethylenediamines, is shown on Figure (5.6), going from 4.5°K for the di substituted to 2.9°K for the tri substituted.

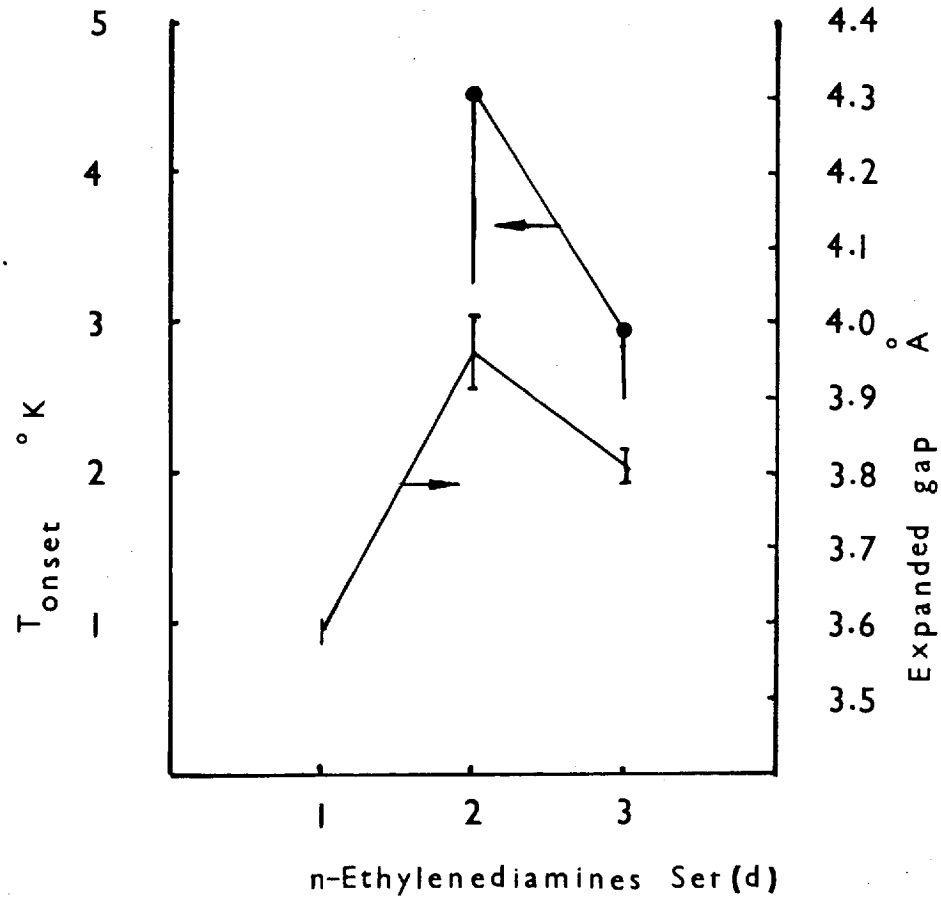


Figure (5.6)

It is believed that the three triamines in the set e) did not intercalate because the bulky substituents made the interaction between the nitrogen of the amine and the TaS_2 sterically unfavourable.

5.4 The Relative Orientation of the Intercalated Triamines Inside the TaS_2

It was explained in the general introduction how the

cases of ammonia and pyridine were difficult cases to determine the molecule orientation as well as the lone pair orientation of the nitrogen atom.

The orientation of the lone pair is important in regard to the bonding model between tantalum disulphide and the intercalated molecule, as was pointed out at the general introduction.

Also it has been suggested that the increment on the superconducting transition temperature is due to the charge transfer from the nitrogen lone pair to the $d_{z}2$ band of the transition metal dichalcogenide by increasing the electronic density near the Fermi surface.

It was found that for the series of triamines intercalated into TaS_2 the orientation of the molecule and the lone pair orientation could be easily determined from the expanded gap.

The construction of molecular models with a Catalin atomic model kit (where the van der Waals radii and the covalent radii are represented on a scale of 1Å=1cm) helped to determine the dimensions of the molecule as well as the orientation of the nitrogen lone pair. Thus the predicted value of Δ for any particular orientation of the molecule could be established.

It was found that for the series of triamines intercalated into TaS_2, the orientation of the molecules and the lone

pair orientation could easily determined from the magnitude of the expanded gap, Δ , the magnitude of which excluded all orientations apart from that in which the alkyl chains were parallel to the layer and in the α_2 orientation.

For example the trimethylamine intercalated into TaS_2 gave a gap of 3.61 Å. By measuring the molecular model values of 5.5 Å (Figure 5.7a) 3.7 Å or 3.3 Å (Figure 5.7b) the last two corresponding to two different positions of the hydrogen atoms of the methyl groups.

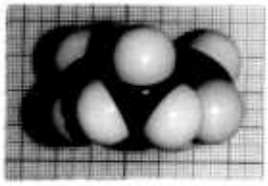
It can be concluded definitely that the trimethylamine molecule inside TaS_2 is oriented with the C_3 symmetry axis lying perpendicular to the TaS_2 layer and that the nitrogen lone pair points towards the TaS_2 layer.

In a similar way the C_3 axis was found to be perpendicular to the TaS_2 layer for all trialkylamine up to tributylamine Figure (5.7). Of interest is to note that these molecules adopt the same orientation in montmorillonite (Chapter I).

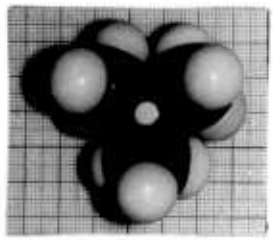
It can be seen that applying the same analysis to the diethylenediamine, the expanded gap of 3.96 Å is in agreement with the boat conformation of figure 5.8 (a) against the chair conformation of figure 5.8 (b).

Side view

Top view

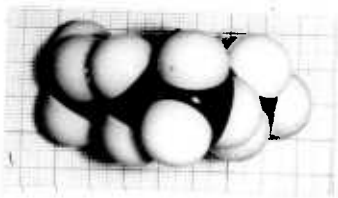


a

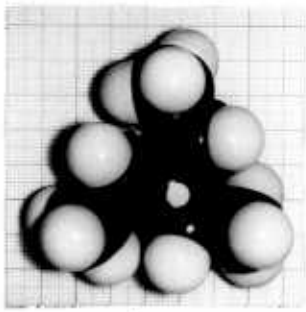


b

Trimethylamine

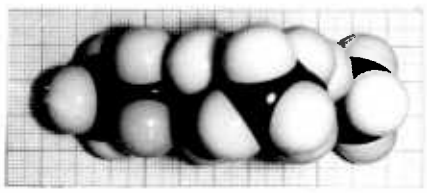


c

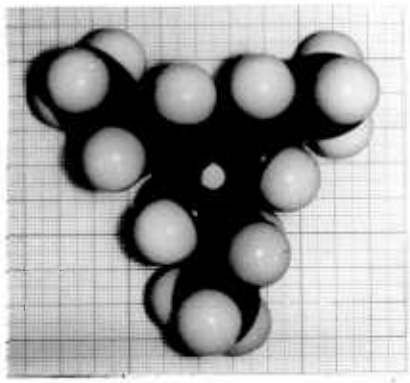


d

Triethylamine

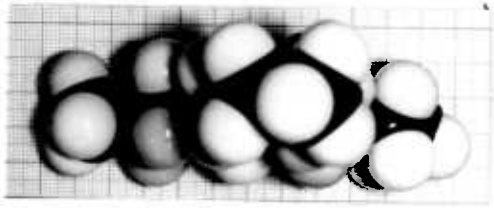


e

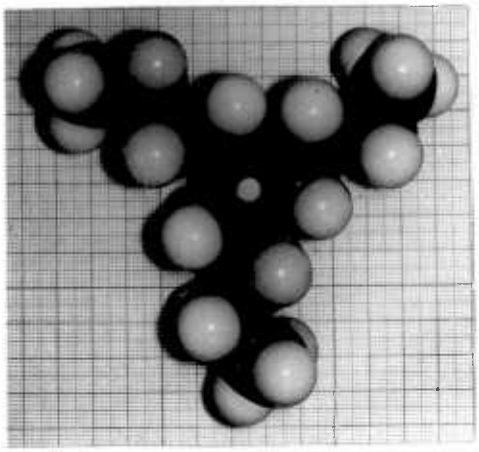


f

Tripropylamine



g



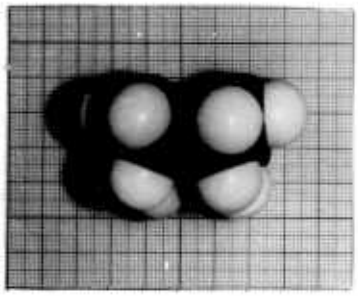
h

Tributylamine

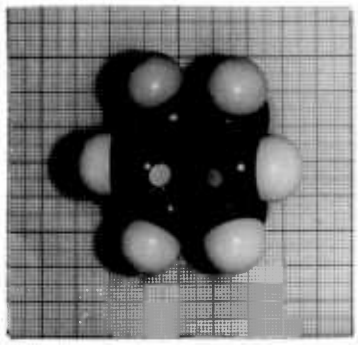
Figure 5.7

Side view

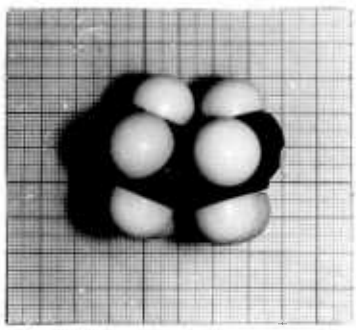
Top view



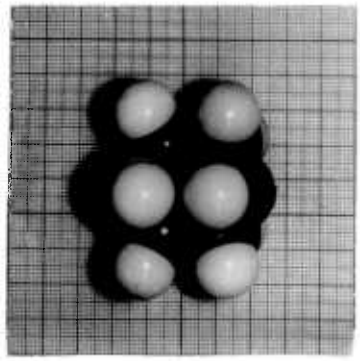
a



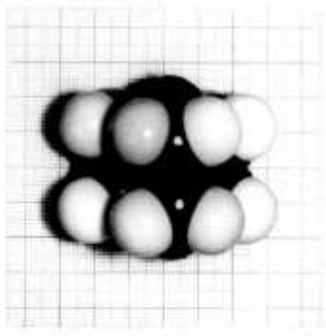
Diethylenediamine boat comformation



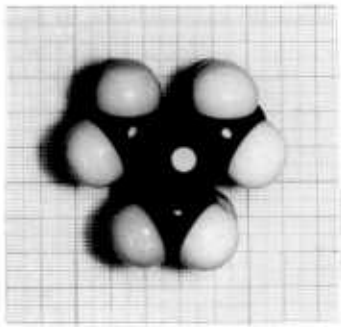
b



Diethylenediamine chair comformation



c



Triethylenediamine

Figure (5.8)

The expanded gap of 3.81 Å for triethylenediamine is quite small according to the photographs of the model on figure 5.8 (c). Furthermore, mass spectrometry has shown no sign of extra degradation, other than the one produced by the mass spectrometer when the mass fragments are formed inside the apparatus.

Clearly this method of analysis does not permit the precise location of the nitrogen within the interlamellar gap but the conclusion that the nitrogen lone pair points towards the tantalum layer is in marked contrast with previous results on ammonia and pyridine (Chapter I).

5.5 Discussion

It is an important conclusion that triamines in general intercalate TaS_2 except when bulky substituents prevent the triamines to intercalate. The intercalation behaviour of the triamines is remarkably similar to the one observed on the intercalation of the same triamines into clays. Even suggesting to attempt to intercalate into TaS_2 every substance that had successfully intercalated montmorillonite clay (Theng 1974).

The nitrogen atom lone pair orientation of the triamines inside TaS_2 lamellae was easily determined from the expanded gap value and again in remarkable agreement with the observed orientation of the triamine molecules inside clays.

The two expanded gaps showed by tributyl and tripropylamine is not unique, e.g. pyridine intercalated into TaS_2 has also shown two simultaneous expanded gaps.

The hypothesis formulated at the beginning of the chapter that the amino group in a molecule acts as tractor for intercalation was proven right in predicting the hydroxyl group attached to an amine, like in the mono, di and tri ethanolamines, will intercalate. The aldehydes were not attempted but is strongly suggested as a next line for future research, because the ability of aldehydes to react with amines to form Schiff bases.

Gamble et. al. (1971) have experimented with -OH, -SH and $-CH_2OH$ groups attached to the pyridine group. They claim to have prepared intercalated samples but stated that they were difficult to characterize. In the case of this work there were no special problems to prepare the ethanolamines.

The T_{onset} plotted against the number of carbons on alkyl chain Figures (5.1) and (5.2) shows a correlation with composition, both decrease with increasing number of carbons on alkyl chain and also have a correlation when the odd and even number of carbons are taken into consideration.

The expanded gap for the case of triethylenediamine shows a smaller gap than the one needed for accommodating the molecule inside, as is shown in section (5.4), couple of photographs of figure 5.8. It was thought that the mole-

cule has fragmented before intercalating but this hypothesis was proved wrong by mass spectrometry. Triethylenediamine intercalation should be studied more carefully by changing reaction temperatures and times before any definite conclusion could be reached.

CHAPTER 6

INTERCALATION OF AMINO ACIDS

6.1 Introduction

Amino acids are substances that have a basic amino group $-NH_2$ and an acid carboxylic group HOOC- on the same molecule. Since the two functional groups in an amino acid are, respectively, basic and acidic, the compounds are amphoteric, and in fact exist as zwitterions or inner salts.

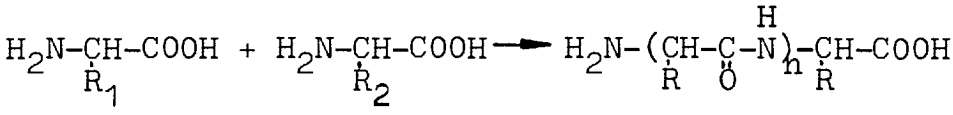
$$H_3\overset{+}{N}\underset{R}{C}HCOOH \overset{-H_1^+}{\rightleftharpoons} H_3\overset{+}{N}\underset{R}{C}HCOO^- \overset{-H_2^+}{\rightleftharpoons} H_2N\underset{R}{C}HCOO^-$$

They have two dissociation constants. The first one is a related to the ionization of the carboxylic group H_1^+ and the second is related to the ionization of the protonated amino group H_2^+. The pK_a may be defined as the negative logarithm of these dissociation constants. As there are two pK_a's for any amino acid pK_1 will relate to the ionization of the carboxylic acid and pK_2 will relate to the ionization of the conjugated acid of the amine.

The amino group of one amino acid reacts with the carboxylic group of another amino acid to form an amide bond. Such a linkage is also called a peptide bond.

$$R_1NH_2 + HOOC\text{-}R_2 \longrightarrow R_1\text{-}\underset{H}{N}\text{-}\overset{O}{\overset{\|}{C}}\text{-}R_2 + H_2O$$

This reaction is very important because it enables the amino acids to polymerize to form polypeptides.



Polypeptides are polymers containing from 2 to about 50 individual units linked by peptides bonds. When the number of amino acids in a very large polypeptide is greater than about 50 units, the molecule is considered a protein.

As stated in the introduction section (1.4) Gamble (1971) has formulated empirical rules governing the properties that chemical species must possess in order to intercalate. The most important rule is that molecules in which the nitrogen is basic ($pK_a > 4$) usually formed stable compounds provided the amine did not have bulky substituents. For certain amino acids, the values of pK_a are significantly larger than this critical value e.g. glycine pK_2=9.78. Thus if the zwitterion is in a state where it can function as a base, it might be expected that the amino acid would intercalate.

It was considered that the amino group at one end of the polypeptide might initiate intercalation of an entire polypeptide, in much the same way as the amino group of a primary amine would intercalate a hydrocarbon chain of up to 18 carbon atoms into the 2H-TaS_2 layers.

For example, it has already been shown in Chapter 5 that

the amino group, not only allowed intercalation of alkyl groups, but also aromatic groups, ring systems and alcohol groups. It was therefore considered possible that the amino group might also permit intercalation of a carboxyl or an aldehyde group.

Furthermore, as it has been established (Weiss and Rudhart 1969) that alkyl acid amides can intercalate layered structures (section 1.4), it was considered possible that a peptide bond might promote intercalation because of its similarity with the amide bond.

6.2 The Peptide Bond

The peptide backbone consists of a repeated sequence of four atoms and their associated substituents, Katon (1968). In principle rotation may occur about any of the three bonds connecting them as shown in figure (6.1).

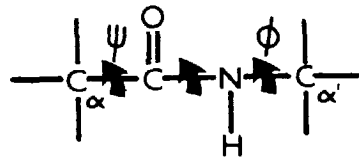


Figure (6.1)

But in the peptide group it is found experimentally that the central C-N bond is not freely rotatable. (Figure 6.2)

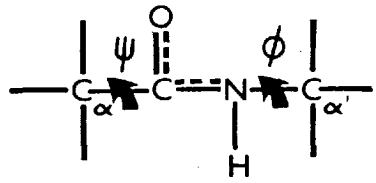


Figure (6.2)

Thus X-ray crystallographic studies of simple peptides have shown that whereas the N-C bond length is 1.47 Å, as expected for a single bond, the C-N peptide bond is only 1.32 Å. This short bond can be compared with the value of 1.24 Å for the C=N double bond length in model compounds and 1.34 Å to 1.38 Å for C=N in an aromatic ring. This is taken as a strong evidence for electron delocalization in the peptide bond. In addition all of the X-ray work on the peptide group has shown that the six atoms C_{α}(N H)(C O) $C_{\alpha'}$ are either coplanar or very close to being coplanar.

The electron delocalization in peptide bond has several very important implications and is worthy of further consideration. The first step is to examine the electron configuration of the atoms directly involved in the bond O,C and N. As all three atoms are involved in π bonding, the atomic orbitals of C and N must have sp^2 hybridization to permit the unhybridized p_z orbitals to overlap.

The nitrogen atom has one electron in each of the three sp^2 orbitals and a lone pair in the p_z orbital lying perpendicular to the plane of the sp^2 orbital as shown in Figure (6.3).

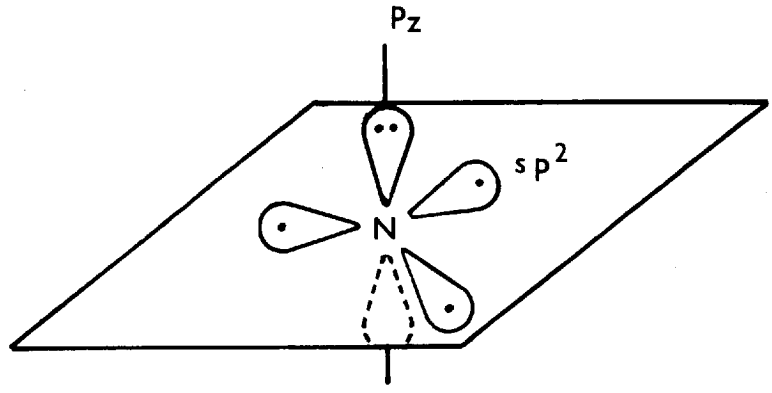


Figure (6.3)

The carbon atom can also be regarded as having three electrons in sp^2 hybrid orbitals and a fourth bonding electron in the perpendicular p_z orbital.

The oxygen atom, which normally contributes one electron to the carbonyl double-bond, may be regarded as having one electron in the bonding sp_x orbital, one in the perpendicular p_z orbital and two in the nonbonding p_y orbital, as shown in Figure (6.4).

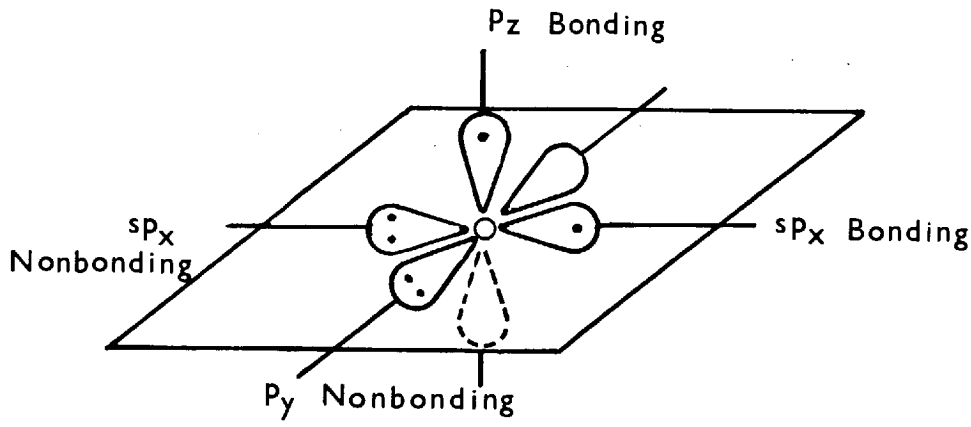
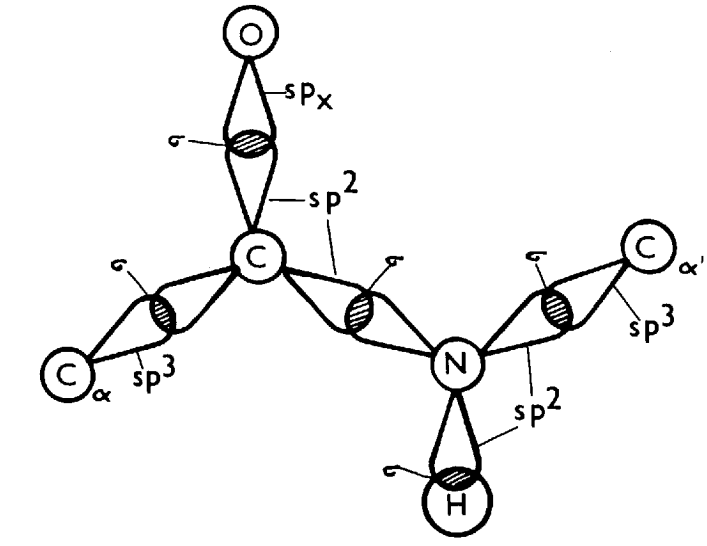


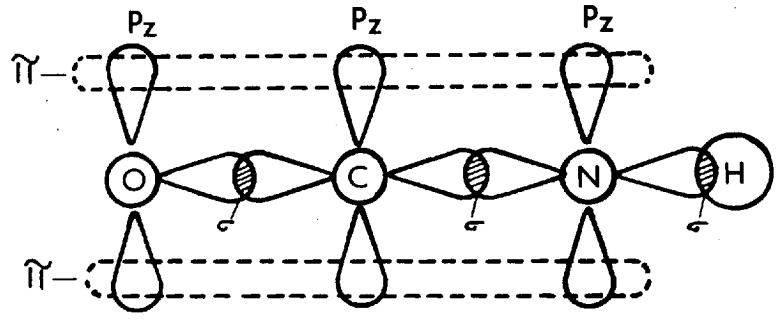
Figure (6.4)

When these three atoms are bonded together, one O (sp_x) and one C (sp^2) overlap to form a single σ bond, as do C (sp^2) and N (sp^2). Since the N-H bond also involves a σ bond in the sp^2 plane of the nitrogen, all six atoms of the peptide group would be expected to be coplanar. The three p_z orbitals are parallel to each other and form a conjugated π bonding system over which the four p_z electrons (one from the oxygen, one from the carbon and two from the nitrogen lone pair) are delocalized.

Schematic representations of the top (A) and side (B) view of the bonding scheme are shown in Figure (6.5)



A



B

Figure (6.5)

Thus the peptide bond, like the amide bond, has a high degree of conjugation, resulting from delocalization of the nitrogen lone pair into the carbonyl group. This delocalization reduces the basicity of the nitrogen and leads to restricted rotation about the C-N bond.

A careful study of the configuration of the peptide group has shown that a nonplanarity of up to about 6°, due to rotation about the C-N bond, can be tolerated and that in most cases the O and H atoms should lie <u>trans</u> to the peptide bond. There are no known examples of the <u>cis</u> peptide bond occurring in polyaminoacids, polypeptides and proteins. Only diketopiperazine (glycine anhydride)

has two cis peptide bonds in its molecule and this configuration is necessary for the ring to close.

The presence of double bonds on portions of the molecule containing delocalized π electrons can give rise to electronic transitions in the near ultraviolet and visible regions.

In this case one can define three energy levels which can be classified as bonding, nonbonding and antibonding (Figure 6.6).

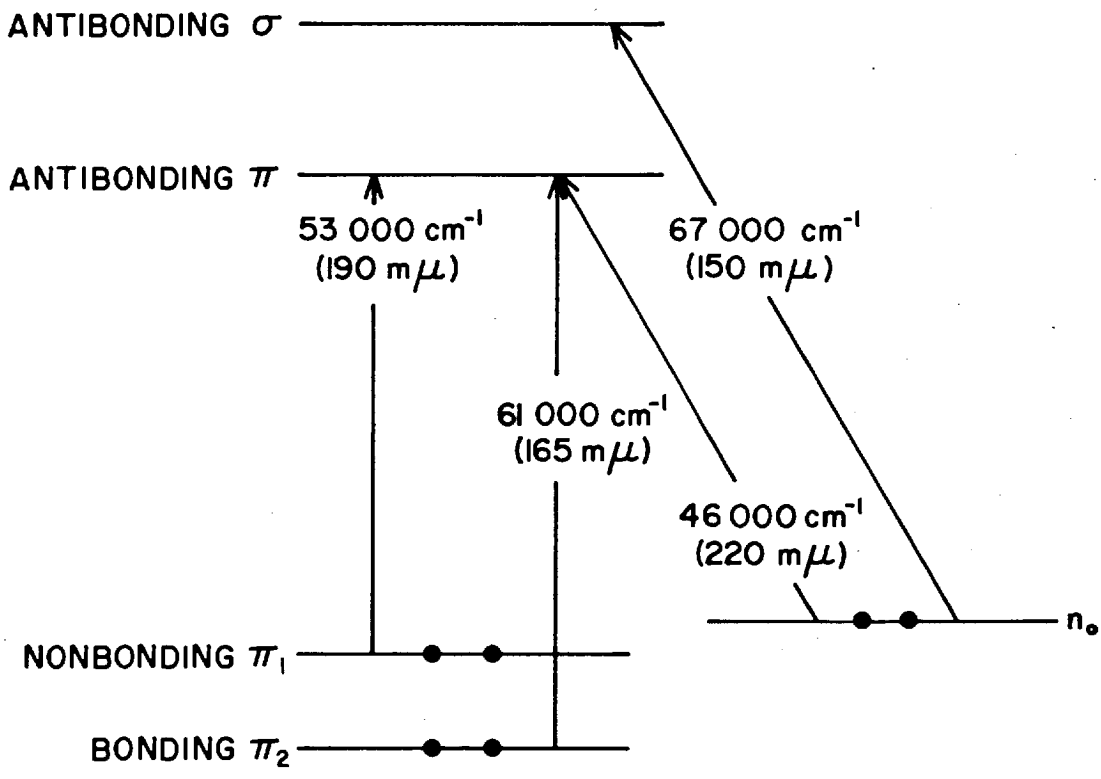


Figure (6.6)

If the oxygen, carbon and nitrogen atoms were equally electronegative, the orbitals would be symmetrical in energy. In practice the energy of the nonbonding orbital is found to be closer to the bonding orbital.

Each of the three orbitals can contain two electrons, so that the four delocalized π electrons fill the two lowest molecular orbitals. The minimum energy required for electronic excitation is that which promotes an electron from the nonbonding to the antibonding orbital, thus producing a π_1-π^* transition.

In addition to the delocalized π electrons, the oxygen atom also possesses two nonbonding electrons in the atomic p_y orbital. One of these electrons can also be promoted to the π^* orbital through the so-called n-π^* transition. The relative energies or wave lengths of these transitions are shown in Figure (6.6) one can see the lowest energy (highest wavelength) transition is the n-π^* followed by π_1 - π^*, π_2 - π and n-σ^*.

The ions over which the charge is distributed and the charge itself vibrate with respect to one another, so that electrons in the ground state may be promoted to a state that is simultaneously excited, both electronically and vibrationally, the so-called vibronic transition. Furthermore, and most important to this presentation, the radiation-excited states in the polymeric amino acid can undergo resonance coupling to give what is known as exciton splitting of the energy level.

The electrical conductivity values for polypeptides suggest a conductivity gap between 2.4 and 3.1 eV. This conductivity gap might be related to the n-π^* transition,

but the observed values are around 5.9 eV. therefore, the lack of agreement between the conductivity measured and optical transition value suggests that the semi-conducting state is optically forbidden.

6.3 Intercalation Experimental Procedures

6.3.1 Procedures to intercalate amino acids and polypeptides

The intercalation was carried out using aqueous solutions of each amino acid. It was necessary to use water as a solvent because the amino acids are, in general, almost insoluble in anything else. Amino acids are soluble in ethyl alcohol but their solubilities are 1000 times smaller than in water. Typically, the solubilities of glycine at 25°C are 25.3 g/100 ml in water and 0.043 g/100 ml in ethyl alcohol 90%.

The substances tried are listed in table (6.1) and are divided into Set (a) contains glycine and polypeptides of glycine with general formula.

$$H_2NCH_2(CONHCH_2)_{n-1}COOH \quad (n=1,2,3,4,5)$$

This is the only sequence of polypeptides readily available. The second set of compounds (b) is formed by pyridines with a carboxyl group attached in the three possible positions corresponding to picolinic, nicotinic and isonicotinic acids. Last set (c) is formed from several other amino acids that were chosen to give a general idea of what

restrictions on the intercalation of amino acids may exist. For example, β alanine would be the second term in the series of aminoacids of general formula

$$H_2N\text{-}(CH_2)_n\text{---}COOH$$

that may be intercalated in future work.

Amino acids (chromatographically homogeneous or laboratory grade purity) were dissolved in distilled water and saturated solutions were normally prepared at 75°C in a pyrex glass tube. The solutions were made by placing 0.2 grams of the amino acid and adding increasing amounts of distilled water until the amino acid was completely dissolved. The amount of water used is listed in table (6.1). 2H-TaS_2 (0.150 grams) was added to the solution and the tube sealed in air. The tubes were then placed in an oven maintained at 95°C for a time which varied between 7 and 14 days.

Another method used was to place 0.200 g of 2H-TaS_2 inside a saturated solution of the amino acid or polypeptide. The suspension was boiled and stirred under reflux as necessary. This procedure shortened the intercalation times to one day for glycine, two days for diglycine and three days for triglycine. This method had two major disadvantages. Firstly it is applicable to powders only because stirring damages large crystals. Secondly when bubbles were formed on the crystals during boiling, they appeared to cause the crystals to exfoliate.

Glycine intercalation was attempted in a 1T-TaS_2 and NbS_2 powders under similar conditions but no positive results have yet been obtained.

During the attempt to intercalate NbS_2 with glycine a complicated X-ray diffractrograph developed at the beginning, but the product was decomposed after 2 weeks reaction time, as judged from the X-ray diffractograph that showed one very broad peak.

6.3.2 Attempts to intercalate polyglycine

Attempts were made to polymerize glycine in situ by exposure to concentrated ammonia solution at 150°C. Samples were intercalated by the method of sealed glass tubes as previously described and checked that intercalation was completed to stage 1. It was confirmed that the sample did not deintercalate in presence of a concentrated ammonia solution at 100°C. The sample intercalated with glycine, after being exposed to the ammonia solution for a week at 100°C, gave the same diffractograph. It was therefore concluded that there was no deintercalation of glycine. A portion of the same sample of TaS_2 intercalated with glycine was previously dried at room temperature and sealed in a glass tube with concentrated ammonia solution. The tube was set in a constant temperature oven at 150°C for 24 hours as was done by Oró (1961) to polymerize glycine. The X-ray diffractograph was now changed indicating that a reaction had taken place in interlamellar space. This will be further discussed in section (6.5).

TABLE 6.1

Substance name	pK_a	Reaction Conditions Water[b] ml	Time[c] days	Composition x moles	Crystalographic data c-axis Å	e.s.d. Å	expanded gap Å	Superconductivity Tonset °K	Width °K
[a] glycine or glycocoll	9.78[a]	0.8	7	0.284	9.71	0.009	3.67	3.4	1.1
diglycine	8.25	1.6	11	0.172	9.43	0.016	3.39	2.6	0.6
triglycine	8.09	1.6	7	0.085	9.40	0.017	3.36	4.2	1.4
tetraglycine		5.5	14	0.076	9.40	0.017	3.36	not	detected
pentaglycine		40.0	7	0.066	9.41	0.049	3.37	not	detected
glycine anhydride		2.5	7	0.158	9.51	0.056	3.47	2.8	0.8
[b] picolinic acid		1.0	7	0.163	9.46	0.036	3.42	3.4	1.4
nicotinic acid		6.0	7	0.165	9.56	0.005	3.52	3.6	1.8
isonicotinic acid		20.0	7		N O T I N T E R C A L A T E D				
[c] D and L valine	9.72	3.6	7	0.255	12.64	0.072	6.60	not	detected
β alanine		4.0	7	0.231	9.38	0.041	3.34	2.5	0.5
L proline	10.64	0.5	7	0.181	10.0	0.014	3.96	4.7	2.7

a) From Streitweiser and Heathcock (1978) page 817
b) 0.2g of aminoacid were dissolved with the given quantity of water
c) The reaction temperature was the same for all cases (95°C)

An attempt was made to intercalate polyglycine. Polyglycine was prepared by a method described by Oró (1961), where a 5g sample of glycine and 1 ml of concentrated ammonia solution 16 molar, were sealed in a glass tube and set inside an oven at 150°C for 24 hours. The mixture was dialyzed inside a cellophane bag for three days against running tap water. The product was lyophilized to obtain polyglycine with a degree of polymerization of the order of 18 glycine units. Using this method 0.5g of polyglycine was obtained and solubilized in a saturated solution of LiBr. The solution of polyglycine with LiBr in water was sealed with a 2H-TaS_2 monocrystal inside a glass tube and set inside a constant temperature oven at 100°C for a week. The product gave a diffractogram indicating an expanded gap of 5.6 Å. This unexpected result suggested that LiBr had intercalated the 2H-TaS_2 crystal and this was confirmed by intercalating another single crystal directly with LiBr aqueous solution.

6.4 Results

The glycine polypeptides in set (a) were successfully intercalated to stage 1. The expanded gap reduced as the number of glycine units increased Figure (6.7). Even though the pK_2 value of the polypeptide as well as its solubility was decreasing with the number of glycine units, as can be noticed on table (6.1), the intercalation behaviour seemed to be influenced by whether the number of glycine units was even or odd. Pentaglycine intercalation was faster compared with tetraglycine, triglycine was as fast as diglycine and glycine. Moreover the quality of

the crystals after intercalation were noticeably better with triglycine and pentaglycine.

The absence of a superconducting transition for tetra-glycine and pentaglycine intercalated samples within the measured range (1.2K° to approximately 15°K) was unexpected and further research is essential before any conclusions can be drawn. Figure (6.7).

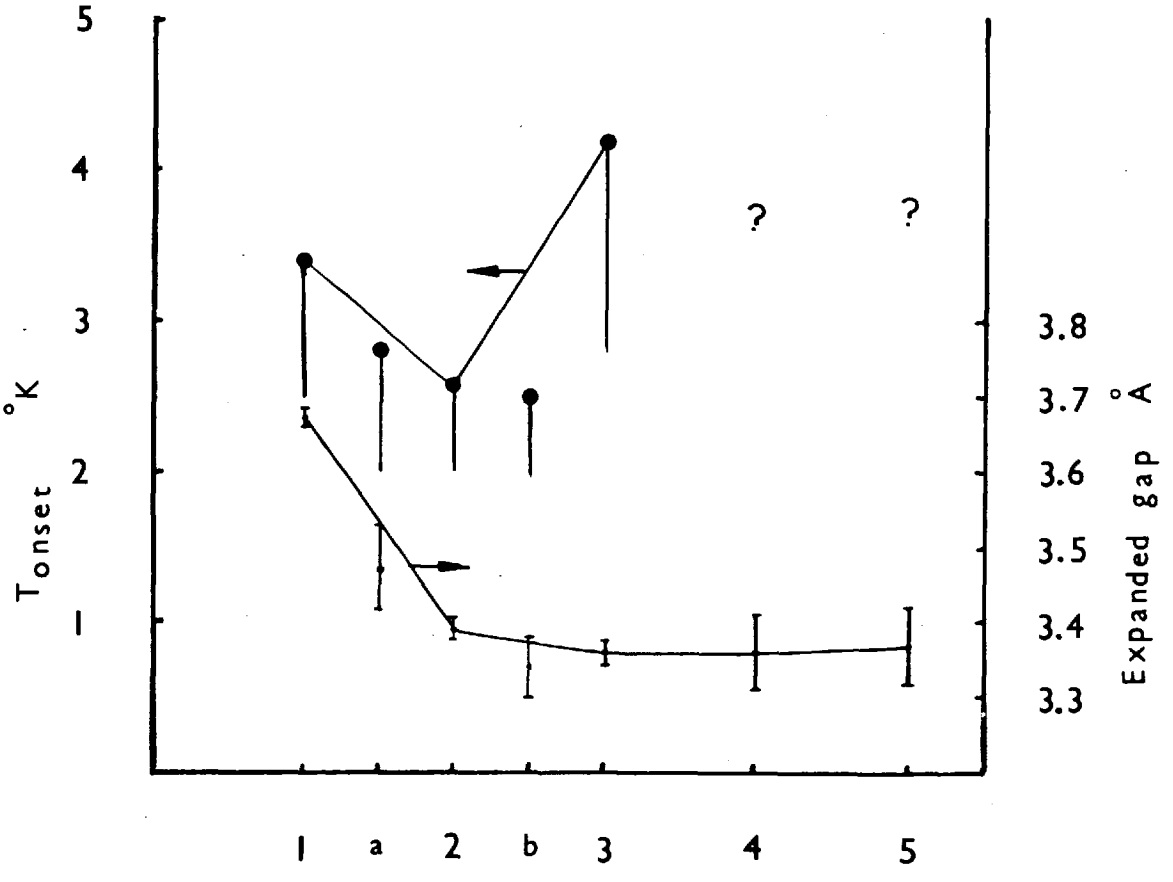


Figure (6.7)

The set (b) picolinic and nicotinic acids intercalated to stage 1 and formed superconducting complexes with TaS_2. In the case of isonicotinic acid it was not possible to obtain an intercalated sample because of the low solubility of isonicotinic acid in water.

The set (c) D alanine and L alanine exfoliated very easily and no X-ray experiments were possible. The intercalation conditions were too violent and would have to be chosen more carefully in future experiments in order to obtain intercalation compounds of adequate quality. No superconducting transition was detected for the valine intercalation compound.

6.5 Discussion

During the research on intercalation of amino acids the main concern was to find a suitable method to intercalate fast without damaging the large crystals of transition metal dichalcogenide. From the fact that glycine was intercalated faster by the stiring-under-reflux method than by the sealed glass tube method an important discovery was made. The intercalation of amino acids is solution-diffusion controlled.

The expanded gap of the n-glycine polypeptide complexes decreases with increasing number of glycine units. This is evidence to predict that the expanded gap for polyglycine intercalated inside TaS_2 would be around 3.35 Å. From the magnitude of the expanded gap of 3.36 Å for pentaglycine, the polypeptide molecule must lie parallel to the TaS_2 layer, and more specifically in the α_2 orientation.

The intercalation of β alanine was achieved with an expanded gap of 3.34 Å which was in good agreement to the asymptotic-limit for the expanded gap of

polyglycine. This suggests that the two CH_2 of β alanine are also in the α_2 orientation and that the two hydrogen atoms attached to the carbon are responsible for the expanded gap.

The intercalation of the first members in the homologous series of n-glycine polypeptide indicates very clearly the possibility that the polypeptide molecule may enter between the TaS_2 lamellae. This may be attempted either by finding suitable reaction conditions for intercalating the polypeptide i.e. choice of solvent, reaction temperature and intercalation methods, or by in situ polymerization of the monomor.

During the experiments where glycine was set to react with concentrated ammonia solution the expanded gap changed from 3.67 Å to 3.47 Å suggesting that glycine anhydride was the reaction product. The necessity of further analyses to confirm what are the products of reaction and whether the reaction could be continued further in order to obtain the polypeptide.

It is believed that the intercalation of amino acids might proceed smoothly by using the double intercalation procedure developed by Di Salvo (1971) of intercalating first with ammonia and then intercalate the amino acids at the same time the intercalation of ammonia is taking place.

It has to be pointed out that during the thermogravimetric analyses any water co-intercalated inside the TaS_2 could not be distinguished from water produced by a polymeriza-

tion. If it is found possible to intercalate amino acids from non-aquous solutions, then it will be possible to study the polypeptide structure and the influence of the hydrogen bond between polypeptides chains on the inter molecular geometry.

From the expanded gap of picolinic and nicotinic acid complexes (3.42 Å and 3.52 Å), the molecular plane must lie parallel to the TaS_2 layer. Hence the lone pair orientation, which is found in the molecular plane, also lie parallel to the TaS_2 lamellae.

In contrast to picolinic and nicotinic acids the absence of intercalation of isonicotinic acid was unexpected. It is interesting to note that Di Salvo (1971) attempted the intercalation of isonicotinamide, but report it unintercalated. This suggests a possible relation between the intercalation behaviour of both substances.

The molratio $\times$ in$(TaS_2$ intercalate$)_x$ for n-glycine polypeptide decreases proportional to the molecular weight of the polypeptide, as might be expected. The values of picolinic acid and nicotinic acid are comparable to diglycine and glycine anhydride. This is to be expected as they lie parallel to the TaS_2 layer, they have roughly similar molecular weight and they have almost the same expanded gap.

The superconducting transition temperature (T_{onset}) of the n-glycine polypeptides correlates with the expanded gap as can be seen from figure (6.7). They both decrease in the following order: glycine, glycine anhydride, diglycine,

ß alanine. The fact that T_{onset} increases for triglycine and that absence of superconducting transition was detected for tetraglycine and pentaglycine in the range from 1.2°K to 15°K was unexpected and no obvious explanation has been found.

The only other amino acid which did not show any superconducting transition was valine. There is nothing unusual about this complex. It shows the largest expanded gap of all the amino acids studied, but this gap is in agreement with measurements made on the Catalin molecular model of the L and D valine molecules.

CHAPTER 7

CHARACTERIZATION OF INTERCALATED CRYSTALS

7.1 Introduction

The first question when attempting intercalation of new substances is if intercalation has actually occurred. The X-ray powder diffraction is a fast technique which also gives an accurate result.

The problem of finding the composition of the intercalated compound was approached using thermogravimetric analysis. The chemical state of the intercalated molecule inside the lamellae was proved with the aid of mass spectrometry.

Electrons, X-rays and neutron diffraction techniques have been shown to be very useful to determine the structure of intercalated complexes section (1.5). The physical properties have been shown to be intimately related to the structure of the intercalated compound section (1.3). Therefore, the structure of the intercalation complexes and its relation with the physical properties has been studied, in the case of this research, first by single crystalls X-ray studies, in order to know what was the intercalated complexes structure and then the superconducting transition temperature of the complexes was determined in an effort to correlate this property with the structure.

7.2 Thermogravimetric Determinations

Gamble (1971) has shown that the intercalation is reversible. He heated the intercalated complexes in vacuum or in a dry nitrogen gas stream. The weight loss difference between high and low temperature was found to correspond to the amount of organic substance intercalated, confirming that the molecules had been completely driven out.

In this work thermogravimetric analysis (T.G.A.) has been used to determine the weight loss of intercalated samples, hence the composition of the complexes.

A weighed sample was set in an aluminium pan inside the furnace of a Perkin-Elmer TGS-1 thermobalance. This furnace consisted of a platinum resistance element on a ceramic cylinder which heated the sample in accordance with a selected temperature programme.

The thermobalance was calibrated with magnetic standards of known Curie point temperature. Alumel, Nickel, Perkalloy and Iron were used as standards, giving fixed temperature points at 163°C, 354°C, 596°C and 780°C respectively. Oxidation of the samples was prevented by using a stream of dry nitrogen gas.

In a typical run, the intercalated sample was weighed on a microbalance (between 2 and 10 mg.) with a 10 microgram precision. The aluminum pan containing the sample was

hung from the electronic microbalance and the furnace raised into its position. The thermogravimetric result was a graph of weight loss of the sample vs. temperature.

From this graph the weight loss was directly measured (every division was calibrated to be 0.01 mg and the total graph amplitude, 1 mg).

The temperature at which the weight is first observed to decrease (T_i) and the temperature by which all of the molecules have been driven out (T_f) are somewhat dependent upon the heating rate and all the experiments were made at a rate of 20°C/min.

T_i and T_f were almost the same for all the intercalated complexes tested. They began to deintercalate at 60°C and deintercalation was complete at 500°C, independent of the different methods used for intercalation or the chemical differences between the intercalated species. From this observation it is thought that there is no correlation between the temperatures of deintercalation, on either the molecules intercalated or the method used to intercalate the samples.

The results were referred to a general formula

$$TaS_2\ (\text{intercalate})_x$$

where x is the mol ratio of intercalated molecules to TaS_2 units. The value of x was established by using the

mass loss measured with the thermobalance, assuming that only one, known, molecule is intercalated. The molecular ratios were very close to rational numbers indicating near stoichiometric relation. Due to the fact that the structures are chemically complicated, the ratios are not exact rational numbers. T.G.A. was used as a fast and easy method to determine the molecular ratio as well as to establish the thermal stability of the intercalated complex.

7.3 Superconductivity Measurements

Superconductivity is a state of a metal (below certain temperature called T_c or transition temperature) in which the metal becomes a perfect conductor i.e. resistance equals zero, and also behaves as a perfect diamagnetic substance. This later property is known as the Meissner effect. There are three commonly used properties to detect superconductivity: electrical conductivity, heat capacity or magnetic susceptibility. The most convenient method is to measure the change on magnetic susceptibility of the sample vs. temperature. Low temperature facilities are needed to detect the superconducting transition temperature which is usually below $20^{o}K$.

The superconducting transition temperature was measured using an A.C. susceptibility bridge method built by Dr. Forgan of the Birmingham University. The arrangement of the primary and secondary coils, and the location of the sample and the thermometer are shown in Figure (7.1).

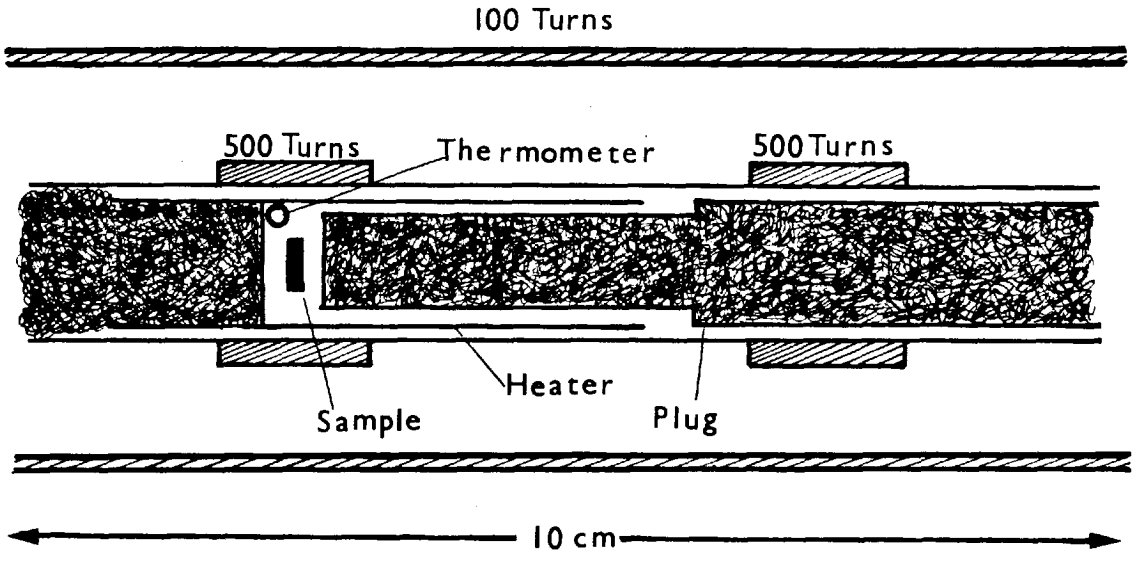


Figure (7.1)

The heater was constructed of 0.01 inch thick copper foil insulated with thin paper to prevent eddy currents. Resistance paper of 800 ohm was thermally bonded with G.E. 7031 varnish as shown in Figure (7.2).

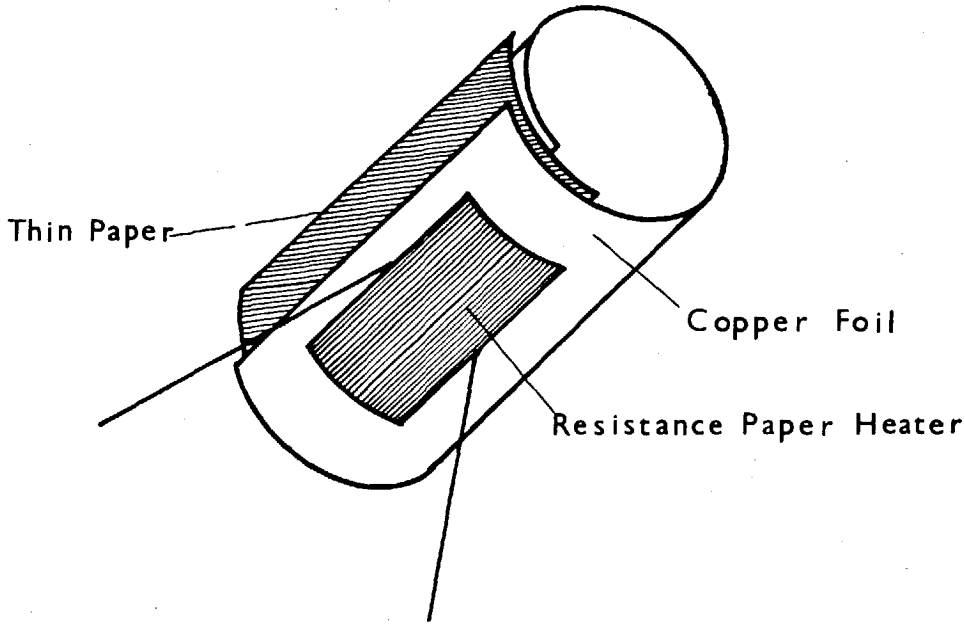


Figure (7.2)

The Allen-Bradley carbon resistance thermometer (470 ohm) was silver painted to copper-platinum wires and bonded with G.E. 7031 varnish to a copper wire wool disc in order to increase the heat conductivity (Figure (7.3)).

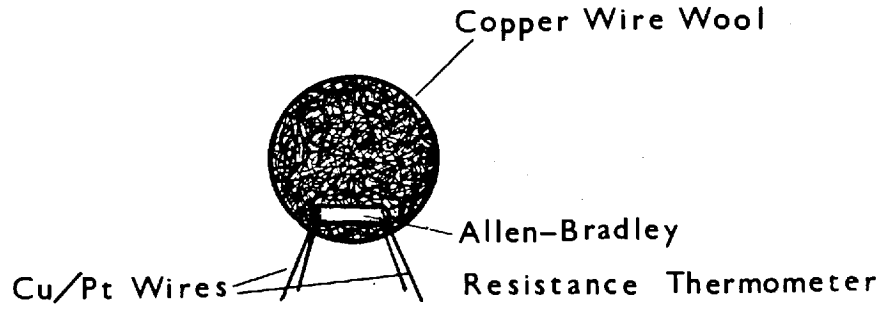


Figure (7.3)

The temperature control was achieved using the following circuit Figure (7.4).

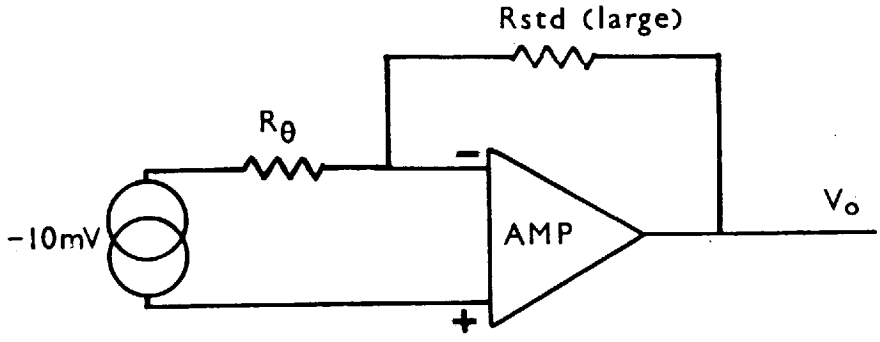


Figure (7.4)

A sample of the intercalated powder was prepared by putting 10 mg of the powder between sticky paper and cutting it to form a flat disc so that it was a sandwich

of sticky paper with the powder as the filling.

A typical run was made when a sample was introduced into the apparatus and the plug put in its place. The whole apparatus was dipped into the liquid helium. The helium Dewar was pumped down until the temperature of the liquid helium was below $2^{o}K$. The apparatus was then lifted above the liquid helium surface. Using the heater, the temperature of the apparatus was allowed to rise to about $10^{o}K$.

A graph of the superconducting transition was obtained on an x-y recorded where the X axis was proportional to the sample temperature and the Y axis was detecting the susceptibility of the superconducting sample. The transition was swept back and forth by slowly increasing and then decreasing of the temperature with the aid of the heater controller. No thermal hysterisis was observed during the transition provided the time constant of the lock-in amplifier was set at 0.1 sec and the temperature was scanned from $2^{o}K$ to $10^{o}K$ over a period of 5 minutes.

Calibration of the Allen Bradley carbon thermometer was achieved by using lead and niobium samples. They provided fixed points at $7.1^{o}K$ and $9.2^{o}K$ respectively. For lower temperatures, the helium vapour pressure was used for calibration. Twelve vapour pressure points were measured between $4.2^{o}K$ (normal boiling point of liquid helium at 1 atmosphere) and $1.2^{o}K$ where the liquid helium vapour pressure is around 3 mm of Hg.

These calibration points were used to make a thermometer scale which was traced over a paper strip. The thermometer that way obtained has a precision of hundreths of Kelvin degree.

The superconducting transition temperature was measured directly from the graph by the use of the thermometer described above.

The definition most commonly used for the superconducting transition is the temperature at which half of the material has become superconductor or at half-height of the transition. The transition temperature reported in this work is actually the onset temperature; in other words the temperature at which the superconductivity begins or sample diamagnetism start to be detectable.

The reason for using T_{onset} instead of T_C (superconducting) is because the transition widths are very broad (of the order of 1^oK). The range of the T_{onset} for the superconducting transitions found in this work is between 1.2^oK and 5^oK.

The transition widths are also reported because the intercalated compounds have a tendency to show very broad transitions due apparently to the intrinsic behaviour of these complexes, as has been noted by Di Salvo et. al. (1971). Such widths are of the order of 2^oK in some cases.

Detailed results are given in the appropriate chapters.

In a few cases, no superconducting transition could be detected in the scanned range of temperatures. This was due to the way superconducting transition measurements were made. In these cases the complexes may have a superconducting transition temperature on temperatures below or above the temperature range stated, for example TaS_2 intercalated with D valine, L valine, monoethanolamine, triethanolamine, tetraglycine and pentaglycine did not exhibit a superconducting transition in the range from 1.2°K to 15°K even though X-ray evidence shows complete intercalation in all cases.

7.4 X-ray Diffractometry

7.4.1 Powder diffractometry equipment

The equipment consisted of a Philips X-ray generator type PW1011, which activated a Philips Cu target X-ray tube.

A Berthold powder diffractometer (Solus-Schall type 50200 with a $\theta/2\theta$ drive) was aligned on the beam and X-rays were detected by a scintillation counter 1A-1 from Nuclear Enterprises.

The scintillation counter was connected to a Scalar-Ratemeter SR3B from Nuclear Enterprises Ltd. which provided the 1.25 Kv high voltage necessary for its activation as well as counting the X-rays sensed by it as shown in Figure (7.5).

The analog out put from the ratemeter was applied to a chart recorded Sunvic Controls Ltd. with a full scale deflection of 100 mv.

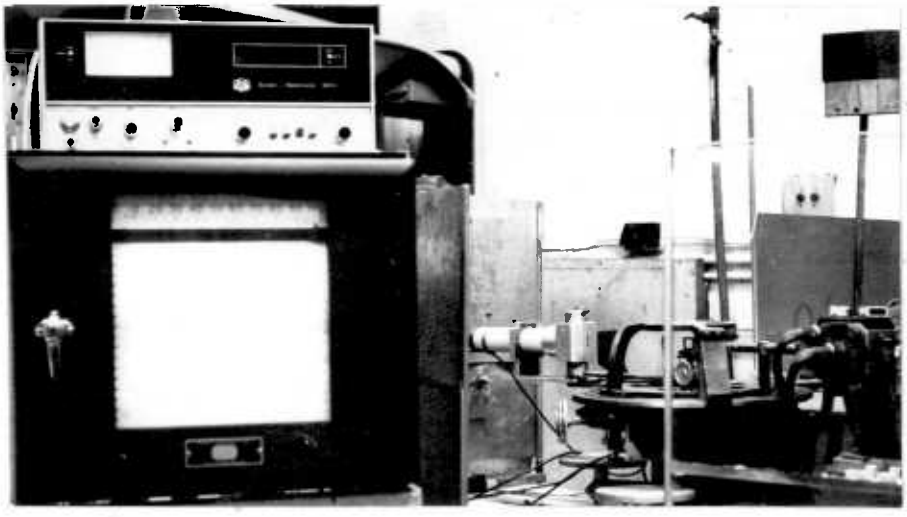


Figure (7.5)

The conditions for taking the diffractographs were standardized for all the experiments. The Cu X-ray tube was set at 30Kv and 10 ma direct current. A thin nickel foil was placed in front of the X-ray-source in order to reduce the CuK_{β} radiation. The scanning rate was 1^{o} a minute. The source slit and the detector slit of the powder diffractometer were set at 0.55 mm and the beam divergence slit was fully open. The ratemeter was set to a 4 sec time constant and the channel width of the pulse height analyzer set 20%. The absolute position of the window in the energy spectrum was made to coincide with pulses due to CuK_{α} by setting the energy range at 0.2 and the energy knob at 1.0.

The only setting that was changed from run to run was the count-rate range which was adjusted to give peaks of reasonable height. Several recordings at the same scan

speed and chart speed were made in order to obtain traces of peaks with both large and small maxima in the number of pulses per second.

7.4.2 Procedure

The powder used on the X-ray diffraction experiments was set in a glass holder specially made to use a very small quantity of sample 150 mg of TaS_2 powder (Figure 7.6). The high X-ray absorption of sample means that only a thin layer (0.15 mm) of powder was needed. Because powder samples were unstable if free standing support in recess of glass plate was necessary. In order to avoid adhesives the sample was slightly compressed with the aid of a microscope slide.



Figure (7.6)

The sample was run from $50^{o}\theta$ to zero at a rate of 1^{o} θ per minute. The powder sample was returned to the vessel if the diffractometer trace was complex, had more peaks than expected and those peaks were not sharp and uniformly distributed.

Special attention was given to establish the angle $\theta=0$ for the recording. This was done by stopping the recording 30 seconds after the diffractometer motor has stopped, this is the time the motor of the diffractometer would have taken to move from the stopping position of half of one degree to zero.

7.4.3 Interpretation

The information obtained from the X-ray powder diffractometer was mainly the expanded gap. This is defined as the difference between the separation of the MX_2 layers in the intercalated complex and the original 2H-TaS_2. A sample of 2H-TaS_2 powder gave a layer spacing of 6.030 (0.025) where the amount between parenthesis is the standard deviation. The expanded gap is then given by measured interplanar spacing of the intercalated minus 6.04 Å.

The X-ray powder diffractometer results can be interpreted by using the general observation that the 001 reflections for intercalated samples dominated the diffraction pattern. In particular 101 were unobserved.

This was due to the fact that the samples used were coarse powders (100 mesh, 50 microns) which would orient preferentially under compression with the layer planes parallel to the plane of the sample, would also make it difficult to detect weak reflections.

The diffractographs obtained were measured with a scale. The positions of the peaks, measured in millimeters, were transformed to θ values using the factor 6.35 mm = $1^{o}\theta$ ($\frac{1}{4}$" = $1^{o}\theta$). The values of θ were transformed to interplanar spacings in $\mathring{A}$ by using the Braggs relation.

$$d = \frac{\lambda}{2\text{Sin } \theta}$$

where λ is 1.5418 $\mathring{A}$ for the CuK_{α} radiation wavelength.

If the sample had been intercalated to a single stage then the 00l reflections will obey the relation.

$$ld(00l) = d\ (001)$$

If there is more than one intercalated layer to the crystallographic repeat distance then

$$c = n\ d_{i}$$

Where d_i is the separation of intercalate layers and n is the number of intercalate layers. In this case observed 00l reflections will be restricted to values of l that are multiples of n.

In the present studies of the expansion geometry, only the separation of intercalate layers is important and so the first recorded 00l reflection will in general be indexed as 001 and values of d (001) obtained by the 1 given equation.

Due to systematic errors, predominantly displacements of sample surface from correct position, made necessary to correct the values of the interplanar spacings. First values for the expression

$$\text{Cos}\ \theta\ \text{Cot}\ \theta$$

were calculated, and by using this value and the corresponding interplanar spacings a extrapolation to $\theta = 90$ was made. Least square fitting (Mandel 1964) method was used to find the interception with the axis and a value for the dispersion of the points. The best interplanar spacing fitting and the standard deviation were obtained by a simple computer programme.

7.4.4 Intercalated Single Crystals

Selected single crystals of 2H-TaS_2 were examined to check for crystal perfection using an oscillation camera (Unicam type S25) (Figure 7.7). The single crystal was mounted over a glass support specially designed to allow the crystal to be mounted using just a little amount of water and a very small amount of NaCl salt so that the samples were not contaminated with organic solvents and adhesives that may interfere with the intercalation.

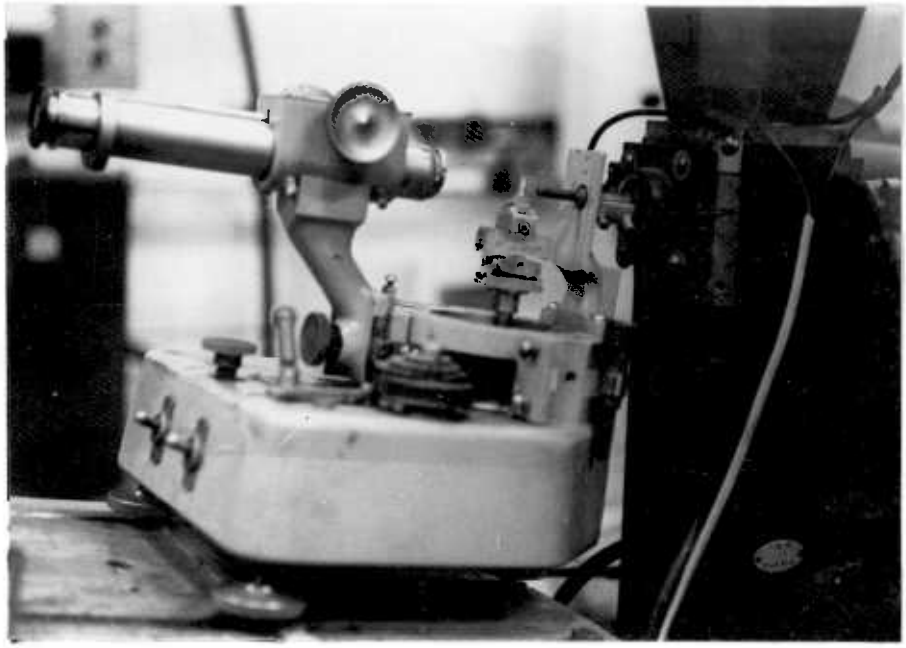


Figure (7.7)

The glass support was a thin glass slab 0.15 mm thick and 4 mm wide; the single crystal could then be mounted by just letting the crystal rest on its largest flat surface and in contact with the glass slab which had been wetted with saline solution. After drying it was mounted on the single crystal goniometer and the diffraction pattern recorded on a cylindrical camera loaded with Ilford Industrial G X-ray film.

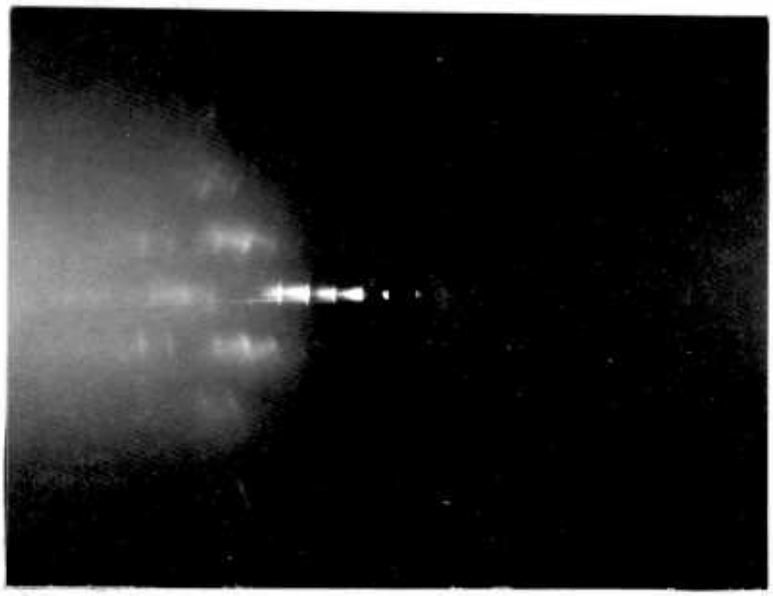
The MoK_{α} X-ray radiation was used (excitation voltage $\sqrt{2}$ 30 kv, filament current 10 ma).

The X-rays were filtered with a zirconium foil to a attenuate the K_{β} radiation. Two methods were used to filter the beam: either the foil was set covering the photographic film (filtrating the diffracted beams) or in front of the beam (filtrating the incident beam). The former was preferred because it also attenuates a

lot of the fluorescent radiation yielding clearer photographs when very long exposure times were needed.

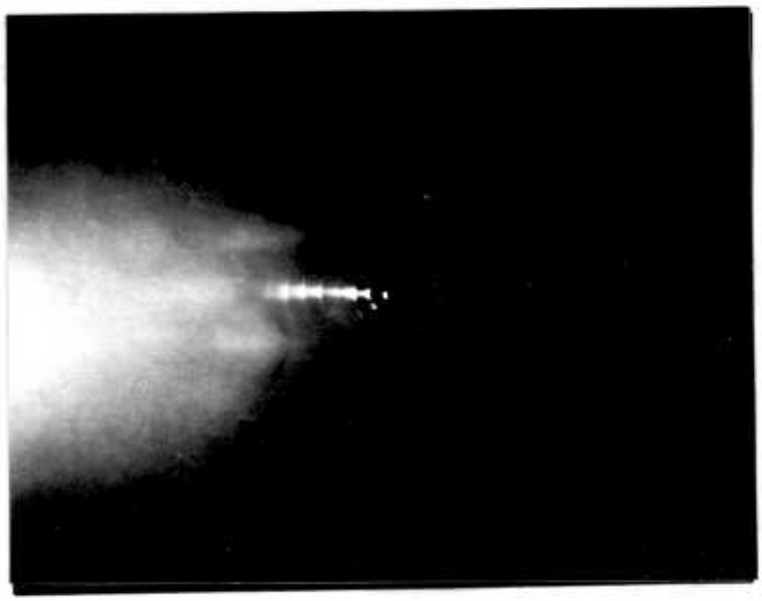
The Figure (7.8) shows a single crystal oscillation photograph which can be indexed as shown in the same figure. A computer programme was used to calculate the intensities of the 10l reflections. It can be observed that the 10l reflections follow the calculated pattern, the odd 10l reflections are stronger than the even reflections confirming that this is the 2H polytype.

Three TaS_2 single crystals were intercalated with glycine, diglycine and triglycine. The oscillation photographs are shown in Figures (7.9) (7.10) and (7.11). It can be observed that these photographs do not show any periodicity in the stacking sequences of the dichalcogenide layers after intercalation, although the orientation of the a axis within the layer remains parallel to that existing before intercalation Figure (7.12) (only (hk) rods are observed, no hkl reflections). Possibly stacking changes such as that found in 2H-TaS_2-pyridine complex also occur in these cases, but the present choice of reaction conditions do not favour a highly ordered reaction product. It was noticed that intercalation was not inhibited by the absence of stacking order.



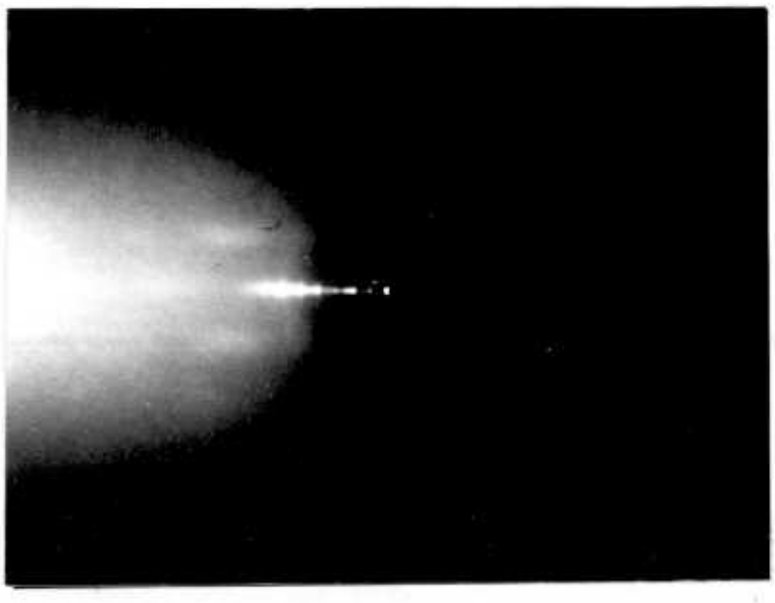
Oscillation photograph of 2H TaS_2 showing strong 10L odd reflexions, single crystal c-axis perpendicular to the beam

Figure (7.8)



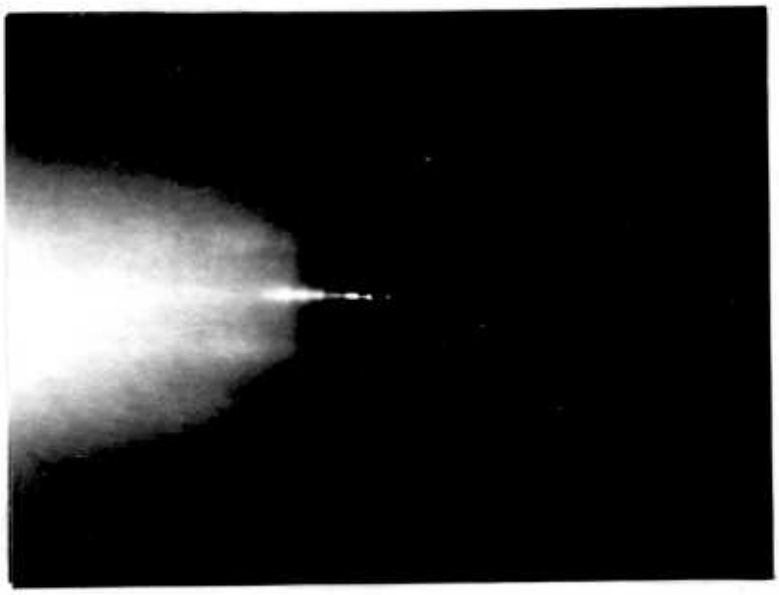
2 H–TaS_2 Intercalated with glycine showing only 00L reflexions, single crystal c-axis perpendicular to the beam

Figure (7.9)



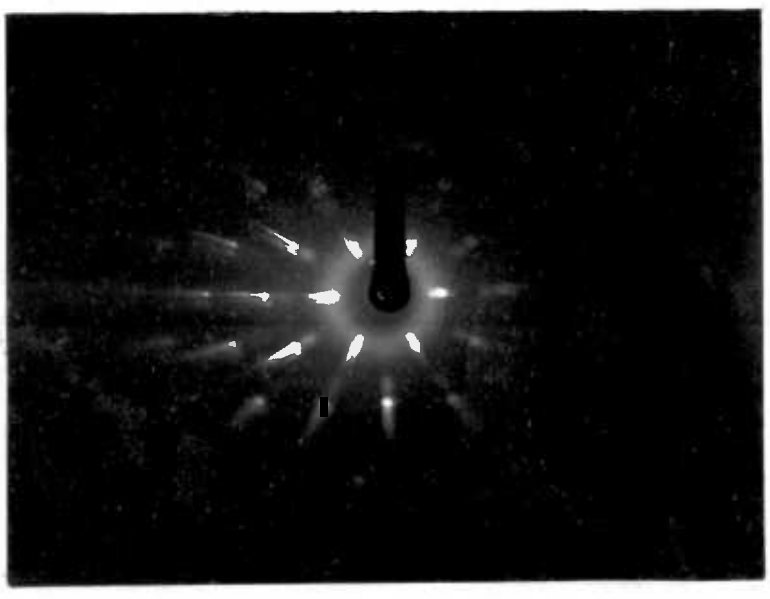
2 H–TaS_2 Intercalated with diglycine showing only 00L reflexions, single crystal c-axis perpendicular to the beam

Figure (7.10)



$2H\text{-}TaS_2$ Intercalated with triglycine showing only 00l reflexions, single crystal c-axis perpendicular to the beam

Figure (7.11)



$2H\text{-}TaS_2$ Intercalated with n-glycines n=1,2,3. single crystal c-axis parallel to the beam

Figure (7.12)

CHAPTER 8

GENERAL DISCUSSION AND FUTURE WORK

The principal concern of this research has been to extend the knowledge of molecules that can be intercalated into 2H-TaS_2 and to identify what chemical factors these molecules have in common.

Thus before intercalation one had to ensure that the material was in its 2H polymorph using the procedures given in Chapters 3 and 7. Other polytypes were identified before optimal conditions were achieved, but no systematic study of the formation of these polytypes was undertaken.

During the intercalation reaction special attention was given to the intercalation techniques in order to explore ways to obtain undamaged single crystals or increase the reaction rate for powder samples. Intercalation was considered complete when molecules had intercalated every space between TaS_2 layers i.e. the compound was first stage.

It is a general observation that the magnitude of the expanded gap for 24 of the 28 complexes obtained during this research lies between 3.3 $\mathring{A}$ and 4.1 $\mathring{A}$.

In an attempt to explain this small expanded gap, scale models of the molecules were made using a "Catalin" Kit. They were squashed between two sheets of cardboard. It was found that the squashed molecules could be used to

select the molecular orientation that was in agreement with the expanded gap. This can be seen from table (8.1).

Therefore, it is believed that the compressed models represent the configuration and orientation of the molecules inside TaS_2. The conformation of the compressed molecular models that explain the expanded gap is planar in all but two cases. In some cases it is possible to identify the α_2 orientation (as defined in section 1.3) within the hydrocarbon and polypeptide chains. (Figure 8.1). The only molecules that show the α_1 orientation are the tetramethyl NNN'N' diaminoalkanes (set (b) Chapter 5). The α_1 orientation is then exhibited by the alkane part of the molecule.

Once the probable configuration of the molecule has been established, it is possible to consider the orientation of the nitrogen lone pair.

The nitrogen lone pair and its relative orientation are considered important because of their relation with initiation of the intercalation reaction, bonding of the intercalated molecule and superconductivity of the complexes, as will be discussed further on.

The atomic orbitals s, p_x, p_y and p_z can be hybridized in molecules to give either tetrahedral sp^3 orbitals or trigonal sp^2 orbitals with an unhybridized p_z orbital. If the nitrogen atom forms three sigma bonds, then the lone pair should be assigned either to a tetrahedral sp^3 orbital or

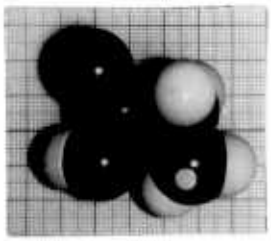
TABLE 8.1

name of the substance	expanded gap measured with X-rays	expanded gap prediction measured from Catalin model	
		side	top
	Å	Å	Å
trimethylamine	3.61	3.5	5.2
triethylamine	4.15	3.8	7.5
tripropylamine	4.08*- 4.44	3.9	9.3
tributylamine	3.95*- 4.11	4.1	11.5
T.M. diaminomethane	3.66	3.6	6.4
T.M. diaminoethane	3.56	3.6	6.0
T.M. diaminopropane	3.74	3.6	6.3
T.M. diaminobutane	3.67	3.8	6.2
T.M. diamino 2-Butene	3.87	4.0	6.3
ethanolamine	3.95	3.9	4.3
diethonolamine	4.42	3.8	4.5
triethanolamine	3.87	3.8	9.1
ethylenediamine	3.59	3.8	4.2
diethylenediamine (boat)+	3.96	4.0+	5.4
diethylenediamine (chair)	3.96	4.7	6.3
triethylenediamine	3.81	5.0	6.0
glycine	3.67	3.7	4.5
diglycine	3.39	3.5	5.2
triglycine	3.36	3.5	5.0
tetraglycine	3.36	3.4	5.0
pentaglycine	3.37	3.4	5.0
glycine anhydride	3.47	3.6	6.6
picolinic acid	3.42	3.0	6.0
nicotinic acid	3.52	3.0	6.0
D and L valine	6.60	6.0	8.0
β alanine	3.34	3.34	4.5
L proline	3.96	4.3	5.2

*majority component (70% for tributylamine, 80% for tripropylamine)

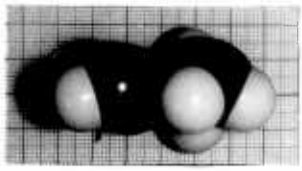
+the molecule can exhibit chair and boat conformations.

Top view

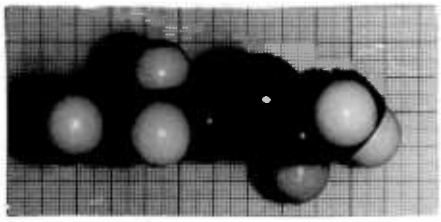


Glycine

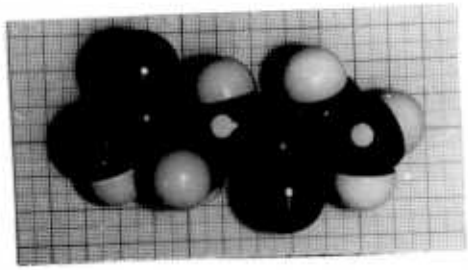
Side view



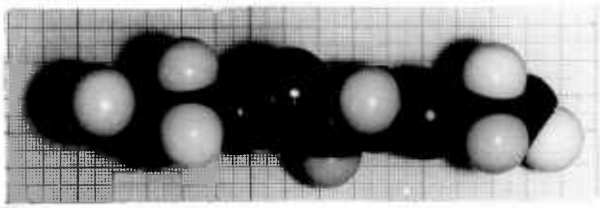
Glycine



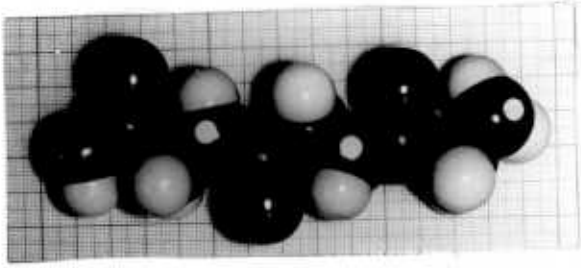
Diglycine



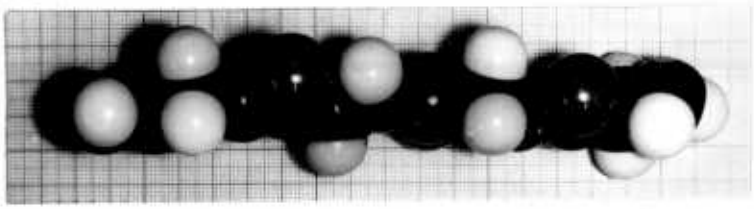
Diglycine



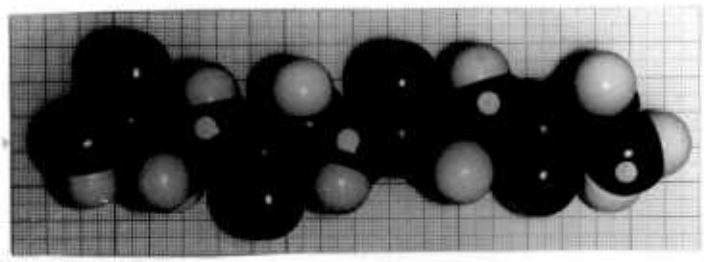
Triglycine



Triglycine



Tetraglycine



Tetraglycine

Figure (8.1)

to a p_z orbital. If just two sigma bonds are formed, as in picolinic and nicotinic acids, then the lone pair should be assigned to the third sp^2 hybrid orbital.

Thus in the triamines, the lone pair must be in one of the sp^3 hybrids. For almost all the triamines studied the plane of the carbon zig-zag lies parallel to the TaS_2 layers (in the α_2 orientation) and the C_3 symmetry axis of the orbital containing the lone pair of electrons lies perpendicular to the TaS_2 layers. Even when the alkyl chain is in the α_1 orientation as in the tetramethyl NNN'N' diaminealkanes this statement regarding the orientation of the lone pair remains valid.

In the case of a polypeptide, two different types of nitrogen can be defined. In the terminal NH_2 group the lone pair of the nitrogen atom must be in one of the sp^3 hybrids and inclined at an angle to the TaS_2 layers. In the peptide bond the lone pair of electrons in the nitrogen atom must be in the p_z orbital. Therefore, in the intercalated compounds containing peptide bonds, the symmetry axis of the p_z orbital containing the lone pair of electrons must be perpendicular to the TaS_2 layer.

In the case of picolinic acid and nicotinic acid, the orientation of the lone pair in the nitrogen atom must be parallel to the TaS_2 layer. A similar orientation must be inferred from the expanded gap measurements reported for 2,6 dimethylpyridine and 2,4,6 trimethylpyridine (Gamble 1971).

It is important to note that in this research the orientation of the nitrogen atom lone pair of the intercalated molecules can be inferred merely from the magnitude of the expanded gap. For the previously intercalated amines and pyridines (Gamble 1970 and 1971), and particularly ammonia and pyridine, as shown in section (1.4), the orientation of the molecule and the lone pair were difficult to establish and were only confirmed after neutron scattering experiments (Riekel 1977).

It is interesting to observe that while the pentadecylamine molecule (18 atoms long) lies perpendicular to the TaS_2 layer (Gamble 1970) with a 39.0 Å expanded gap, pentaglycine (18 atoms long) lies parallel to the TaS_2 layer with a 3.42 Å expanded gap. The glycine anhydride (diketopiperazine) intercalation also adds evidence to the idea that the terminal amino group is not the only element of the polypeptide helping to initiate intercalation. Hence the peptide bond has to be considered an active element regarding intercalation.

The interpretation that the nitrogen lone pair is responsable for initiating the intercalation of the organic molecules (Gamble 1970) is consistent with the findings of this research.

It is generally accepted that intercalation involves charge transfer. Hence the processes involved in intercalation can be visualized as:

1) diffusion through the liquid or solution to the crystal edge

2) initiation of intercalation by charge transfer to the layers

3) opening of the layers

4) diffusion between the layers

In the amino acid intercalation the diffusion from the solution to the crystal edge is found to be the rate controlling step of the reaction.

The most interesting processes, from the point of view of this research are steps (2) and (3) the initiation of the intercalation by charge transfer to the layers and the opening of the layers. It is proposed that a charge transfer compound is formed by a co-ordination reaction between a tantalum atom and a nitrogen lone pair and is responsible for the initiation of the intercalation.

There is evidence by Thompson (1974) that sulphur is released during intercalation of ammonia, which supports the view that tantalum atoms at the edge of the TaS_2 layers must be exposed during the intercalation reaction. It is believed that these are the only possible sites for the co-ordination reaction to take place.

A charge transfer complex or compound is defined chemically as a bonding interaction between two atoms A and D (Acceptor and Donor), in which the bonding energy is attributable to a partial transfer of charge between the same atoms. It is considered to be a resonance hybrid (Cotton and Wilkinson 1972) of the unbonded representation A····D and the charge

transfer bonded representation A^{-}——D^{+}.

The proposed charge transfer compound formation between the edge tantalum and the nitrogen lone pair, can be visualized in an ideal case as shown in figure (8.2).

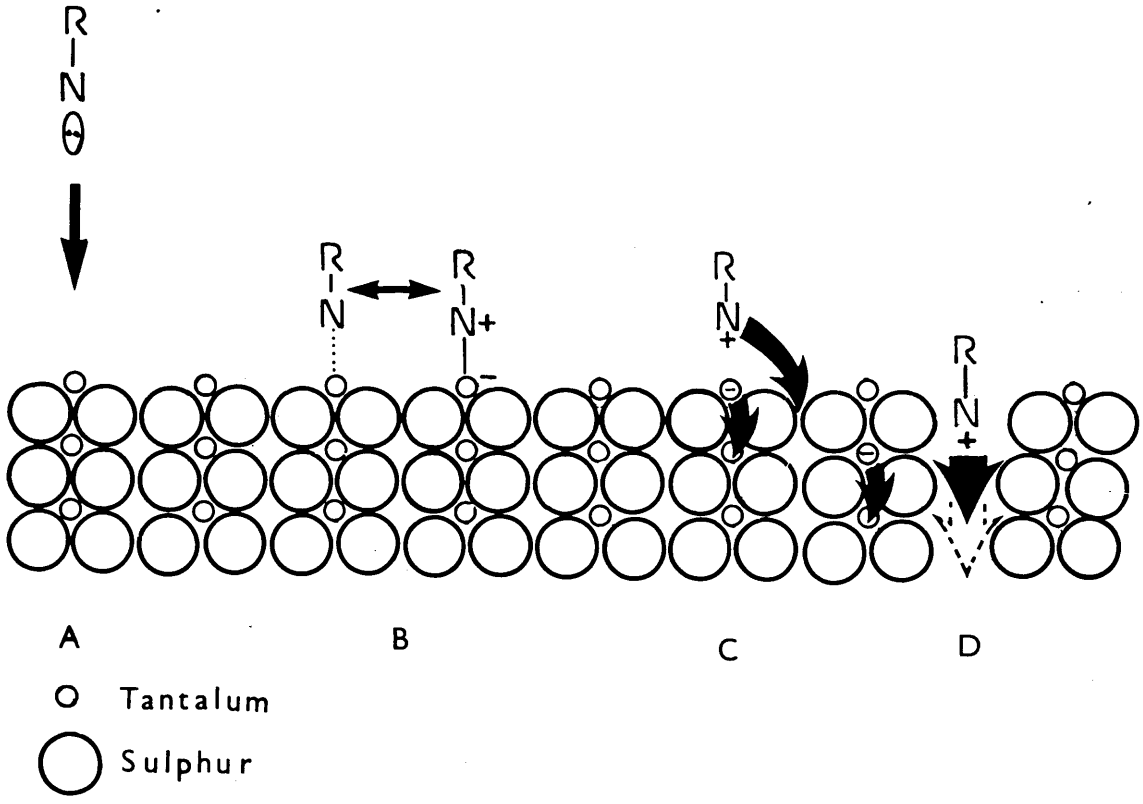


Figure (8.2)

(A) describes the nitrogen atom and its lone pair of electrons approaching the edge tantalum atom, R represents the rest of the molecule. (B) shows the two representations of the resonance hybrid in which charge transfer has occurred and (C) is the unconventional chemical step where formation of the ions takes place.

The opening of the layer involves three phenomena that will be described separately but they are very clearly interlinked.

1) When two adjacent layers are negatively charged, they will tend to repel making it energetically favourable for the layers to open up.

2) The positively charged nitrogen atom is then able to enter between the layers and carry with it the rest of the molecule.

3) The negative charge is delocalized within the conduction band, but as this is a narrow band conductor the electron will reside predominantly at a tantalum atom dorbital.

Now, the cation (the positively charged nitrogen atom) and its associated negative charge can diffuse towards the interior, allowing another molecule to form a charge transfer compound with the edge tantalum atom. So the intercalation can proceed as shown on figure (8.2D).

It is difficult to have back charge transfer to the intercalate molecular ion to obtain the uncharged intercalated molecule. Hence there is no requirement for the nitrogen lone pair to point in the direction of a tantalum atom as is required in the simple chemical charge transfer model.

The orientation of the charged molecule and its lone pair is determined mainly by Coulombic and van der Waals forces. Hydrogen bonding and dipole-dipole interactions between intercalated molecules may also influence the orientation of the molecule.

As the nitrogen atom is positively charged and the layers are negatively charged, for electrostatic reasons the nitrogen atom will tend to reside midway between the layers. The position of the nitrogen atom in the intercalated molecules of this work is consistent with this explanation. Even though the orientation of the lone pair often happens to be perpendicular to the TaS_2 layer, clearly the van der Waals forces are important in determining the orientation of these molecules and there is no need to consider that the molecules occupy specific sites over the surface of the layer.

So far, the importance of the lactam-lactim tautomerism on the peptide bond has not been mentioned but it deserves discussion. Although the proton attached to the nitrogen atom can migrate to the oxygen atom and form the less stable lactim structure, it is not affecting the nitrogen lone pair in the unhybridized P_z orbital of the peptide bond. Hence the argument that the peptide bond is helping to promote intercalation remains unchanged.

Superconductivity in transition metal dichalcogenide intercalated compounds has been explained in terms of charge transfer to the Fermi surface (Gamble 1970). This increases the density of states at Fermi level which according to BCS theory will increase the superconducting transition temperature. The measured superconducting T_{onset} for the complexes prepared in this work are within $1.2^{o}K$ and $5.0^{o}K$, in agreement with the generally observed temperature range for intercalated TaS_2. It is believed

that the T_{onset} observed is consistent with the charge transfer model and there is no evidence to invoke the superconducting excitonic mechanism.

The absence of a superconducting transition in tetraglycine, pentaglycine and ethanolamines intercalation complexes was unexpected. This is an important point that needs further study and may be combined with future work on the in-situ polymerization of glycine between the layers of TaS_2, or other transition metal dichalcogenide.

Such a composite of polyglycine intercalated in between a TaS_2 would give opportunity to study the electronic properties of a semiconductor polypeptide intercalated between a superconducting layer dichalcogenide.

REFERENCES

Bach, B., and Thomas, J.M., 1972, J. Chem. Soc. Chem. Comm., 6, 301-2.

Balchin, A.A., 1976, Crystallography and Crystal Chemistry of Materials with Layer Structures (F. Lévy D. Reidel Publishing).

Beal, A.R., and Liang, W.Y., 1973, Phil. Mag., 27, 1397-416.

Becke-Goehring, M., 1960, Inor. Synth., 6, 123-8.

Che-Hsiung Hsu, Labes, M. M., Breslin, J.T., Edmiston, D.J., Winter, J.J., Leupold, H.A., and Rothwarf, F., 1973, Nat. Phys. Sci., 246, 122-3.

Chianelli, R.R., Scanlon, J.C., Whittingham, M.S., and Gamble, F.R., 1975, Inor. Chem., 14, 7, 1691-6.

Cotton, F.A., and Wilkinson, G., 1972, Advance Inorganic Chemistry, (Interscience Publ.) 463

Cousseau, J., Trichet, L., and Rouxel, J., 1973, Bull. Soc. Chim. Fr., 872.

Dines, M.B., 1974, Science, 188, 1210-11.

Di Salvo, F.J., 1971, Ph. D. Stanford University.

Di Salvo, F.J., Schwall R., Geballe, T.H., Gamble, F.R., and Osiecki, J.H., 1971, Phys. Rev. Lett., 27, 6, 310-13.

Ehrenfreund, E., Gossard, A.C., Gamble, F.R., 1972,Phys. Rev., 5, 5, 1708-11.

Gamble, F.R., and McConnell, H.M., 1968, Phys. Rev., 26A, 4, 162-3.

Gamble, F.R., Di Salvo, F.J., Klemm, R.A., and Geballe, T.H., 1970, Science, 168, 568-70.

Gamble, F.R., Osiecki, J.H., Cais, M., Pisharody, R., Di Salvo, F.J., Geballe, T.H., 1971, Science, 174, 493-7.

Gamble, F.R., Osiecki, J.H., and Di Salvo, F.J., 1971, J. Chem. Phys. 55, 7, 3525-30.

Gamble, F.R., Silbernagel, B.G., 1975, J. Chem. Phys., 63, 2544.

Geballe, T.H., Menth, A., Di Salvo, F.J., and Gamble, F.R., 1971, Phys. Rev. Lett., 27, 6, 314-6.

Gesierich, W., 1954, Diplomarbeit Heidelberg.

Ginzburg, V.L., 1968, Contemp. Phys., 9, 4, 355-74.

Ginzburg, V.L., 1972, Annual Rev. Mat. Sci., 2, 633-696.

Glover III, R.E., and Sherrill, M.D., 1960, Phys. Rev. Lett., 5, 6, 248-50.

Gmelins, 1968, Handbuch Der Anorganischen Chemie, (Verlag Chemie).

Goehring, M., 1956, Quat. Rev., 10, 4, 437-50.

Greene, R.L., Grant, P.M., and Street, G.B., 1975, Phys, Rev. Lett., 34, 2, 89-92.

Greene, R.L., Street, G.B., and Suter, L.J., 1975, Phys. Rev. Lett., 34, 10,577-79.

Grim, R.E., 1968, Clay Minerology, (McGraw-Hill).

Huisman, R., de Jorge, R., Haas, C., and Jellinek, F., 1971, J. Solid State Chem., 3, 56.

Jolly, W.L., and Becke-Goehring M., 1962, Inor. Chem., 1, 76-8.

Katon, J.E., 1968, Organic Semiconducting Polymers (Edward Arnold, Marcel Dekker).

Little, W.A., 1964, Phys. Rev., 134, 6A, A1416-24.

Little, W.A., 1973, J. Low, Temp. Phys., 13, 3, 365-69.

Lippincott, E.R., and Tobin, M.C., 1951, J. Amer. Chem. Soc., 73, 4990.

Lippincott, E.R., and Tobin, M.C., 1953, J. Chem. Phys., 21, 1559.

Mandel, J., 1964, The Statistical Analysis of Experimental Data, (Internscience, John Wiley and Sons), 274-8.

Nitsche, R., 1964, Z. Krist., 120, 1.

Nitsche, R., Bolsterli, H.U., and Lichtensteiger, M., 1961, J. Phys. Chem. Solids, 21, 199.

Nitsche, R., and Richman, 1962, Z. Elektrochemie, 66, 709.

Nitsche, R., 1967, J. Phys. Chem. Solids (supp.) 1, 28.

Oró, J., and Guidry, C.L., 1961, Arch.Biochem. Biophys., 93, 166-71.

Parry, G.S., Scruby, C.B., and Williams, P.M., 1974, Phil. Mag., 29, 3, 601-12.

Riekel, C., Hohlwein, D., and Schöllhorn, R., 1976, J.C.S. Chem. Comm. 863-4.

Riekel, C., and Schöllhorn, R., 1976, Mat. Res. Bull., 11, 369-76.

Rüdorff, W., and Sich, H.H., 1959, Angew. Chem., 71, 724

Saito, Y., Makino, M., Yamazoe, N., and Seiyama, T., 1977, Denki Kag, 45, 12, 746-52.

Schaefer, H., 1964, Chemical Transport Reactions (Academic Press).

Schöllhorn, R., and Zagefka, H.D., 1977, Angew. Chem. Int. Ed. Engl., 16, 3, 199-200.

Scruby, C.B., Williams, P.M., and Parry, G.S.,1975, Phil. Mag., 31, 2, 255-74.

Streitweiser, A., and Heathcock, C.H., 1978, Introduction to Organic Chemistry (Collier Macmillan Co., Inc.), 817.

Subba Rao, G.V., and Tsang, J.C., 1974, Mat. Res. Bull., 9, 921-26.

Theng, B.K.G., 1974, The Chemistry of Clay-Organic Reactions, (Adam Hilger).

Thomas, J.M., Evans, E.L., Bach, B., and Jenkins J. LL., 1972, Nat. Phys, Sci, 235, 126-7.

Thompson, A.H., 1974, Nature, 251, 492-4

Ubbelohde, A.R., 1977, Proc. Franco American Conf. Intercalation Compounds of Graphite, La Napoule France, (Vogel-Hérold).

Villena-Blanco, M., and Jolly, W.L., 1967, Inor. Synth., 9, 98-102.

Walatka, V.V., Labes, M.M., and Perlstein, J.H. 1973, Phys. Rev. Lett., 31, 18, 1139-42.

Walton, A.G., and Blackwell, J., 1973, Biopolymers (Academic Press).

Weiss, A., and Ruthardt, R., 1969, Z. Naturforsch., Ser. B, 24, 335.

Wilson, J.A., and Yoffe, A.D., 1969. Advan. Phys., 18 193-335.

Yoffe, A.D., 1973. Fest. Prob. XIII, 1-29.